TotalControl

Advanced integrated supervisory and wind turbine control for optimal operation of large Wind Power Plants

Control algorithms for primary frequency and voltage support
Deliverable no. D4.1

Delivery date: 28.02.2020
Lead beneficiary: DNV GL
Dissemination level: Public

Author(s) information (alphabetical):

Name	Organisation	Email
Ervin Bossanyi	DNV GL	ervin.bossanyi@dnvgl.com
Salvatore D'Arco	SINTEF	salvatore.darco@sintef.no
Liang Lu	DTU	lilu@dtu.dk
Ander Madariaga	ORE Catapult	ander.madariaga@ore.catapult.org.uk
Wouter de Boer	DNV GL	Wouter.deBoer@dnvgl.com
Wouter Schoot	DNV GL	Wouter.Schoot@dnvgl.com

Document information

Version	Date	Description		
		Prepared by	Reviewed by	Approved by
1	28.02.2020	The authors	Ervin Bossanyi	Ervin Bossanyi

TABLE OF CONTENTS

EXECUTIVE SUMMARY

This report is concerned with the addition of special features to wind plant controllers so that they can actively contribute to the stable operation of the electricity grid system and make it possible for larger penetrations of wind power to be integrated. After an brief overview of relevant grid codes in Section 2.1, section 2.2 describes how wind farms may contribute to both frequency and voltage stability. The remainder of the report is concerned mainly with grid frequency support.

Section 3 investigates control algorithms implemented at the wind turbine level which can be used for frequency support. A wind farm simulator and a grid simulation code are coupled together, permitting time-domain simulations of an entire grid system to be performed. The closed-loop response of the system is simulated, whereby the wind plant power output is made to depend on the grid frequency, and that frequency is in turn determined by the grid power balance with the inclusion of the wind plant output. This allows the system effects of any control algorithms to be evaluated. A set of simulations based on the Irish grid system and using historical time-history inputs has shown that the system response can indeed be improved by an appropriate choice of control algorithms, which include inertia emulation but can also include other features. The results show that the frequency nadir following recorded system trip events can be improved, and controller parameters adjusted to achieve the best response.

The Virtual Synchronous Machine (VSM) concept of offers the possibility to provide inertial support directly from power converters. Section 4 uses a hardware-in-the-loop setup in the laboratory to test a VSM system together with a grid emulator. Some classical VSM schemes may not work well for wind turbines, so alternative schemes are investigated. The experimental tests demonstrate that a modified VSM scheme can be implemented within a WT conversion system and can offer inertia support during grid disturbances, with enough flexibility in modulating the amount of support to provide and a satisfactory speed response.

1 INTRODUCTION

This report is concerned with the addition of special features to wind turbine or wind farm controllers so that they can actively contribute to the stable operation of the electricity grid system and make it possible for larger penetrations of wind power to be integrated. Grid voltage and frequency can be affected when wind turbines are connected to the grid, and this can be seen as an impediment to the integration of large quantities of renewable power, but with appropriate controller modifications, it is possible for negative effects to be mitigated, and even for wind power plant to contribute positively to grid stability.

Most of the report is concerned with the issue of frequency stability. With large amounts of wind power connected through inverters, their physical inertia is disconnected from the grid frequency, reducing the overall system inertia resulting from directly-connected conventional synchronous generators. This results in wider frequency swings, and the possibility of bigger frequency dips when a large power plant or transmission line trips out, which could cause system instability. However, the physical inertia of wind turbines is very significant, and controller changes can bring it into play, so that it can contribute to system inertia. Furthermore, because this is done

programmatically rather than by a direct physical link, it is should be possible to devise control algorithms which do more than just provide effective inertia, but instead can be tuned to provide the best possible response to help the grid, while remaining within the allowed operational parameters of the wind turbines.

In this report, Section 2 introduces the topic: in Section 2.1, some of the relevant grid codes which currently govern the operation of the system are described, and Section 2.2 goes on to describe in general terms how wind power plant may be able to contribute.

Section 3 is concerned specifically with grid frequency response by changing the active power output of the wind plant, and aims to provide a simulation framework which can be used to investigate and test wind plant control algorithms designed to help grid stability. This is achieved by coupling together a wind power plant simulator capable of time-domain simulations of wind farm performance including the control systems, to a grid simulator which combines the resulting wind power with the rest of grid, and predicts grid frequency variations resulting from the short-term power imbalances. This provides a closed-loop simulation environment, where the wind plant responds to grid frequency by changing its power output, and the grid responds to this power output resulting in changes to the frequency which are detected by the wind plant.

Section 4 is concerned with a particular way to achieve changes in wind plant power output in response to frequency variations known as the virtual synchronous machine (VSM) concept, whereby the inverter controller is configured to provide the appropriate response. Section 4 reports on a laboratory test setup of a VSM system working together with a grid emulator, to allow the resulting system behaviour to be studied by hardware-in-the-loop simulation.

2   GRID FREQUENCY AND VOLTAGE SUPPORT

2.1   GRID CODES

Grid Codes, also known as Connection Network Codes, are regulations that provide the framework and rules for operating electricity transmission and distribution networks. Among other conditions, they set acceptable operational ranges for a number of electrical parameters at the point of common coupling between a user and the network. In this way the grid codes impose control response capability requirements on any user seeking connection rights. In a nutshell, they set the conditions under which power networks can be accessed by licensed market participants. Figure 1 below shows graphically the legal context of power networks and the place network codes play in them.

In the specific case of generation assets, some of the conditions set in the codes are given in terms
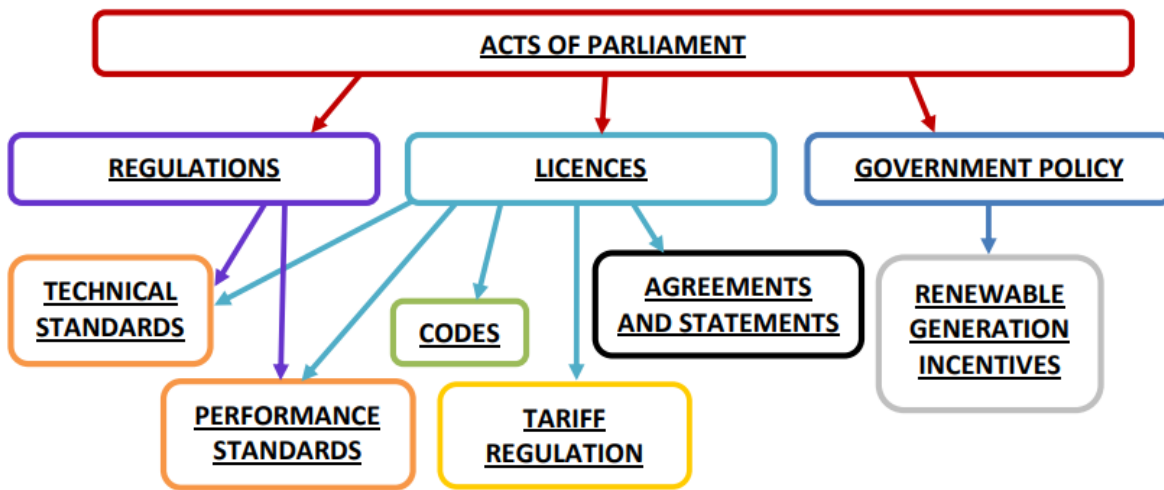
Figure 2-1 Codes, Standards and Regulations relationship diagram **[10]**

of electric power output control capability requirements in a number of real-world scenarios. These requirements are, in some cases, applicable to all generators within a given power/voltage range [independently of the technology of choice]. In other cases, the requirements are specific for a given generation technology, i.e. intermittent sources like onshore and offshore wind power plants.

With regards to active and reactive power (P and Q) response control for frequency and voltage support, electricity system operators (ESOs) have historically get access to it in one of the following two ways:

1. by setting, in the relevant codes, grid connection requirements for network users that include adequate automatic P and Q responses to voltage and frequency variations in normal operation; and,
2. by procuring ancillary services directly from generators able to perform in excess of the minimum requirements (set in the grid code) when required from the control room, e.g. firm frequency response, enhance reactive power output, others.

In terms of the first option, generators applying for connection agreements must ensure grid code compliance for their generation assets. This generally includes some form of P and Q response control in normal operation. In the UK for instance, the Grid Code [1] and CUSC – Connection and Use of System Charges [2] set up these conditions in the form of (P,f) response ramps, acceptable (P,Q) operational envelops, or others (see Figure 2). These operation envelopes are designed to provide power networks with a degree of frequency and voltage self-regulation. At EU level, equivalent requirements are set up in the Requirements for Generators and additional documents related to its implementation by Member States [3].
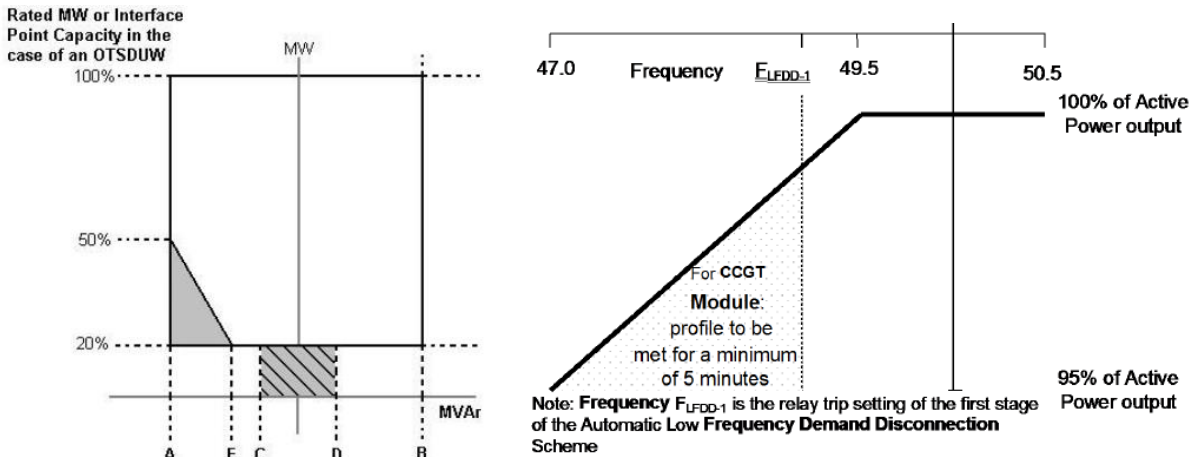
Figure 2-2 examples of P, Q, f, U operation conditions as in the grid code

According to these codes, during the past two decades [offshore] wind power plants have been required to operate within certain active and reactive power response conditions, which depend on the status of the plant, weather conditions and network constraints. Strictly speaking, they have generally been excluded from ancillary service markets. It is therefore understandable that, from an owner-operator perspective, most of the interesting OWPP control developments have been aimed at maximising profits within a market that determines the value to society in terms of the energy produced. Grid codes have therefore been generally considered as constraints, and compliance reassurance has been provided by means of technical assessment, test, measurement, validation and simulation [4]. Other standards like IEC 61400 series have been developed to reassure that wind turbines and plant controls designed, manufactured and tested according to them will operate reliably in real world conditions.

In terms of the second option, the ESOs also procure ancillary services like enhanced frequency response and reactive power support, directly from generators able to provide them. Historically, these services have been provided by conventional power plants with big synchronous generators. However, with the continuous increase of [offshore] wind and other asynchronous generation in power systems, operators are looking into different ways of procuring ancillary services. Several European Countries have set up initiatives intended to rationalise, simplify and improve frequency response and other products by retiring a few now obsolete services, standardising procurement windows, and improving the transparency of market information.

At the time of writing, new frequency response products are being designed and brought to the market, and a significant increase in the market share of non-conventional power plants is envisaged. In the UK for instance, a recent power park module signal best practice guide for intermittent generation defines the requirements for the provision of additional information from power park operators into ESO control rooms. Power Available for example is defined as an operational metering signal that combines live weather readings with plant capability to provide a dynamic, real-time indication of maximum potential output. This Power Available signal provided by Power Park Modules is being integrated into ESO processes and systems, which in time will improve control room visibility of intermittent generation and facilitate wind participation in new frequency response products being proposed by the ESO, like dynamic regulation-moderation-containment, and static containment [5].

On the other hand, other technologies like demand side response and electricity storage are also willing to take part in these new ancillary service markets. Electricity storage seems well placed to be considered in conjunction with [offshore] wind power because it increases its 'dispatchability' and therefore, also increases its chances of taking part in future ancillary service provision markets. More generally, the inclusion of electricity storage assets in conjunction with (or in the vicinity of) renewable electricity sources (RES) would increase the overall dispatchability of the renewable energy, and therefore, increase the chances of RES participating in the provision of ancillary services to the ESO.

And recent advancements provide a pathway on connection arrangements with electricity storage. A recent study by the European Union GC ESC expert task groups [8] recommend categorising electricity storage into synchronous and non-synchronous devices with standalone, mixed and a variation of co-located sites shown in Figure 3.
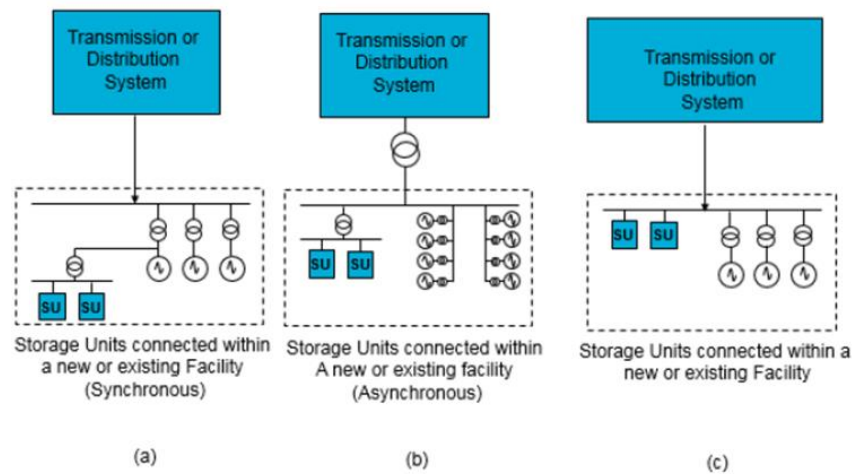
Figure 2-3: recommended co-located configurations by task group

Finally, the Danish Grid Codes [9] take a streamlined approach setting out clear requirements and guidelines on electricity storage 'battery plants' based on the point of connection (POC) or point of common coupling (PCC) as shown in Figure 4. This approach contrasts with the UK grid code which is a bit more open in nature setting out minimum requirements and allowing some flexibility with bilateral agreements with the system operator.
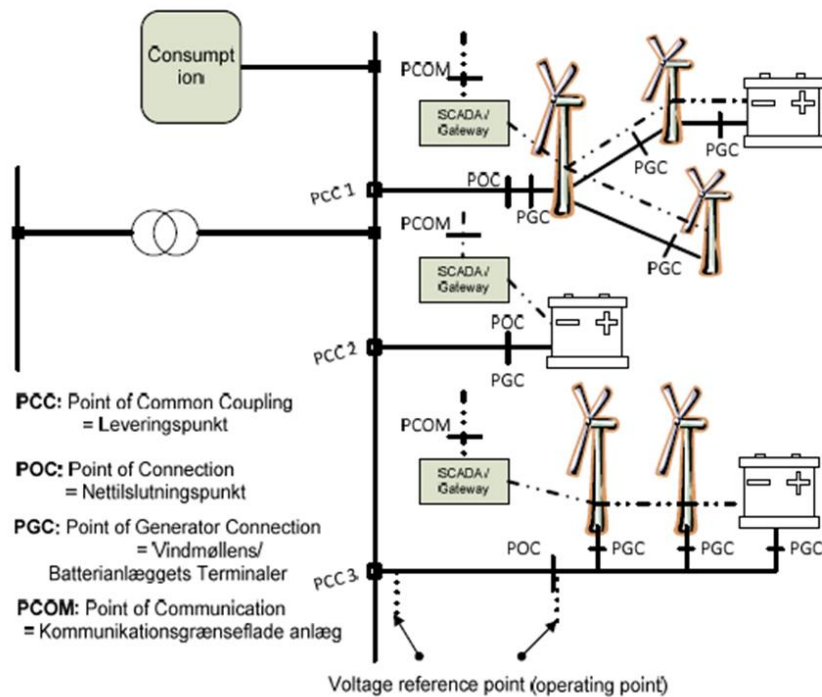
Figure 2-4: An example of grid connection of a plant in Danish grid code

2.1.1 GRID CODE REFERENCES

[1]   The Grid Code, "nationalgrid ESO," 4 September 2019. [Online]. Available: https://www.nationalgrideso.com/codes/grid-code?code-documents .

[2]   Connection and Use of System Code, "nationalgridESO," 1 April 2019. [Online]. Available: https://www.nationalgrideso.com/codes/connection-and-use-system-code-cusc?code-documents.

[3]   Requirements for Generators, "Entso-e," 16 April 2016. [Online]. Available: https://www.entsoe.eu/network_codes/rfg/.

[4]   DNV GL - ST - 0125, "Grid code compliance standard," 2016.

[5]   nationalgridESO, "Power Park Module Signal Best Practice Guide for Intermitent Generation v1.0," July 2019. [Online].

[6]   A. M. Urban, M. de Batista, H. G. Svendsen, S. D'Arco and S. Sahcez, "Turbine controller adaptation for varying conditions and ancillary services: Deliverable TotalControl Project," DNV GL, 2019.

[7]   N. Ding, Z. Lu, Y. Qiao and Y. Min, "Simplified equivalent models of large-scale wind power and their application on small-signal stability," *J. Mod. Power Systems, Clean Energy,* vol. 1, no. 1, pp. 58-64, 2013.

[8]   Q. Gao and R. Preece, "Improving frequency stability in low inertia power systems using synthetic inertia from wind turbines," in *IEEE PowerTech2017*, Manchester , 2017.

[9]   nationalgridESO, "Future of Frequency Response - Industry Update," February 2019. [Online].

[10] Power Networks Demonstration Centre (PNDC), "PNOR Phase 1 report," The University of Strathclyde, Glasgow, 2018.

[11] R. Eriksson, N. Modig and K. Elkington, "Synthetic inertia versus fast frequency response: a definition," *IET Renewable Power Generation,* vol. 12, no. 5, pp. 507-514, 2016.

[12] ENTSO-E, "ENTSO-E Network Code for Requirements for Grid Connection Applicable to all Generators," ENTSO-E, Brussels, 2013.

2.2 POTENTIAL CONTRIBUTION FROM WIND FARMS

As the penetration of wind farms on the grid system increases, a number of issues may arise which are of concern for the stable operation of the grid. This report is concerned with two of these issues, voltage and frequency regulation, and investigates how the wind power plant itself can help to mitigate the problems.

The frequency of an AC grid undergoes small variations which are important in ensuring a constant match between power supply and demand. Conventional power stations use directly-connected synchronous generators whose speed of rotation is tied to the grid frequency. This provides a natural regulation mechanism to help match supply and demand known as inertial response: if more power is being consumed than generated, the extra current drawn increases the generator torque, causing it to slow down; so some of its kinetic energy is used to supply the excess demand, and the grid frequency decreases; and vice-versa if there is excess supply. All such generators are locked together through the grid frequency, so they act together like a single giant flywheel stabilising the system.

Wind turbines also have plenty of rotor inertia [16], but they operate at variable speed, disconnected from the grid frequency by the power converter, and therefore do not contribute to the inertia of the grid. This means that the greater the penetration of wind power, the lower the effective inertia of the system provided by the remaining conventional plant, which means that grid frequency variations will increase, and could lead to system collapse.

However, it is perfectly possible to bring the large inertia of wind turbine rotors into play, so that they contribute after all to frequency stability of the grid. This can be done by appropriate modifications to the turbine control, covered in Section 3 of the report, or by modifying the way in which the power converter itself is controlled, as covered in Section 4.

2.2.1 FREQUENCY RESPONSE USING TURBINE CONTROL

Section 3 of the report describes how a variable speed pitch regulated wind turbine controller can be modified to bring the rotor inertia into play. A sensor detects changes in grid frequency and the controller responds by changing the instantaneous torque or power command sent to the power converter. This is sometimes called synthetic inertia, or inertia emulation: it cannot be identical to the true inertial response of a synchronous generator, because of control loop delays such as:

a) the response of the grid frequency sensor, which typically has to measure several cycles of the voltage sinusoid in order to arrive at a reasonably clean estimate of frequency

b) the calculation time needed for the controller to process the frequency signal and calculate the required change in power command

c) the response of the power converter to the power command

d) communication delays between sensor, controller and power converter

On the other hand, using the controller gives the freedom to implement any desired algorithm for modifying the power command. In fact it could try to mimic both inertial response and primary frequency response. To emulate inertial response, the controller should demand additional power proportional to minus the rate of change of grid frequency. For primary response it can emulate the droop curve response of a steam turbine governor by demanding a further power increment proportional to the difference between the measured frequency and the nominal frequency (actually the small delays mentioned above imply that primary response can actually be a lot faster than in conventional plant which relies on adjustment of steam valves etc.). However the response can be generalised further: the controller can shape the response in any arbitrary way designed to enhance grid stability while staying within the limits of feasibility for the wind turbine in the current wind conditions (including any effect on turbine loading). Here the term 'fast frequency response' is used to indicate any such generalised response of power output to grid frequency variations.

The strategy should achieve two things. Perhaps the most important is to help keep the frequency nadir as high as possible (the lowest point in the frequency dip which follows a worst-case event such as the sudden loss of a major generating station). In normal conditions, it is also important to minimise the amount of frequency variation to keep it within the statutory range.

In order to understand the best strategy to adopt, it is necessary to model the wind plant and the grid system in combination. This is the topic of Section 3.

2.2.2 THE VIRTUAL SYNCHRONOUS MACHINE

It is also possible to arrange the wind turbine's power converter controller to respond automatically to frequency changes, responding in a similar way to a conventional synchronous generator. This is known as the virtual synchronous machine concept, and is covered in Chapter 4. Of course, if significant changes in active power flow are needed, the main turbine controller may also have to respond.

2.2.3 VOLTAGE / REACTIVE POWER CONTROL

Integration of wind farms to the power system brings several challenges to the voltage / reactive power control of the system. First of all, the uncertainty in wind power output leads to a fast change of active power flow in the grid, and consequently a fluctuation in reactive power and voltage. Secondly, long-distance transmission of wind power from wind farms to load centres may bring conflicts among different voltage controllers at different regions and hierarchical levels, if there is no proper coordination between these voltage controllers. Thirdly, significant fluctuations of reactive power along transmission lines will increase operation time and switching times of shunt reactors, which will shorten their life expectancy and increase maintenance cost. In addition, the participation of wind farms in voltage / reactive power control presents challenges to the payment and cost allocation in reactive power markets.

Various voltage / reactive power control methods have been proposed to deal with these challenges. Generally these methods can be classified into three categories:

(1) Decentralized voltage / reactive power control

Local voltage / reactive power controllers receive local or partial information of the power system states, calculate, analyse and send control inputs to local voltage / reactive power control devices. There are three modes of control: local power factor or reactive power control, local voltage control, and remote voltage control. They are used to regulate the power factor, reactive power, or voltage at a local bus or a selected remote bus, within limits or according to a setpoint.

Decentralized voltage / reactive power control does not have complete observation of the power system states and has no coordination with other local controllers. Thus, decisions are not made from the perspective of the global optimum, and this category of control cannot address problems coming from interconnected but not coordinated power grids. Local power factor or reactive power control can reduce the uncertainty of reactive power output; however, the reactive power output is not adjusted according to the voltage, and large voltage variations may happen. Local / remote voltage control works better to maintain the voltage profile at the target bus and avoid voltage collapse.

(2) Centralized voltage / reactive power control

Centralized voltage / reactive power controllers receive all the information of power system states, calculate, analyse and send control inputs to all the voltage / reactive power control devices in the system. In order to mitigate the influence of uncertainty of wind power in each control period, forecast values or probability distribution of wind power can be used in the voltage / reactive power control models. To prevent control devices from excessive operation and switching, their operation cost is taken as part of the objective function. As for the challenge of reactive power market, the model can be improved to compromise system payment and voltage security margin, and reactive power cost from wind farms needs to be discussed. Centralized voltage / reactive power control provides some solutions to the challenges above, however, its coordination among different interconnected power grids has not been well researched.

Centralized voltage / reactive power control can be divided into online optimization and offline optimization based on the time of executing the optimization process. Online optimization helps to achieve stable and economic operation of the power system with integration of wind farms. However, considering the fluctuating wind power, the optimization calculation should be finished in a short control period, or consider multiple wind power scenario simultaneously, which will be a computation burden. Offline optimization can reduce computation burden greatly, but the control rules can be very complex and difficult to realize in a large power system.

(3) Hierarchical voltage / reactive power control

Hierarchical voltage / reactive power controllers are organized in a hierarchical structure and receive partial or all the information of power system states. The control inputs are divided into different layers. The controller at a lower layer complies with the decision made by the controller at an upper layer. One way to do this is that the controller at a lower layer gets control inputs at a higher frequency while the controller at an upper layer operates at a lower frequency. The other

way is that the controller at a lower layer fulfils the requirement from the controller at an upper layer and sends feedback information to it.

Hierarchical voltage / reactive power control has all the advantages of centralized control. The difference between them is that hierarchical voltage / reactive power control can set different control periods for discrete and continuous devices and thus is flexible to coordinate different device characteristics. In addition, it is also flexible to coordinate different objectives between the transmission system and wind farms. However, the design and implementation of hierarchical voltage / reactive power controllers are more complicated than those of centralized control. Hierarchical voltage / reactive power control also needs high capacity of computation and communication.

The different architectures of these three different categories of voltage / reactive power control methods are illustrated below in Figure 2.1.
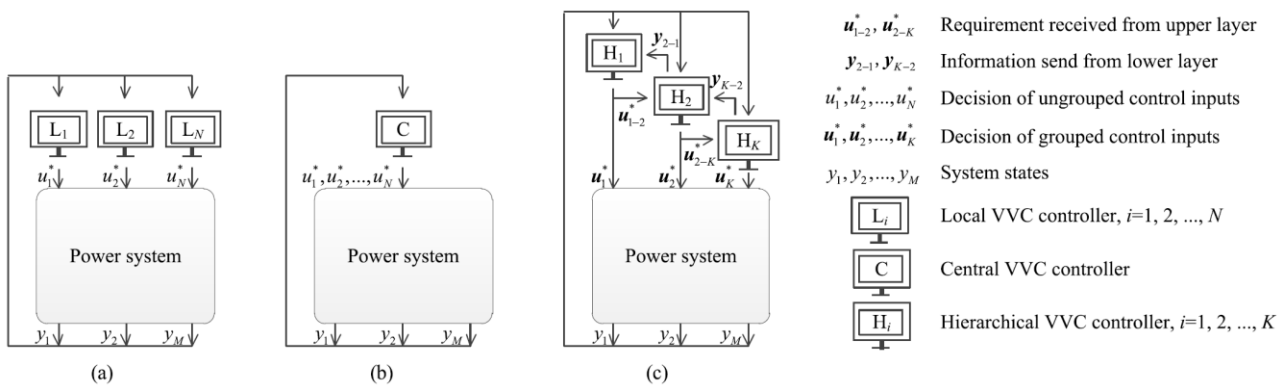
Figure 2-5: Voltage / reactive power control: (a) decentralized (b) centralized (c) hierarchical. Reproduced from [1].

In order to meet power factor requirements (e.g. -0.95 to 0.95) at the point of common coupling (PCC), most wind farms are equipped with switched shunt capacitors for static reactive power compensation. However, as nowadays wind farms are going offshore and getting further away from the shore through longer transmission cables, wind farms are connected to electrically weak power grids, characterized by low short circuit ratios and under-voltage conditions. In this case, dynamic power electronic devices such as static var compensators (SVC), static synchronous compensators (STATCOM) and unified power flow controllers (UPFC) have been increasingly utilized in wind farms to provide rapid and smooth reactive power compensation and voltage control. Research has found that for wind farms which are based on type-4 wind turbines, STATCOM proves to be a better alternative in voltage / reactive power control, and also enhances the fault ride-through (FRT) capability of wind farms.

A STATCOM generates a set of balanced three-phase sinusoidal voltages at the fundamental frequency, with rapidly controllable amplitude and phase angle. It is installed near the point of common coupling (PCC) to help the voltage or power factor at PCC meet the requirements from grid codes. From the perspective of power system dynamic stability, a STATCOM provides better damping characteristics than SVC as it is able to transiently exchange active power with the system. In particular, it has very fast response time (1-2 cycles) and superior voltage support capability with its nature as a voltage source. With the recent innovations in high power semiconductor switches, converter topologies and digital control technologies, faster STATCOMs

(quarter cycle) with low cost are emerging, which is promising to help achieve more cost-effective and reliable integration of renewable wind power into the grid.

Most research on voltage / reactive power control of wind farms with STATCOMs focuses on independent functionalities from wind farm controllers and the STATCOM separately. It seldom focuses on the coordination between wind the farm controller and the STATCOM to fulfil the voltage / reactive power control together. Problems may occur if there is no good coordination.

Take the blackout in UK on August 9th 2019 as an example. In this event, offshore wind farm Hornsea de-loaded from 799 MW to 62 MW immediately, which was one of the main losses of generation in this event. The reason that most of the wind turbines shut themselves down is that turbine controllers reacted incorrectly due to an insufficiently damped electrical resonance in the subsynchronous frequency range, so that the local Hornsea voltage dropped and the wind turbines shut themselves down because of overcurrent protection. The insufficiently damped electrical resonance can be seen at the onshore connection point, and unexpected large swings in active power and reactive power occurred (shown below in Figure 2.2 and Figure 2.3).
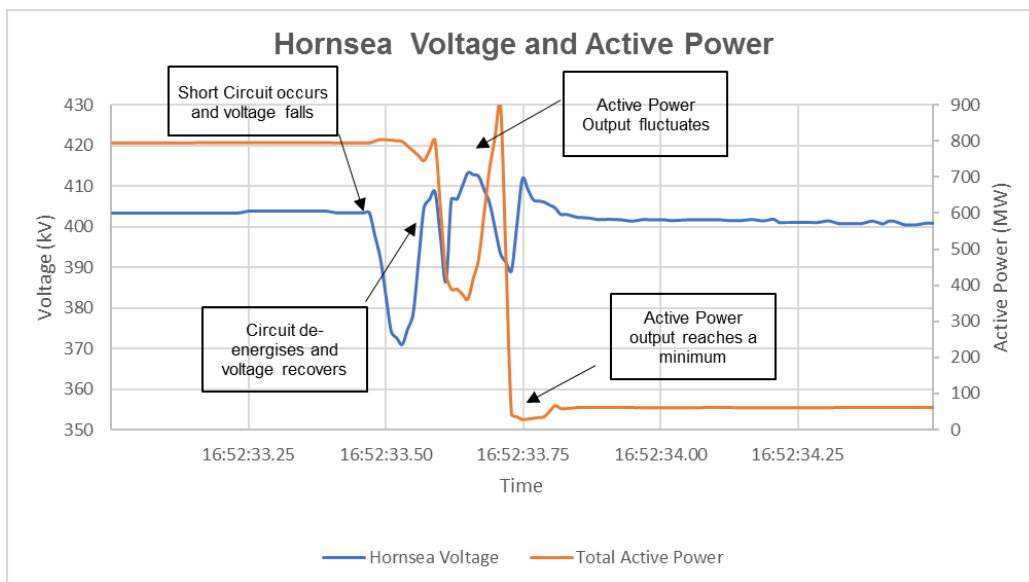
Figure 2-6: *Voltage and active power at Hornsea. Reproduced from [2]*
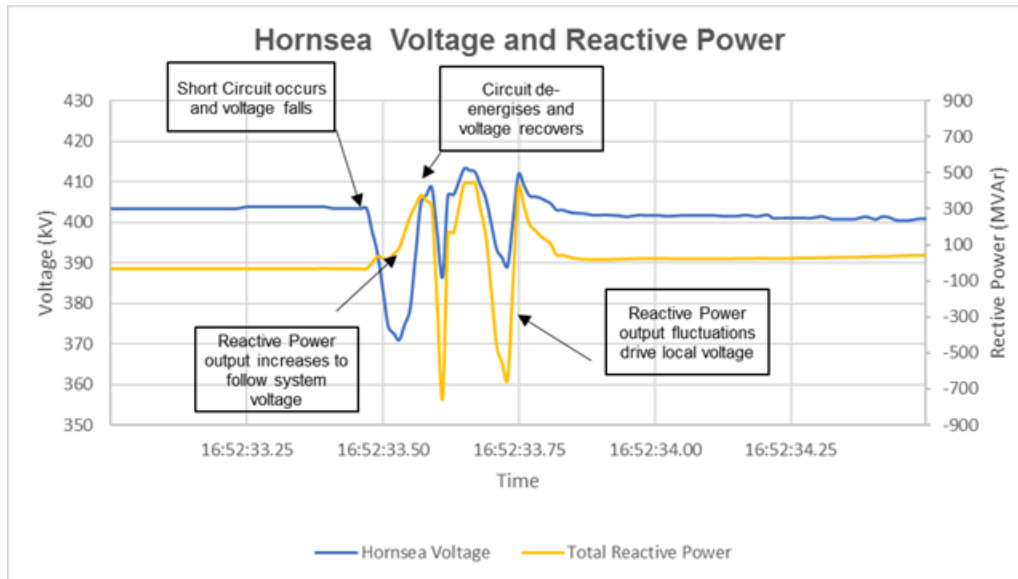
Figure 2-7: Voltage and reactive power at Hornsea. Reproduced from [2]

One possible reason for this insufficiently damped electrical resonance is that there is no proper coordination between wind farm controllers with the STATCOM in voltage / reactive power control. If both of wind farm controllers and STATCOM are controlled to regulate the voltage at PCC, oscillations can very easily occur because the control effects from wind farm controllers and STATCOM will not reach at PCC simultaneously. A wind farm is connected to the PCC via long transmission lines while a STATCOM is located much closer to the PCC. It is possible that the reactive power support from the wind farm just arrived at PCC when STATCOM has supported the voltage back into a suitable range, then unavoidably the voltage at PCC would fluctuate and consequently influence the reactive power outputs from the wind farm and STATCOM. The total reactive power at PCC will show oscillations, because of the non-synchronization in voltage / reactive power control from the wind farm controller and STATCOM and they are both trying to control one target – voltage at PCC. This is one possible reason that in the blackout event, the voltage and reactive power at PCC were oscillating fiercely and consequently the wind turbines shut down because of overcurrent protection.

Therefore, it is vital to research on the coordination between wind farm controllers and STATCOM in voltage / reactive power control. There has been some work relevant with this.

An interface neuro-controller (INC) is proposed for the coordinated reactive power control between a wind farm equipped with doubly fed induction generators (DFIGs) and a STATCOM [3]. The INC is based on heuristic dynamic programming (HDP) techniques and radial basis function neural networks (RBFNNs). It effectively reduces the level of voltage sags and over-currents in DFIG rotor circuits during faults, and therefore, greatly enhances the FRT capability of the wind farm. The INC also works as a coordinated external damping controller for the wind farm and STATCOM, and therefore, improves power oscillation damping of the system after grid faults.

A PID damping controller is proposed for the STATCOM using a pole-assignment approach to render adequate damping to the dominant modes of the studied system [4]. It is based on modal control theory to assign the mechanical mode and the exciter mode of the studied synchronous generator (SG) on the desired locations of the complex plane. The STATCOM with the PID damping

controller effectively suppresses inherent SG oscillations and improves system stability under different operating conditions.

An optimal voltage control scheme for wind farms with STATCOMs is proposed, which ensures that the voltages within the wind farm and the voltage at the high voltage side are within limits and maximizes the dynamic reactive power reserve of the wind farm [5]. This voltage control is to optimize both the voltage profiles of all elements and the reactive power distribution within the wind farm. It has three modes: corrective voltage control, coordinated voltage control and preventive voltage control. The corrective voltage control mode is to ensure that all the bus voltages of wind turbines are within limits. The coordinated voltage control mode is to mitigate the voltage fluctuations at PCC of the wind farm. If all the terminal voltages of all the wind turbines and STATCOM are within limits, and the voltage deviation at the high voltage side of the wind farm is larger than the threshold, the wind farm will operate in the coordinated mode. The preventive voltage control is to maximize the dynamic reactive power reserve of the STATCOM and replace the reactive power output from the STATCOM with that from wind turbines. It tries to drive the reactive power output of the STATCOM to the middle, and therefore, the STATCOM maintains both upward and downward reactive power regulation capability.

3   SIMULATION MODELLING FOR FREQUENCY SUPPORT

3.1   WIND FARM SIMULATION WITH LONGSIM

LongSim is an engineering tool developed by DNV GL for wind farm analysis, both steady-state and dynamic, aimed at designing and testing of wind turbine and wind farm controllers. It is designed to run rapidly, to allow fast design iterations and long simulations. Turbine wakes can be represented by a range of engineering models of wake deficits and added turbulence. The wakes are embedded into a realistic ambient flowfield. The flowfield used for dynamic simulations can be generated from site data. The model was described in detail in TotalControl deliverable D1.9 [6].

For the purposes of the work reported here, the following LongSim developments were used:

- A wrapper was designed so that LongSim could be called from a grid simulation model. At each timestep, the grid model passes information such as the grid frequency to LongSim, which executes one timestep of the wind farm simulation, and returns the total wind farm power output to the grid simulator.
- A means was provided to parameterise the fast frequency response and delta control logic in the turbine controller code within LongSim, so that the turbines would respond appropriately to the changes in grid frequency.

3.1.1   WIND FARM CHARACTERISTICS

A system based on the Irish grid has been used as a basis for the work reported here, as it is typical of a European grid system with a large wind power penetration. However, the aim of the work is to explore the feasibility of improving frequency regulation using wind power, and to demonstrate the use of the combined simulation tool for designing appropriate control strategies, so it is not important to model every aspect of the system in precise detail.

In particular, it is not necessary to model each one of the thousands of wind turbines actually present in Ireland. Instead, one or a small number of turbines can be modelled, making the assumption that they all experience the same grid frequency variation and respond to it in a similar way, and the resulting wind power output is then scaled up by an appropriate factor to represent the actual wind power output on the system.

The simplest LongSim simulation would be for a single turbine, with the output scaled up to match the output of all the turbines. While this might be acceptable for testing the frequency response strategy, it would not take into account the statistical and geographical smoothing of power output caused by the fact that the turbines are spatially separated, and would result in a total wind power output which is very much more variable than it is in reality. Even without simulating all the turbines individually, LongSim can correct for this in different ways. One is to run several instances in parallel, each using wind data from a different geographical location to represent different wind farms, capturing the effect of geographical diversity. Another is to scale up the low frequency power output by the number of turbines, and to scale up the higher-frequency variations according to the square root of the number of turbines, which assumes that the high frequency variations are uncorrelated between turbines. For the purposes of this study, the higher-frequency variations are of greater significance, so the latter approach has been used initially. The way this is done is described in section 3.1.3.

For greater realism, the study has also been extended to model wake effects within wind farms. This means that the turbines will not all be at the same point on their operating curve at any instant, so their frequency response capabilities at that instant will not all be the same. Geographical diversity will have a similar effect. However the main conclusions are unlikely to be dramatically different as a result of these effects.

3.1.2 WIND SPEED DATA

For a dynamic simulation, LongSim needs wind data time histories as a starting point. In this study, some specific historical periods have been selected in which significant frequency transients occurred on the Irish system. For each of these periods, the total power generation, and demand is available as 15-minute averages (Section 3.2.9.1.1), along with the total wind power generation and the forecast wind power, which would have been used to schedule generation from other plant.

The simplest way to generate a suitable wind time history is to take the total wind power generation, and run it back through a typical turbine power curve to obtain a wind speed time history. If this is used as input to the a LongSim simulation which uses the same turbine characteristics as were used to calculate the power curve, then the resulting power output should match the original 15-minute data. Wind direction is not required for modelling a single turbine, as wind farm wake effects are not considered. Turbulence intensity is required, but is not critical to the study especially if wake effects are ignored, so a representative uniform turbulence intensity of 12% was chosen.

The procedure used was as follows:

- A generic 2MW turbine was selected for the study, since all the necessary information was readily available.
- The steady power curve and C_p-lambda-pitch surface were calculated using Bladed steady-state calculations.
- Using the chosen turbulence intensity, the steady power curve was smeared to generate a dynamic power curve, which would better represent the 15-minute average performance of the turbine.
- Select a suitable rated power for all the wind generation. Eirgrid data gives the maximum wind generation as 3900 MW in 2018, so a rated power of 4000 MW was selected, corresponding to 2000 turbines of 2MW rating each.
- Use the dynamic power curve, scaled up to 4000 MW rated power, to convert the actual wind power generation for each 15-minute sample into a 15-minute average wind speed.

This 15-minute wind speed data was then used to drive a LongSim simulation using 2000 of the 2MW reference turbines, running with a timestep of 0.1 s. LongSim adds synthetic turbulence to the smoothed 15-minute average wind speed. The turbulence intensity was assumed to be 12%, with a Kaimal spectrum as defined in the IEC 1400-1 standard. LongSim generates both the point wind speed and the rotor-average wind speed. The rotor-average wind speed defines the aerodynamic performance using the C_p-lambda-pitch surface from the Bladed model. The generator torque and blade pitch demands are generated by a standard PI-based turbine controller, which also includes frequency response logic.

Data is also available for the available wind power, with the difference between available and actual wind power representing the output lost to curtailment. Therefore, rather than using actual wind generation, it would be more precise to generate a wind speed from the available wind power, and have the turbine controllers in LongSim respond to the curtailment demand so that the correct power output is generated. Since a curtailed turbine has a readily-available margin of extra power available, its ability to respond to a frequency drop would be greater. Ignoring curtailment is therefore a conservative approach, in terms of frequency response capability of the wind plant. On the other hand, the study could be extended to demonstrate how the presence of a wind turbine frequency response capability could reduce the amount of curtailment required. Either way, the main purpose of the study is demonstrate a tool which can be used to design and test the actual frequency response algorithms which are of most use to the system while remaining within the physical capabilities of the wind turbine system.

3.1.3 WIND FARM CONFIGURATIONS

Initial simulations were done with the simplest configuration, also because it has the fastest run times. In this case, a single 2MW turbine was simulated (T1), with stochastic turbulence added to the (smoothed) 15-minute wind speed data, and another identical one (T2) running with no added turbulence (but seeing the same grid frequency variations). To represent the correct amount of wind power on the Irish system, the power of one turbine was multiplied by N = 2000 to represent that number of turbines, giving a total installed capacity of 4GW. Since the turbulent variations are uncorrelated between the turbines, the low-frequency power was multiplied by N while the variations due to turbulence were multiplied by $\sqrt{N}$. Thus the total power P is given by $NP_{T2} + \sqrt{N}(P_{T1} - P_{T2})$. A second setup was also used for final simulations, to illustrate how wake effects can be accounted for. This means that each wind turbine sees a different wind speed, and therefore its frequency response capability will be different – there is generally more potential to respond when the wind speed is higher. In this case a 9-turbine wind farm was simulated, as shown in *Figure 3-1*.
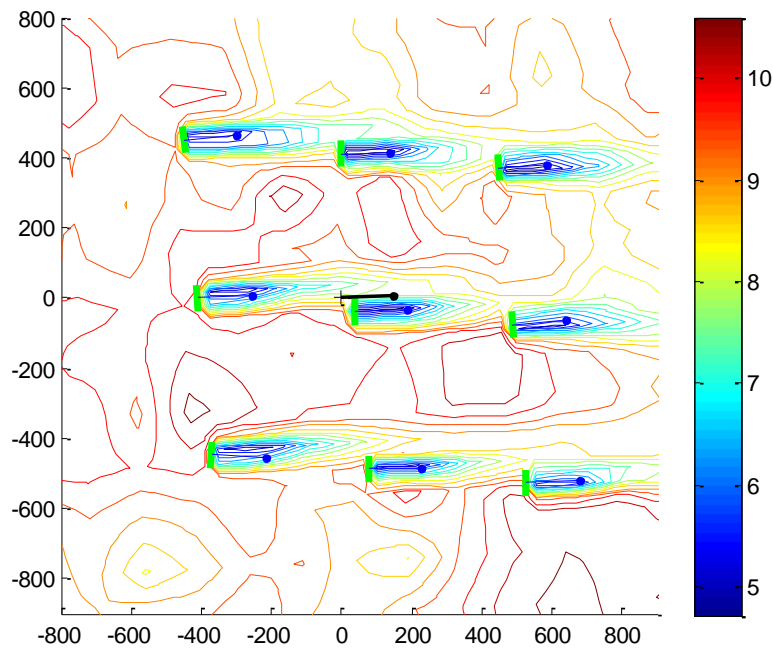
Figure 3-1: *Example wind farm layout, showing wake effects*

By again simulating turbines with and without added turbulence, the power output was scaled up to represent the system wind power production. A scaling factor of 266 (corresponding to 2394 turbines) was used to give the correct total power at a chosen point in time. Note that this requires more turbines in total than before, because of the wake losses. It would be difficult to match the output exactly over a period of time, because the wake losses vary with wind direction and depend on the layout of individual wind farms. However, the simulation result confirms that the precise modelling of these effects is not critical for the conclusions of the study.

For this case, a stochastic spatial wind field is generated from the wind speed data obtained as in Section 3.1.2. Ideally, some real wind farm layouts would be used together with real wind direction data for the period in question. However, as the simulation is only intended for illustrative purposes, some realistic but fictitious wind direction variations were used.

Figure 3-2 shows a typical power output from a single turbine, while *Figure 3-3* shows the power output scaled up as explained above, either from a single turbine (red line) or from the 9-turbine wind farm (black line), scaled to give a similar total power around 150s. Note how the power variations are much reduced in the scaled power. In the wind farm case, the initial 100s of the simulation should be ignored – the higher power level is due to the time taken for the wakes generated at the start of the simulation to advect to the downstream turbines. The remaining power variations due to wake effects would probably be further reduced by modelling more wind farms with different layouts, with wind direction variations appropriate to the location of each farm. The small sharp spike around 130s, which is an example response to a frequency event (as described in Section 3.1.4), remains similar in both cases, suggesting that at least for initial tuning of the frequency response, wind farm effects can probably be ignored.
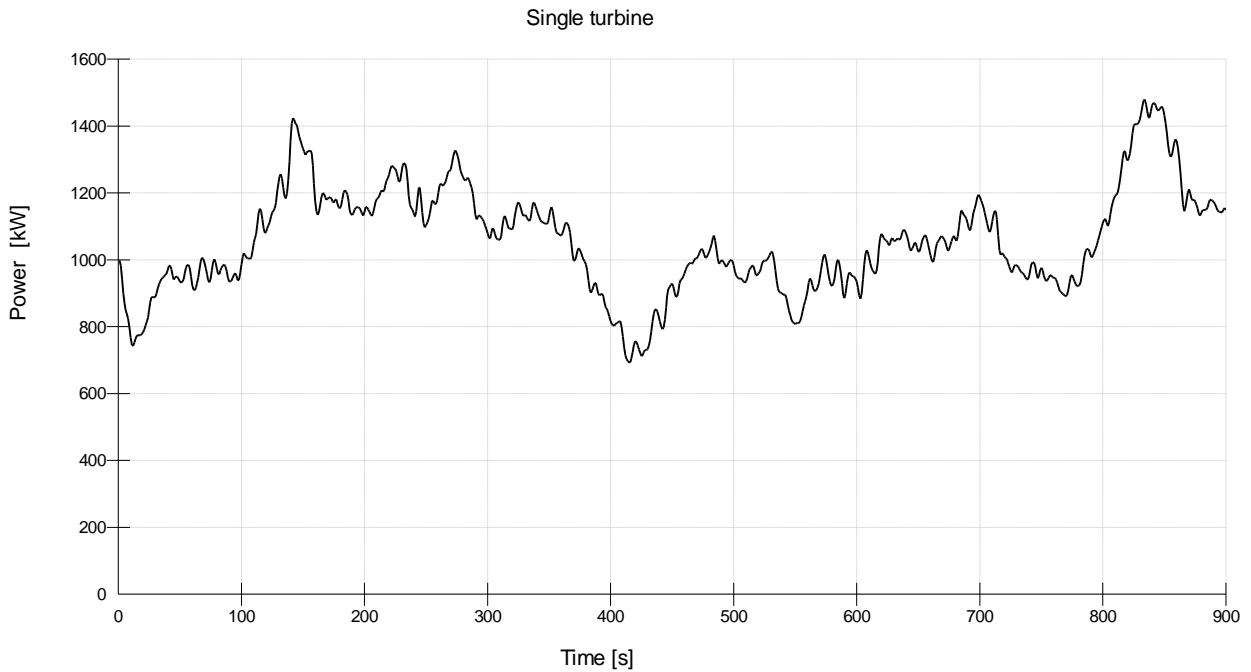
Figure 3-2: *Example of power output of a single turbine*
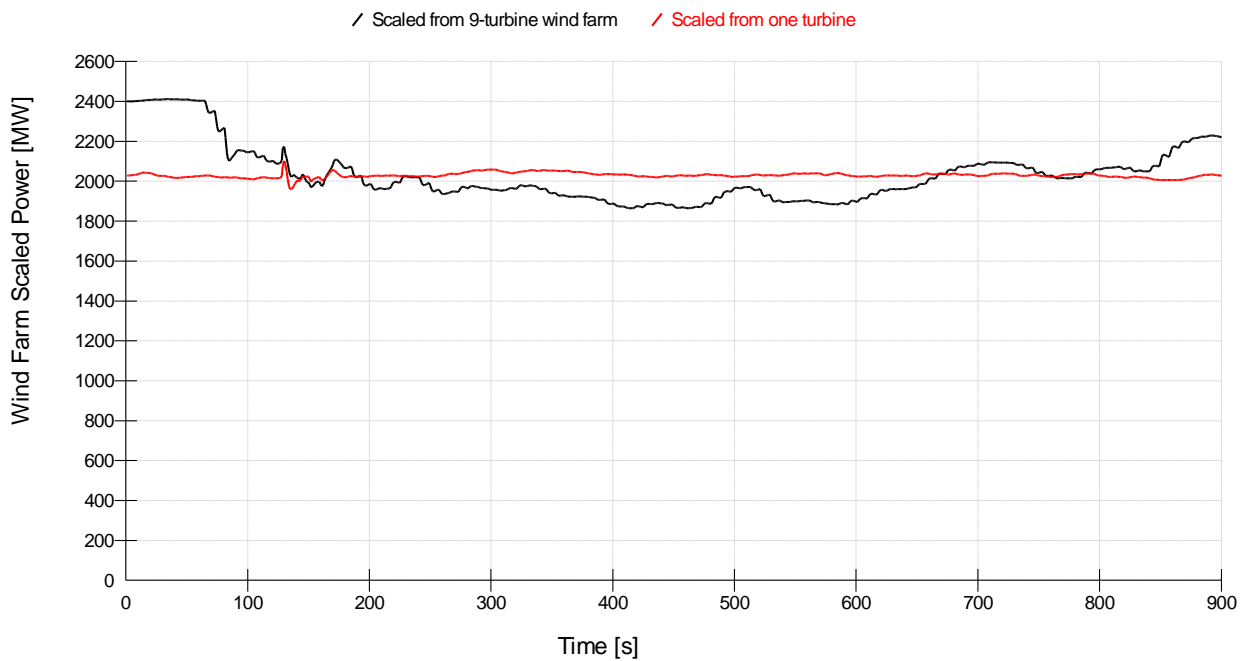
Figure 3-3: *Total power output scaled up from a single turbine (red) or from the 9-turbine wind farm (black)*

3.1.4   FREQUENCY RESPONSE STRATEGIES IMPLEMENTED IN LONGSIM

The turbine controllers implemented in LongSim already included a fast frequency response algorithm, which included three different ways in which a change in power output can be calculated as a function of the grid frequency:

Droop control

Droop control is a proportional action, where the power is changed according to the frequency deviation, beyond a certain deadband. This is similar to primary control (FCR) described in section 3.2.5, but the LongSim implementation can be specified in a more general way as a lookup table of power change versus frequency deviation.

Synthetic inertia

For synthetic inertial response, the change in power is proportional to the rate of change of frequency (RoCoF). An arbitrary value can be selected for the proportionality constant. The constant can be interpreted as the speed of a directly-connected synchronous generator, such that the emulated inertial response is the same as that of the synchronous generator with the same inertia as the turbine rotor (the response is actually slightly different because of measurement and control loop delays, including filtering and a small dead band on the RoCoF).

Boost

The boost is a pre-determined increase in power maintained for a pre-determined length of time following the detection of a frequency drop below some threshold value.

Other strategies

These three strategies are independent and can be used individually or in combination. Other strategies could easily be tried, such as a PI controller responding to grid frequency, which would be similar to a combination of inertia and droop control.

Other parameter settings

If a power increase is provided below rated, the extra energy must be provided by extracting rotor kinetic energy, slowing the rotor. For all strategies, additional parameter settings are used to limit the overall allowable increase in power at any time, including a further limit when the rotor speed is low, to prevent the tip speed ratio falling to a level where there is a risk of aerodynamic stall (which would cause the turbine to shut down). If kinetic energy has been extracted, a subsequent recovery phase is needed so that the rotor speed can return to normal. Further parameters are used to implement a delay to the recovery, if possible, and to control the smoothness and duration of the recovery. Further details can be found in [16].

3.2 GRID SIMULATION WITH KERMIT

3.2.1 BRIEF INTRODUCTION TO FREQUENCY CONTROL

To maintain system frequency within the defined limits, system operators must constantly balance between active power produced and consumed. By definition, this requires that they are able to ensure a very quick, or even instantaneous, response to any frequency deviations. To do so, system operators have to rely on resources, which thus cannot be (fully) used for the scheduled supply of active power in case of generators. Due to the limited availability of such resources, and the (opportunity) costs of not being able to use them for the scheduled supply of active energy, system operators typically try to replace frequency control (primary, secondary) by other types of (operating) reserves. In principle, frequency control (primary, secondary) and operating reserves thus serve different purposes as illustrated by Figure 3-4, based on the conventions applied in Europe:

- Primary reserves serve to arrest any frequency deviations by a fast increase or decrease of active power supply or demand.
- Secondary reserves are aimed to restore system frequency to its target level and release primary reserves employed within a defined period, often using a mix of automatic and/or manual activation of different resources.
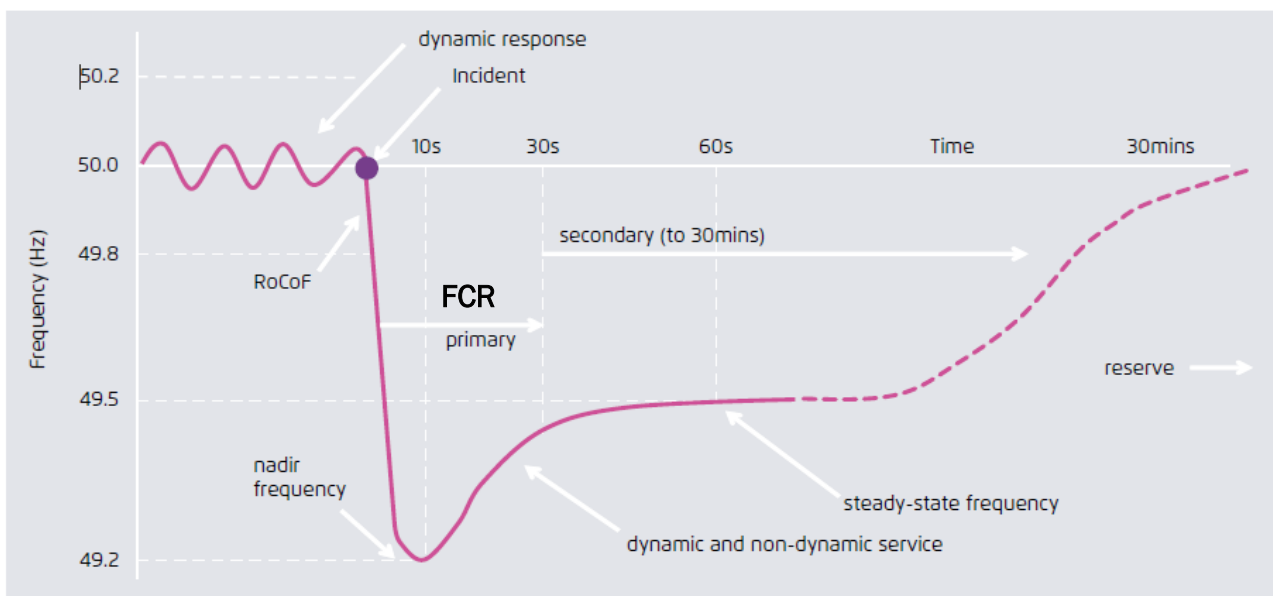
Figure 3-4: *Typical frequency response behaviour in the event of a loss of generation*

Source: p22, https://www.agora-energiewende.de/fileadmin2/Projekte/2018/Japan_Grid/148_Agora_Japan_grid_study_WEB.pdf

Whilst the different types of load frequency control thus serve slightly different purposes, they are all essentially driven by four different types of system imbalances:

- Sudden disturbances, such as a loss of generation, load or HVDC links with other interconnections,
- Continuous, stochastic variations of load and/or generation, such as load noise or the minute-by-minute variability of wind or solar power,
- Forecast errors of load or generation (e.g. wind, solar or run-of-river hydro power),

- Any deterministic deviations caused by market imperfections.

The first three drivers reflect fundamental features of any power system, i.e. their relative role and impact depends on the size and structure of the system.
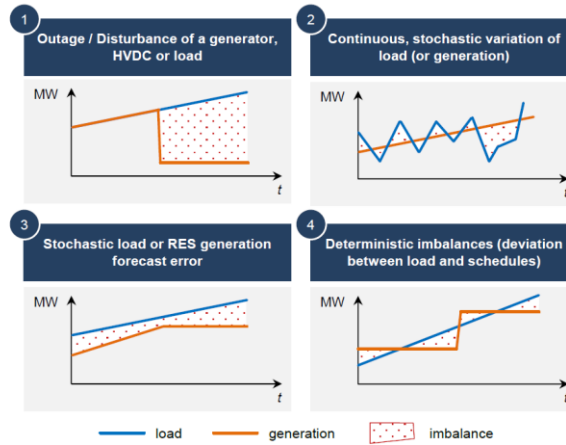
Figure 3-5: *Potential drivers of system imbalances*

Source: ENTSO-E. Supporting Document for the Network Code on Load-Frequency Control and Reserves. Brussels. 28.06.2013, p. 56

As mentioned, corresponding imbalances may principally occur during the entire timeframe of load frequency control. But as indicated by *Table 3-1*, not all factors are equally important for different reserves. For instance, continuous variations and deterministic imbalances are of a temporary nature and are thus mainly relevant for primary and secondary control. Conversely, forecast errors are of a more persistent nature and are thus hardly relevant for primary control but must be addressed by secondary and tertiary control.

Table 3-1: *Relation between types of system deviations and frequency control reserves*

Reserve	Disturbances	Continuous variations	Forecast errors	Deterministic imbalances
Primary reserves	⯑	⯑		(⯑)
Secondary reserves	⯑	⯑	⯑	⯑
Tertiary reserves	⯑		⯑	

Source: DNV GL

3.2.2 SIMULATION ENVIRONMENT FOR GRID SIMULATION

KERMIT (KEMA Equilibrium Renewable Integration Tool) is a proprietary DNV GL tool that is used to simulate the frequency behaviour of a (future) power system and its interconnections, inertia and the operation of primary and secondary regulation. KERMIT was originally designed to study the impact of variable non-dispatchable resources on electric power systems, yet it is finding a variety of new applications with grid operators, ranging from assessment of long-term expansion plans to installation as a control room tool.

KERMIT allows analysis of dynamic grid performance in future scenarios or during events such as generator trips, sudden load rejection, and variable renewable resource (wind, solar) ramping events. The software runs on the MATLAB/Simulink platform and incorporates inertial, governor and regulation response, balancing market logic and control of new technologies such as energy storage. Model inputs include data on power plants, wind and solar production, daily load profile and generation and interchange schedules. The outputs include power plant generated power, area interchange and frequency deviation, real-time dispatch requirements, and numerous other dynamic variables on a second-by-second time scale.

KERMIT also provides the unique capability to model Automatic Generation Control (AGC) and system inertia on a continuous basis over an extended period of time, taking into account not only the performance of resources but also the state of other potentially interconnected systems. It is well suited to investigate how variable energy resources (VER) and energy storage systems (ESS) technology integration affects operational performance.

In Figure 3-6 an illustration of the different inputs & outputs of the KERMIT model is provided.
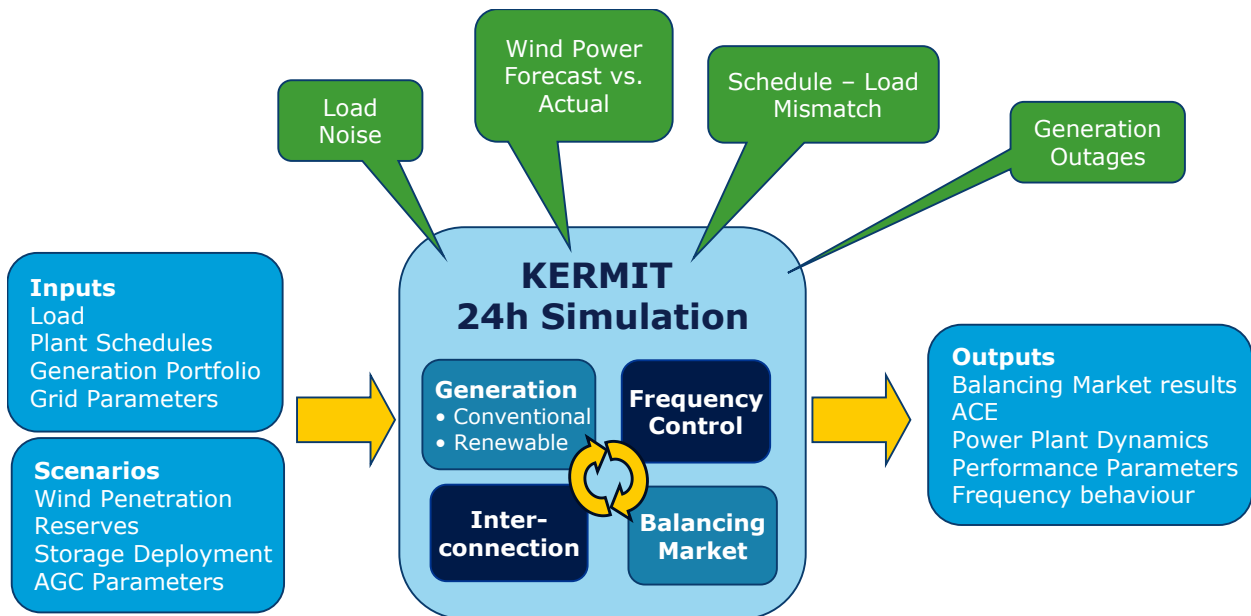
Figure 3-6: *KERMIT model structure.*

Source: DNV GL

The KERMIT implementation of primary control, secondary control, inertia, self-regulating load and plant response will be described in sections 3.2.3 - 3.2.6.

3.2.3 INERTIA

An increasing penetration of VER leads to decreased system inertia, and thus potential issues for system frequency stability. This phenomenon relates to the lack of synchronous connected rotating energy of VER technology, resulting in less-damped frequency behaviour. In systems dominated by conventional units, any frequency deviations lead to a change of the speed of every synchronous generator connected to the grid. The kinetic energy available in the rotating inertia of

these units provides useful support during supply and demand mismatches. If the system inertia is decreased, system imbalances result in larger frequency deviations, as inertia is directly related to the rate of change of frequency (RoCoF). Therefore, also the frequency nadir can be negatively affected. The frequency nadir is defined is defined as the minimum value of frequency reached during a transient period. An example is visualised in *Figure 3-4.*

To evaluate the frequency nadir value in cases of loss of generation, we will make use of KERMIT. The effect of system inertia is included in KERMIT as part of the interconnected system model. In KERMIT the rate of change of frequency versus accelerating power model is obtained by deriving the kinetic energy model (function of the inertia constant H and the frequency deviation Δf) to obtain a time function for the kinetic energy of the system. Based on the assumption that the angular velocity does not deviate much from its nominal value, it is then possible to link the accelerating power to frequency [9]. This allows KERMIT to model the impact on frequency by changes in the system inertia and assess the impact of for example (high) VER penetration and addition of interconnections.

3.2.4 FREQUENCY MODELLING

KERMIT is designed for Control Area analyses where all the generators in a Control Area are connected to a common electrical area. The approach is to define a composite kinetic energy as the sum of the individual kinetic energies, based on the assumption that the set of generators in a Control Area "swing" together at the same Control Area common frequency [9].

3.2.5 PRIMARY CONTROL

The response of primary control upon frequency deviations is an important characteristic for the KERMIT model. It has a large impact on frequency deviations. In KERMIT, the requirements for primary control are currently covered in a deadband and droop setting.

The amount of allocated primary reserve is dependent of the disturbance size and the droop value. In continental Europe the maximum amount of primary control (100%) is typically allocated at a -200 mHz frequency disturbance. The primary control droop setting is calculated according to the following formula in KERMIT:

$$\frac{\Delta P}{P_{nom}} = \frac{100}{x} \frac{\Delta f}{f_{nom}}$$

where:

$\Delta f = $ frequency deviation $[Hz]$
$f_{nom} = $ Nominal frequency $[Hz]$
$x = $ droop setting $[\%]$
$\Delta P = $ Power deviation $[Hz]$
$P_{nom} = $ Nominal power of a unit $[MW]$

Based on the frequency and the droop setting, the volume of required primary power per unit can be determined. The delivery of primary power by a unit is modelled in KERMIT as a first order model to reflect typical grid code requirements for the delivery of primary power, however more complex governor models are also available within KERMIT. The time constant of the first order model can

be changed based on required time for full activation by a unit. In example, when a time constant of 5 seconds is applied as primary control will be delivered within 30 seconds as visualised in *Figure 3-7*. Changing the droop setting for primary activation or the time constant for delivery of primary response will have an impact on the frequency nadir and the steady-state frequency value (*Figure 3-4*).
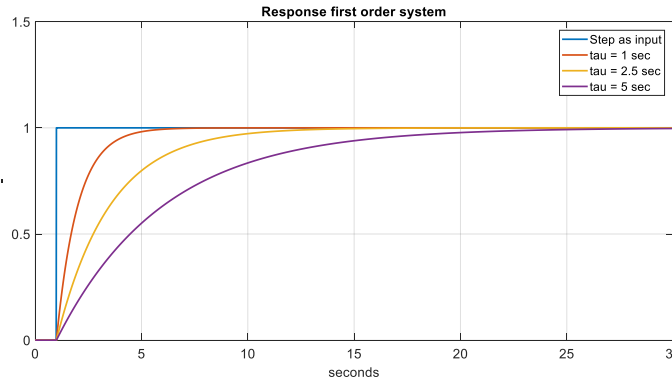
Figure 3-7: *Generic relation between time constants and speed of Primary frequency response*

Source: DNV GL

3.2.6   SECONDARY CONTROL USING AUTOMATIC GENERATION CONTROL (AGC)

The AGC controller structure implementation in KERMIT is illustrated in Figure 3-8.
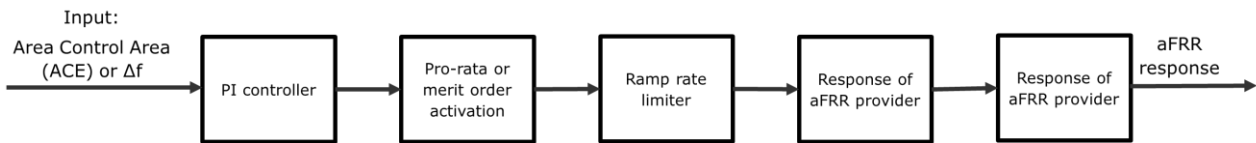
Figure 3-8: *aFRR control scheme*

Source: https://docstore.entsoe.eu/Documents/MC%20documents/balancing_ancillary/160229_Report_aFRR_study_merit_order_and_harmonising_FAT_%28vs_1.2%29.pdf

As illustrated in *Figure 3-8* the PI controller output in KERMIT is converted to an AGC signal on unit level, on a merit order or pro-rata base. In *Figure 3-9* the difference in Pro-rata and Merit order activation is explained, together with effect on the resulting ramp rate.
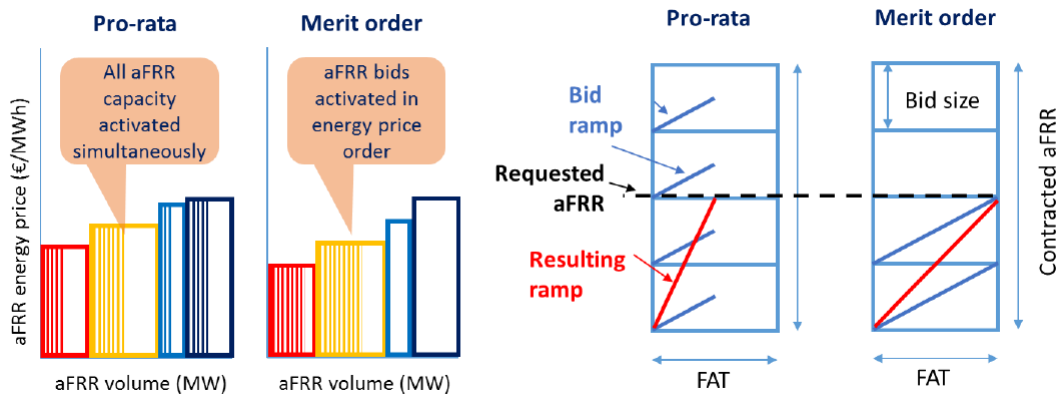
Figure 3-9: *Pro-rata versus merit order aFRR activation*

Source: https://docstore.entsoe.eu/Documents/MC%20documents/balancing_ancillary/160229_Report_aFRR_study_merit_order_and_harmonising_FAT_%28vs_1.2%29.pdf

In *Figure 3-8* also the response of the aFRR provider is visualised, which is modelled in KERMIT using a configurable delay [sec] and ramp rate [MW/min]. Settings can be chosen according to the specific unit configuration or based on the requirements specified by the system operator. An example of the aFRR response of the aFRR provider is illustrated in *Figure 3-10*.
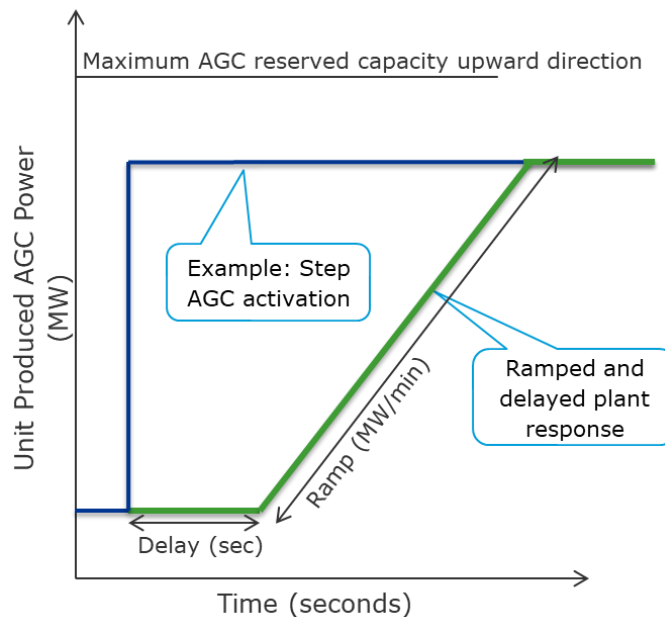
Figure 3-10: *Generic relation between AGC activation and AGC plant response*

Source: DNV GL

3.2.7 CONFIGURATION AND CALIBRATION OF KERMIT MODEL

By combining the DNV GL dynamic wind farm model (LongSim) and the DNV GL developed grid model (KERMIT), it possible to evaluate the effect of different control strategies implemented in the turbine or wind farm controllers on the grid frequency. The control actions may vary from turbine to turbine owing to local variations in wind conditions, including wind turbine wake effects.

Section 3.1.4 describes the different wind turbine controller strategies have been implemented in LongSim.

As defined in [15] a controller which emulates the inertial response of a synchronously-connected generator can be included in a non-synchronously-connected production unit. Inertial response produced by such a controller is often referred to as a synthetic, emulated, artificial, or virtual inertial response. In general the possible effect of additional virtual inertia is illustrated in *Figure 3-11*. Depending on the controller strategy the improvement in frequency nadir will change. The quasi steady state behaviour is not affected, as the FFR power is only maintained for a short period of time.
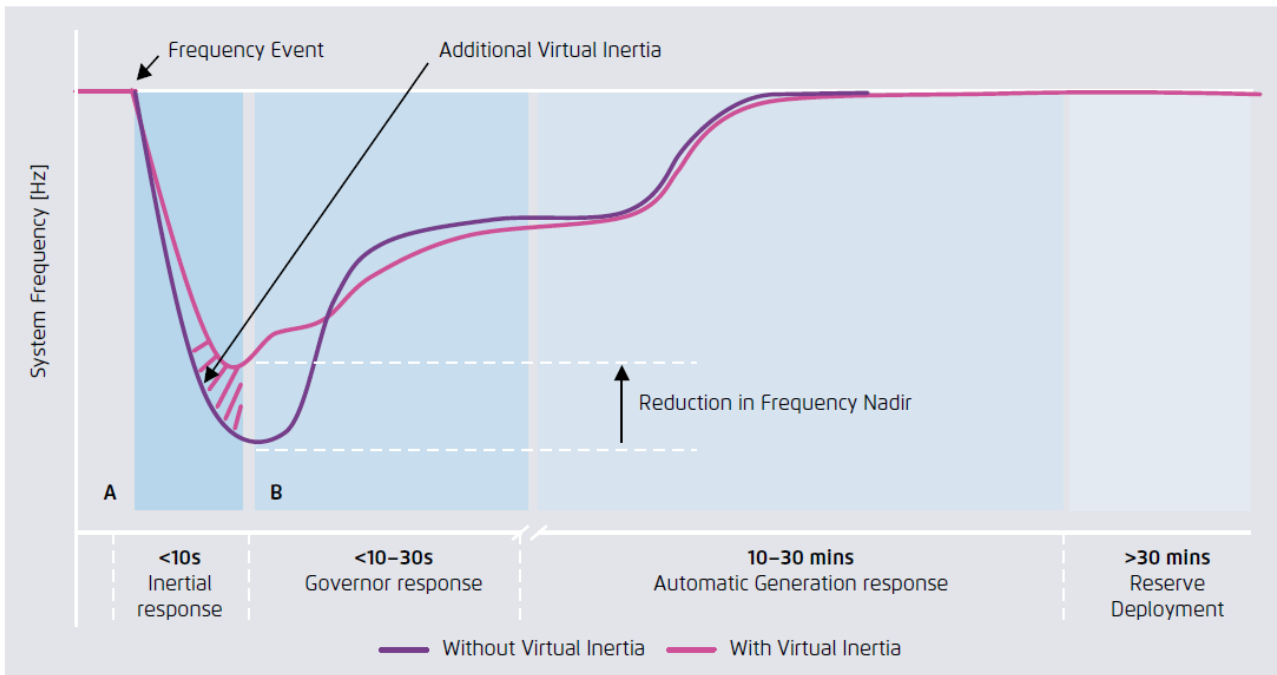
Figure 3-11: Virtual inertia response time frame

Source: p99, https://www.agora-energiewende.de/fileadmin2/Projekte/2018/Japan_Grid/148_Agora_Japan_grid_study_WEB.pdf

To simulate the effect of the different wind turbine controller strategies using LongSim, historical frequency events as well as "normal operation" for the Irish grid are modelled in KERMIT. The Irish grid was chosen as it has a relatively high share of wind power and it is a relatively small grid. Ireland and Northern Ireland have a target of 40% of their electricity produced by renewable sources by 2020, in 2018 a peak all-island wind generation output of 3,990 MW was achieved on 12 December [12]. Additionally, there is public wind, load, synchronous generation (15-min sample time) and frequency data (5-sec sample time) available that can be used to calibrate and validate the modelled grid in KERMIT.

3.2.8   GRID SIMULATION IRELAND (INCLUDING NORTHERN IRELAND)

In *Figure 3-12* an overview of the Irish grid is provided, showing two HVDC connections to England. No AC interconnections are currently present. Therefore, the Irish grid was modelled as one synchronous area with two HVDC interconnections to the UK.

In terms of operating reserve categories, Ireland has defined different categories as indicated in *TABLE 3-2*. In Ireland no automatic secondary control using an AGC is used, instead for secondary

control (SOR) droop settings are used as illustrated in *Figure 3-13* [14]. In case both POR and SOR are delivered on one unit, the different products are differentiated in terms of delivery time as indicated in *Table 3-2*.
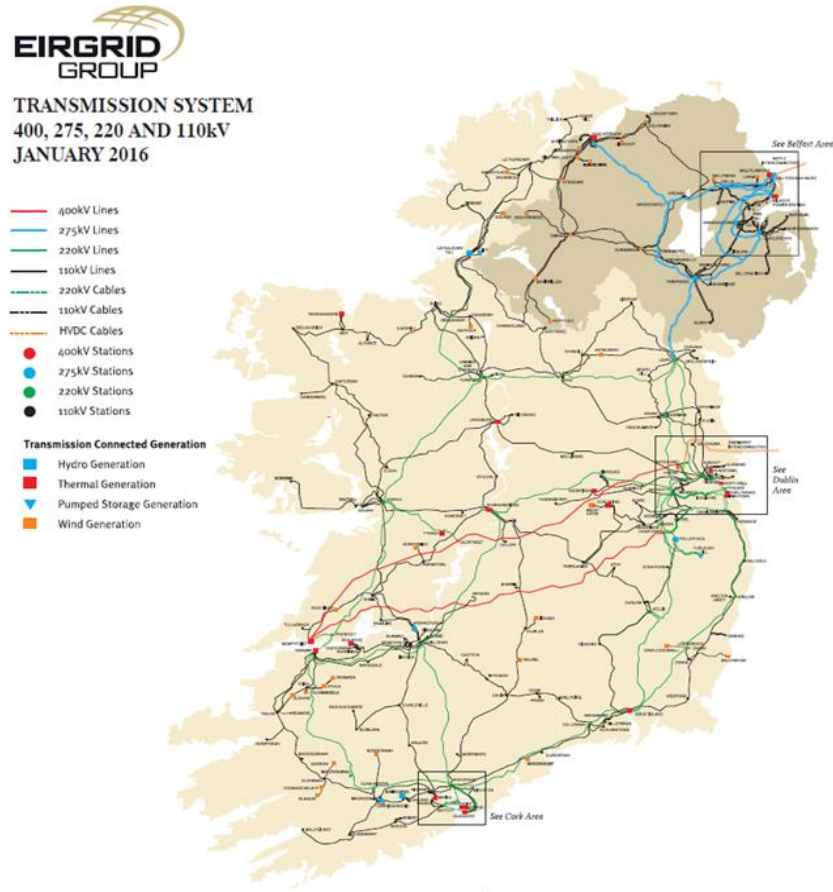
Figure 3-12: *Irish grid*

Source: p12, http://www.eirgridgroup.com/site-files/library/EirGrid/DS3-System-Services-Protocol-Regulated-Arrangements_final.pdf

Table 3-2: *Operating Reserve categories*

Category	Delivered By	Maintained Until
Primary (POR)	5 seconds	15 seconds
Secondary (SOR)	15 seconds	90 seconds
Tertiary 1 (TOR1)	90 seconds	5 minutes
Tertiary 2 (TOR2)	5 minutes	20 minutes

Source: Eirgrid, Soni - Operational Constraints Update 29/03/2019
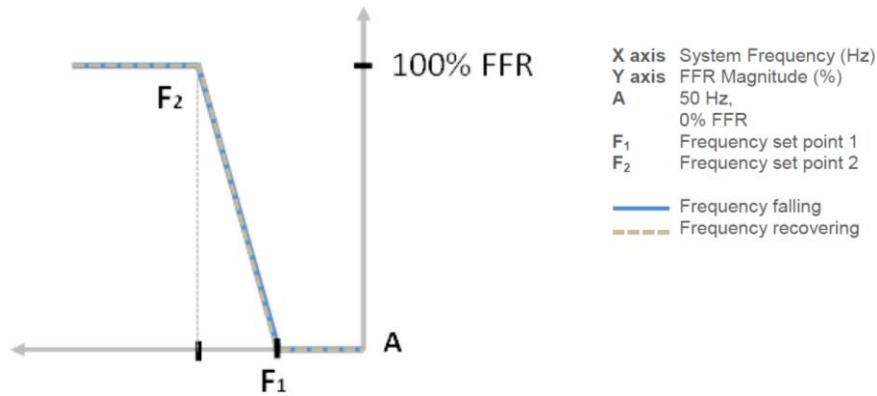
Figure 3-13: *FFR Dynamic Capability Frequency Response Curve*

Source: p12, http://www.eirgridgroup.com/site-files/library/EirGrid/DS3-System-Services-Protocol-Regulated-Arrangements_final.pdf

Based on the response curve visualised in Figure 3-13 the deadband was implemented in the KERMIT grid model. We have assumed that the primary power will also be delivered outside the range of 200 mHz as illustrated in Figure 3-14. Reason for this assumption is that no public information was found on the unit settings and in Ireland controls are implemented outside the range of 200 mHz.
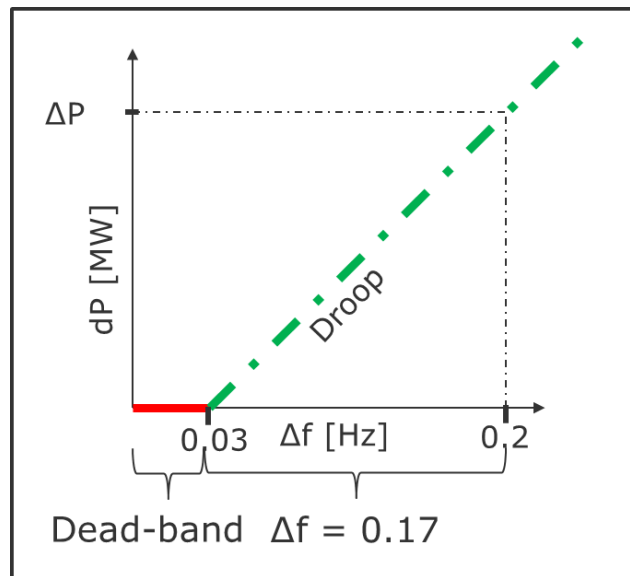
Figure 3-14: *Relation between deadband for primary control and droop configuration*

Source: DNV GL

3.2.9 MODEL ASSUMPTIONS IRISH GRID

KERMIT can be calibrated against system historical performance both in terms of routine daily operations (e.g. ACE and frequency statistics) as well as against events such as unit outages. Once calibrated, the inputs to KERMIT (load and renewable production time series and unit schedules) can be adjusted to reflect future scenarios with high Distributed Energy Resources (DER) penetration, high wind penetration, use of new resources such as storage, synthetic inertial response, and so on, to enable studies of system performance and new control and dispatch schemes.

3.2.9.1 KERMIT CALIBRATION DURING HISTORICAL FREQUENCY EVENTS

The historical frequency data (5 sec sample time) of the Irish grid was retrieved from the SMART grid dashboard [10]. This full day frequency data was retrieved for three of the four Frequency Excursion Incidents that are reported in the in the Transmission System Performance Report 2018 [7]. A summary of three Frequency Excursion incidents in 2018 is provided in *Table 3-3*.

The Dublin Bay Frequency Excursion incident is also described in the Transmission System Performance Report 2018 [7], however this event was not evaluated using the KERMIT model as the historical data could not be retrieved in the SMART grid dashboard [10] for this event.

Table 3-3: Summary of the Frequency Excursion incident [7]

Cause of Incident	Date	Time	MW Lost	Nadir (Hz)	Maximum Rate of Change of Frequency (Hz/s)
Tynagh TYC	15/06/2018	21:14:11	377	49.596	-0.14
Aghada AD2	12/07/2018	00:39:18	342	49.561	-0.20
Whitegate WG1	22/12/2018	06:53:40	316	49.565	-0.29

Definitions used in Table 3-3 [7]:

- Time = Considered to be when the frequency falls through 49.8 Hz.
- Nadir = Minimum system frequency from t 0 to t + 6 minutes.
- Maximum Rate of Change of Frequency = Maximum rate of change of frequency calculated over 500 ms during the period t – 5 seconds to t + 30 seconds.

The frequency events from the Transmission System Performance Report 2018 [7] are illustrated in *Figure 3-15* to *Figure 3-17* below. These visual representations contain more detailed information (i.e. second sample time) compared to the data downloaded from the SMART grid dashboard [10]. The downloaded 5-sec data was sub-sampled to 1-sec data and manually updated based on the visual representations in *Figure 3-15* to *Figure 3-17*.
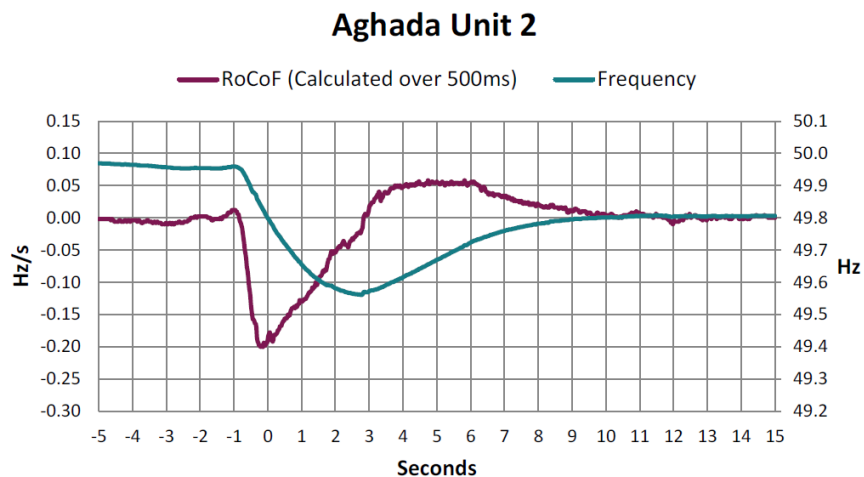
Figure 3-15: Aghada Unit 2 Frequency Excursion Incident (12/07/2018)

Source: Eirgrid & Soni - All-Island Transmission System Performance Report 2018 [7]
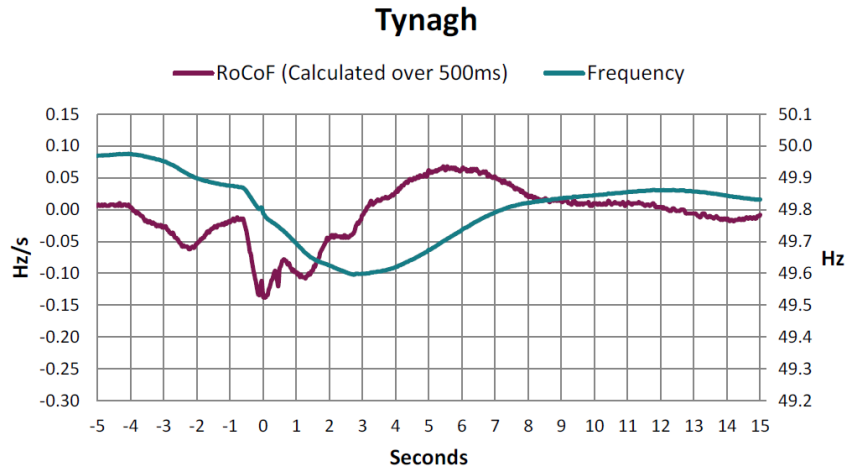
Tynagh

Figure 3-16: *Tynagh Frequency Excursion Incident (15/06/2018)*

Source: Eirgrid & Soni - All-Island Transmission System Performance Report 2018 [7]
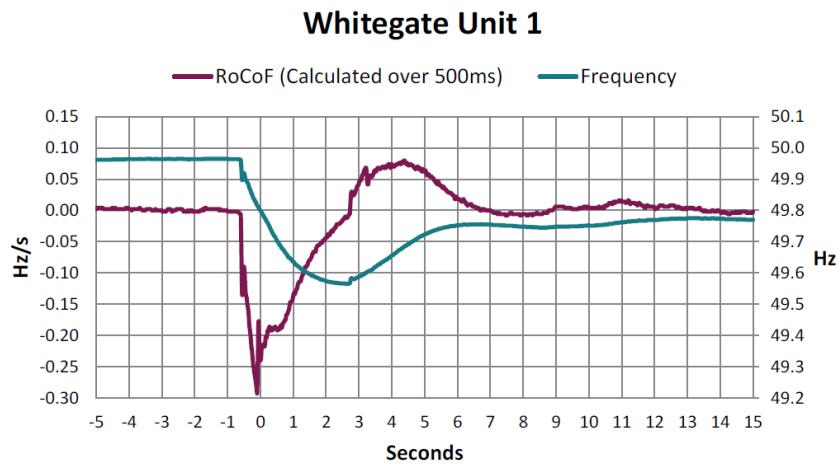
Whitegate Unit 1

Figure 3-17: *Whitegate Unit 1 Frequency Excursion Incident (22/12/2018)*

Source: Eirgrid & Soni - All-Island Transmission System Performance Report 2018 [7]

3.2.9.1.1 POWER BALANCE IN KERMIT DURING THE HISTORIC TRIPS

In order to set up the KERMIT model and be able to simulate the frequency behaviour using the different ancillary services according to the actual frequency measurements described in the previous section, the power balance must be defined in KERMIT. For the integrated KERMIT/ LongSim grid a power balance was chosen driven by the availability of public data. The power balance used for the Irish grid model is provided in *Figure 3-18*. The different parts in the power balance will be briefly described in this section.

Primary & Secondary control

As defined in *Table 3-2* primary and secondary control are defined as "droop" setting in the Irish grid. The operating reserve for POR and SOR equal to 75% of the largest in-feed. Minimum reserve of 135 MW (Ireland) + 49 MW (Northern Ireland) [13]. No detailed settings for deadband and droop (*Figure 3-14*) on unit level could be found, therefore the deadband and droop settings are chosen during the calibration of the model against the historic frequency events.
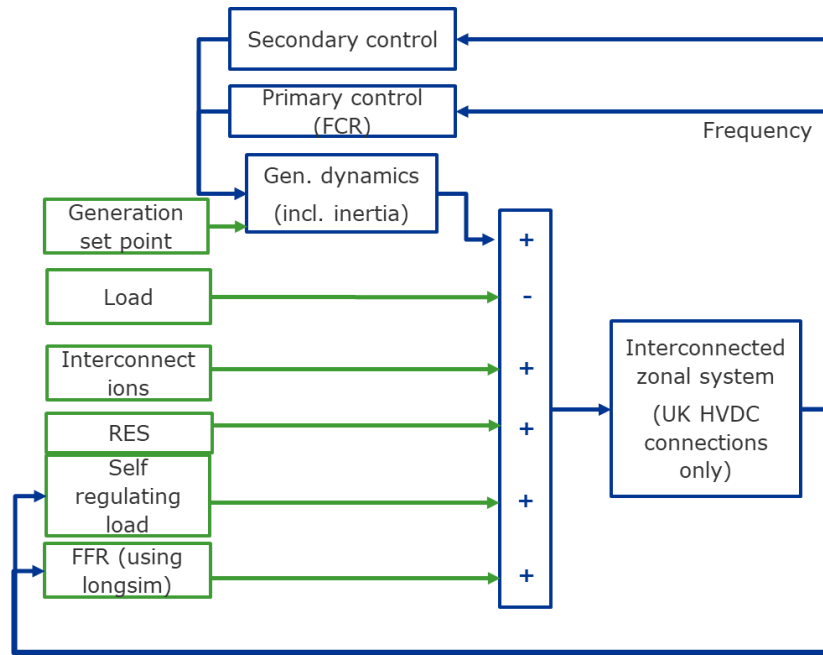
Figure 3-18: *KERMIT power balance*

Source: DNV GL

Synchronous Generator dynamics

Although more detailed generator models are present in KERMIT, it was decided to simplify the generator dynamics to a first order model response with a configurable time constant, which is set differently depending on the type of generator. The total synchronous generation during the days of the frequency excursion incidents is illustrated in *Figure 3-19*. The data is available with a sampling time of 15 minutes and in the KERMIT simulation this is used as dispatch schedule in KERMIT.
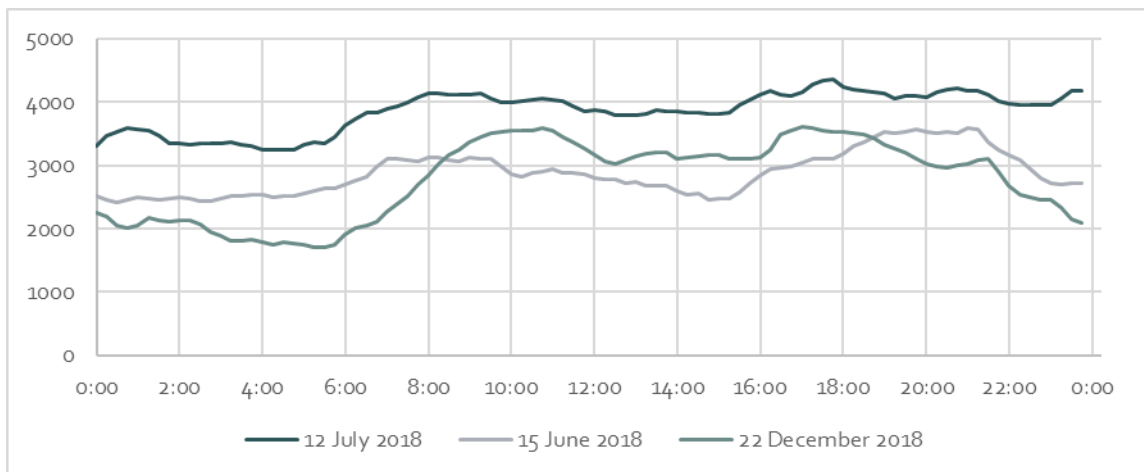
Figure 3-19: *Synchronous generation during the frequency excursion incidents (day of data)*

Source: data downloaded from web portal [10] and from spreadsheet [11]

Inertia

The effect of system inertia is included in KERMIT is described as section 3.2.3. The all-island installed capacity of conventional generation in 2018 was 8,548 MW and the minimum all-island inertia of 23 000 MWs [12]. Based on an assumed inertia constant and installed capacity connected to the grid, the inertia was calibrated according the frequency response after a trip during the frequency events.

Self-regulating load

During the simulations, the frequency dependent load is assumed to be 4%/Hz.

Demand

In 2018 the all-island peak demand reached 6,508 MW and the minimum all-island demand was 2,520 MW [13]. The total synchronous generation during the days of the frequency excursion incidents is illustrated in *Figure 3-20*. The data is available with a sampling time of 15 minutes and in the KERMIT simulation is interpolated between the samples.
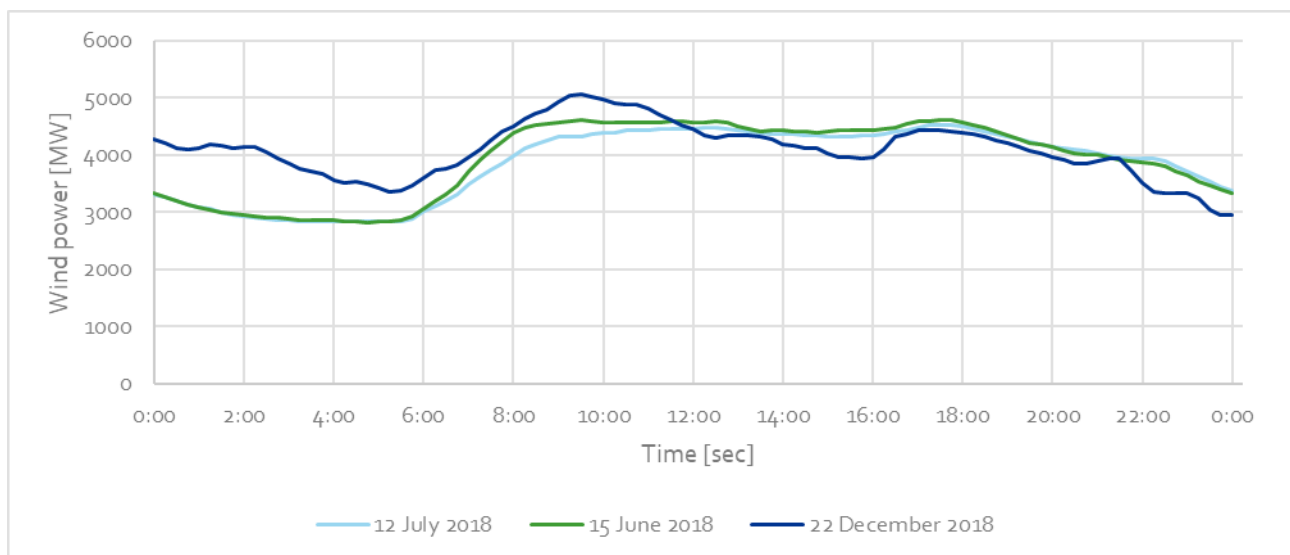
Figure 3-20: *Demand during the frequency excursion incidents (day of data)*
Source: data downloaded from web portal [10] and from spreadsheet [11]

HVDC interconnections

The total power of the two HVDC interconnections (East-West interconnector and the Moyle interconnector) is illustrated in *Figure 3-21* for the days of the frequency excursion incidents. The data is available with a sampling time of 15 minutes and in the KERMIT simulation is interpolated between the samples.
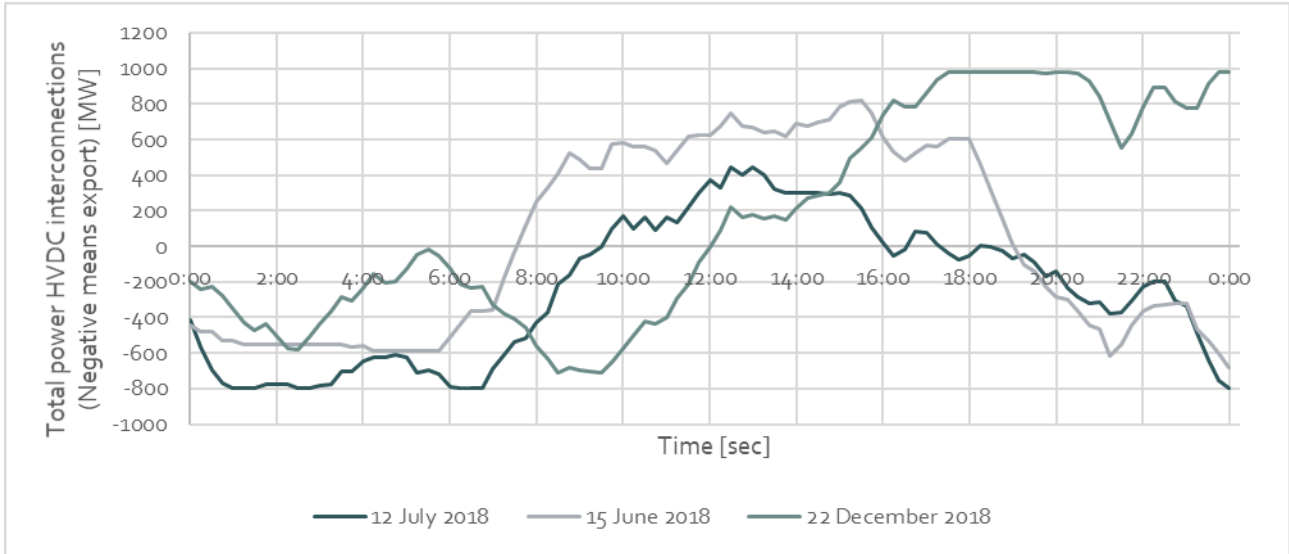
Figure 3-21: Power HVDC connections during the frequency excursion incidents (day of data)
Source: data downloaded from web portal [10] and from spreadsheet [11]

RES - Wind data

Maximum Wind Generation was 3,297 MW in 2017 and 3,990 MW in 2018 [12]. For the calibration events in *Figure 3-22 - Figure 3-24* the wind data is provided. This includes the forecasted and curtailed data. The data is available with a sampling time of 15 minutes and in the KERMIT simulation the "Total Ireland Wind Generation" data is used to simulate the wind generation. Without using LongSim the data is interpolated between the samples, when LongSim is used these wind schedules have been used to determine the windspeeds.
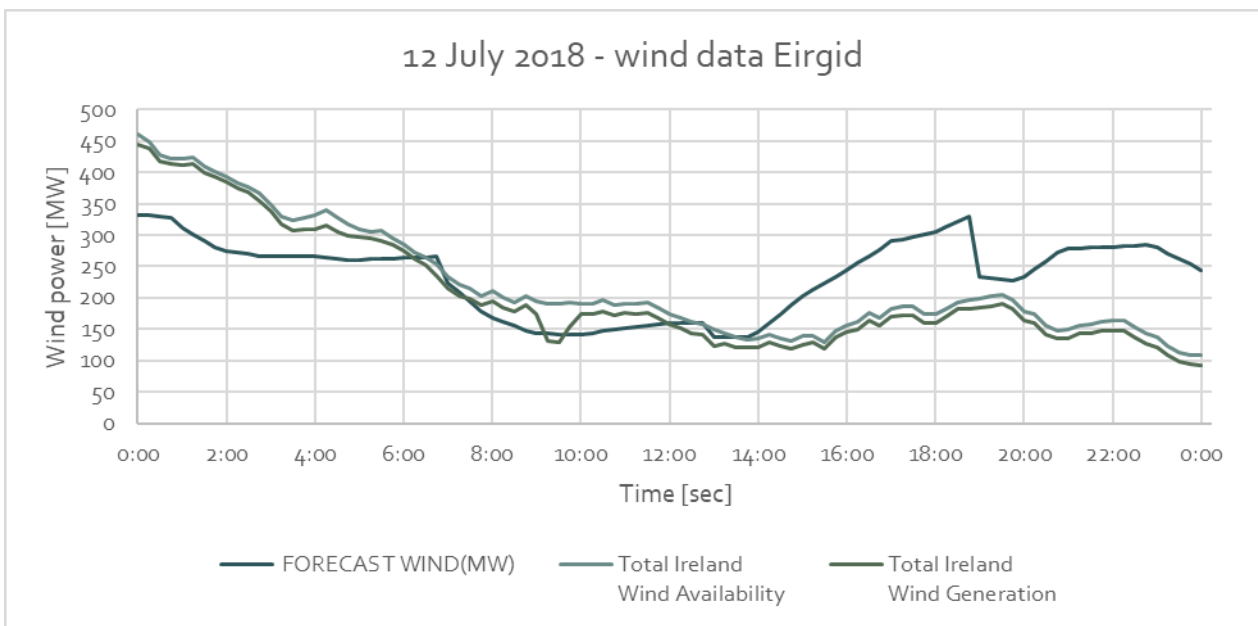
Figure 3-22: 12 July (event 2) wind data Eirgrid
Source: data downloaded from web portal [10] and from spreadsheet [11]
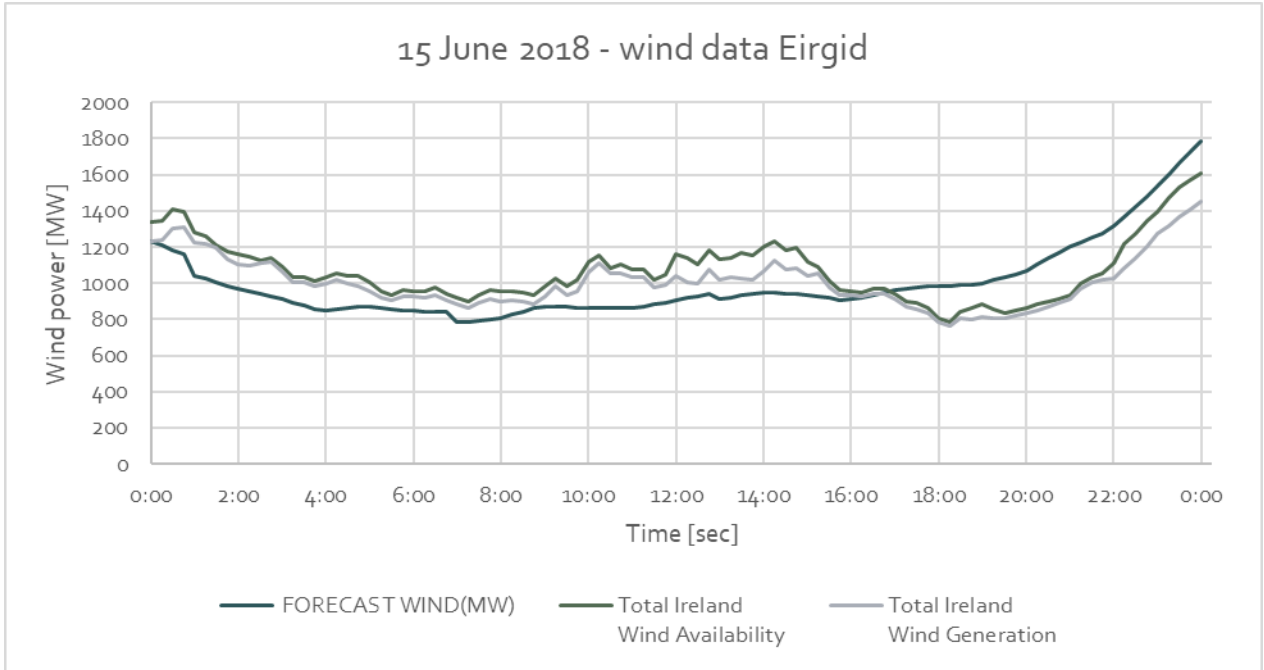
Figure 3-23: *15 June (event 1) wind data Eirgrid*
Source: data downloaded from web portal [10] and from spreadsheet [11]
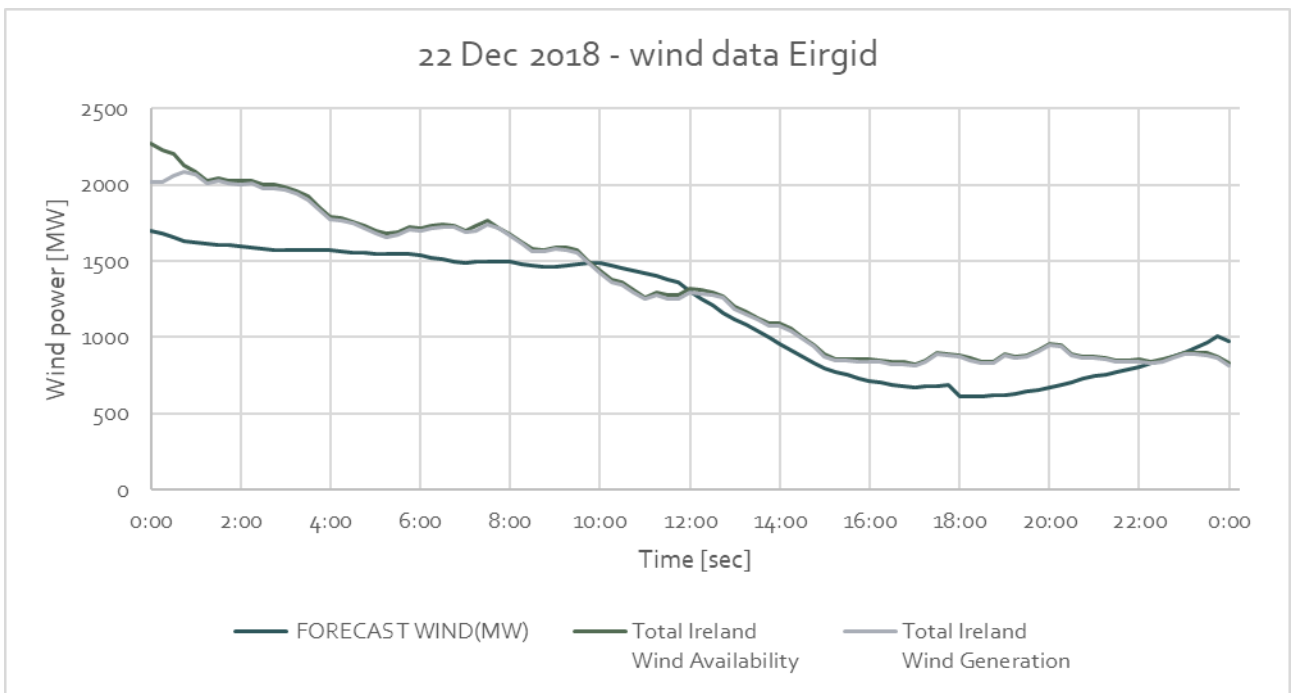
Figure 3-24: *22 December (event 3) wind data Eirgrid*
Source: data downloaded from web portal [10] and from spreadsheet [11]

The determined wind speed is illustrated in *Figure 3-25*.
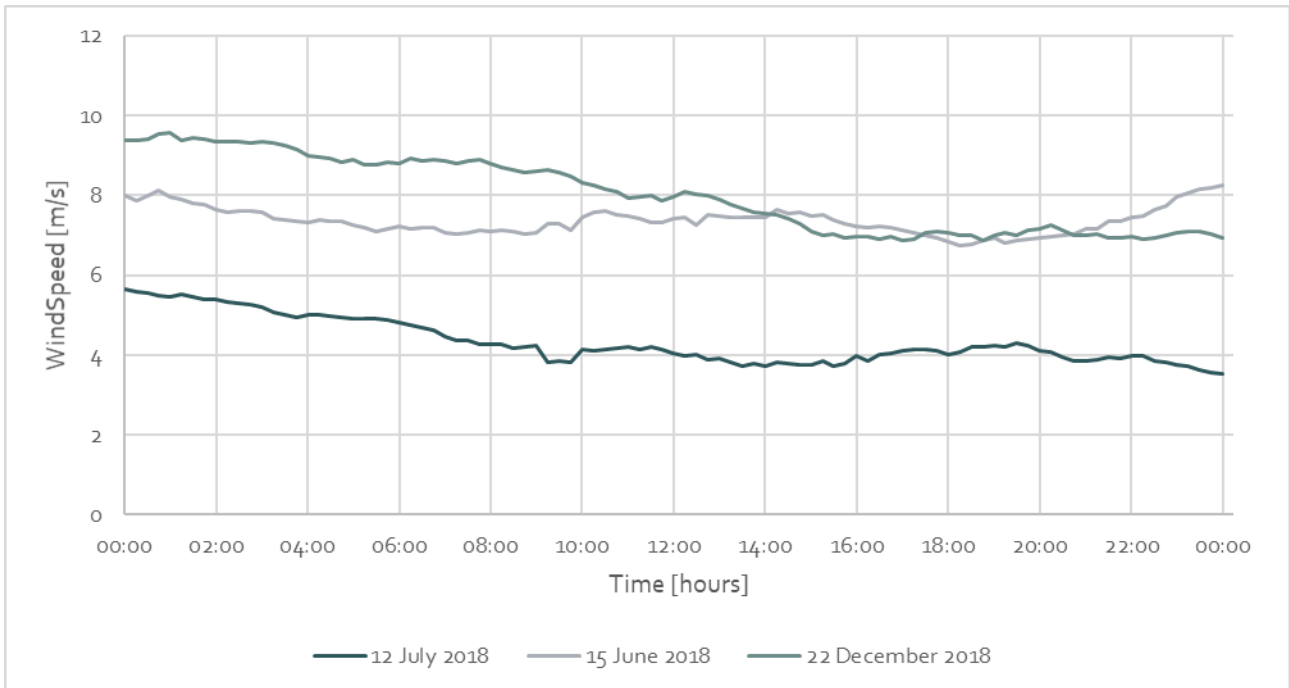
Figure 3-25*: Wind speed*
Source: DNV GL simulation

3.2.9.1.2 CALIBRATION OF KERMIT DURING THE HISTORIC TRIPS

The results of the Irish grid calibration and simulation during the frequency events is provided in
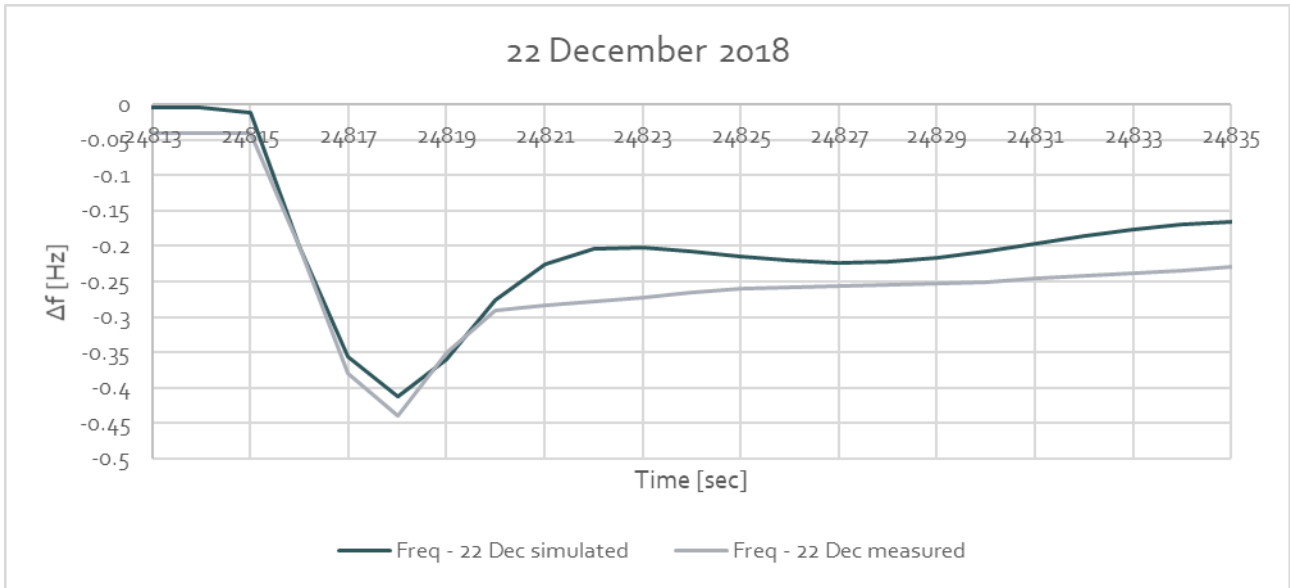
Figure 3-26 - Figure 3-28. The model was calibrated for the 22nd of December and the choice was made to keep primary and secondary controller assumptions identical for the other two days. Only the system inertia was chosen differently: as no detailed unit information was available this was chosen in relation to the total synchronous conventional generated power at the time of the trip.
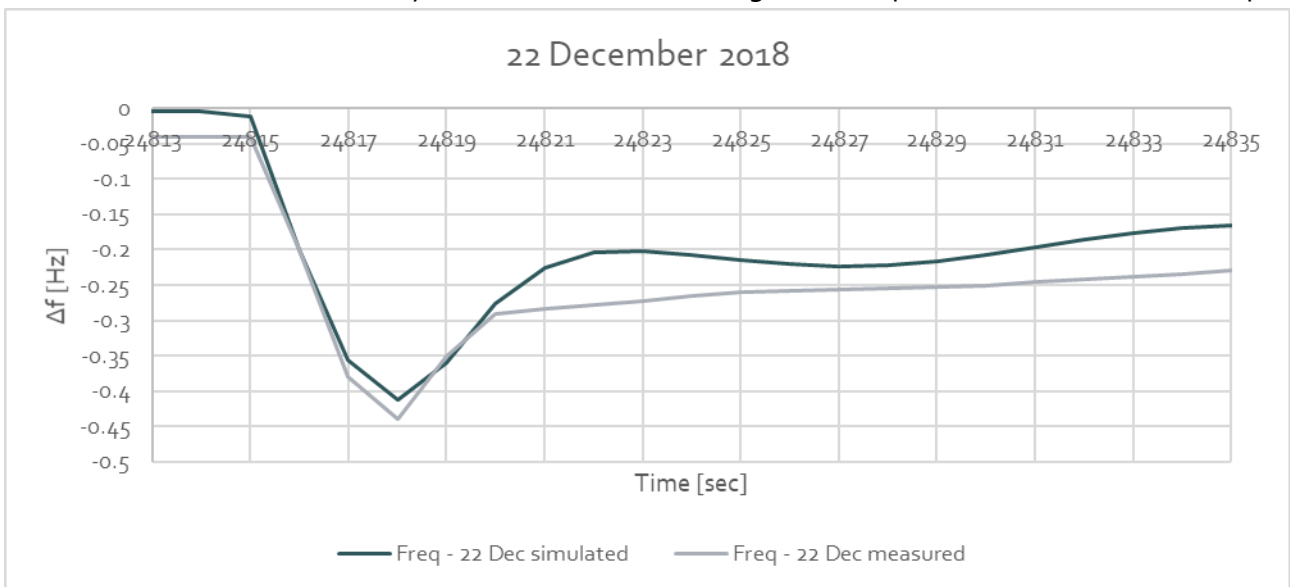
Figure 3-26: *Calibration model - 22 December*
Source: data downloaded from web portal [10] and from spreadsheet [11] and DNV GL simulation
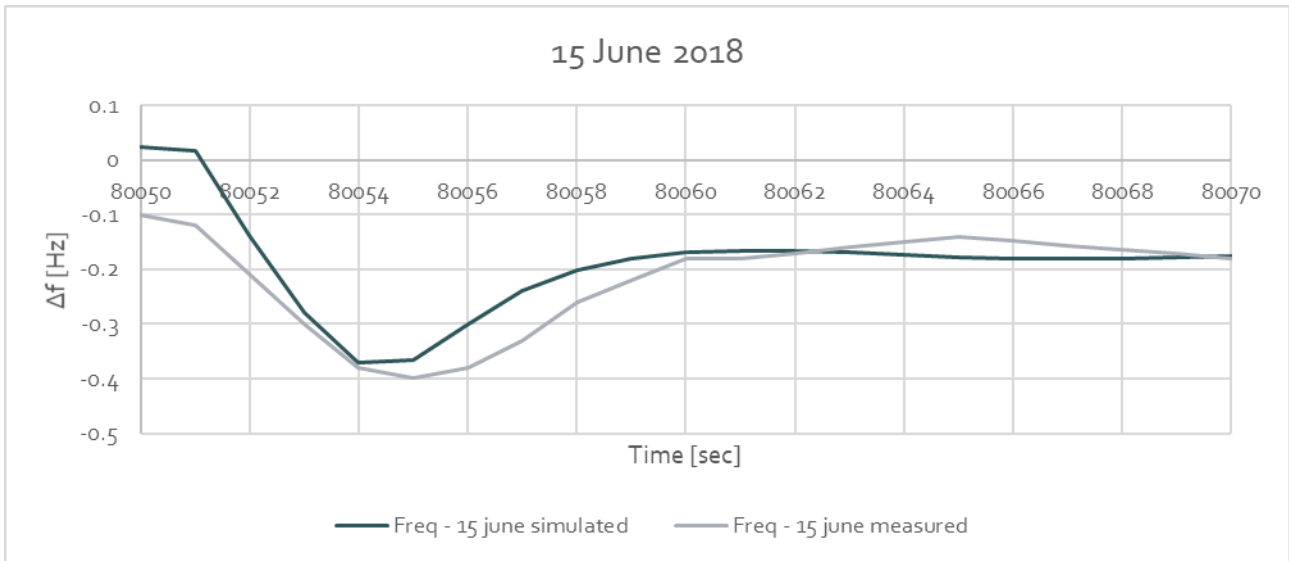
Figure 3-27: *Calibration model - 15 June*
Source: data downloaded from web portal [10] and from spreadsheet [11] and DNV GL simulation
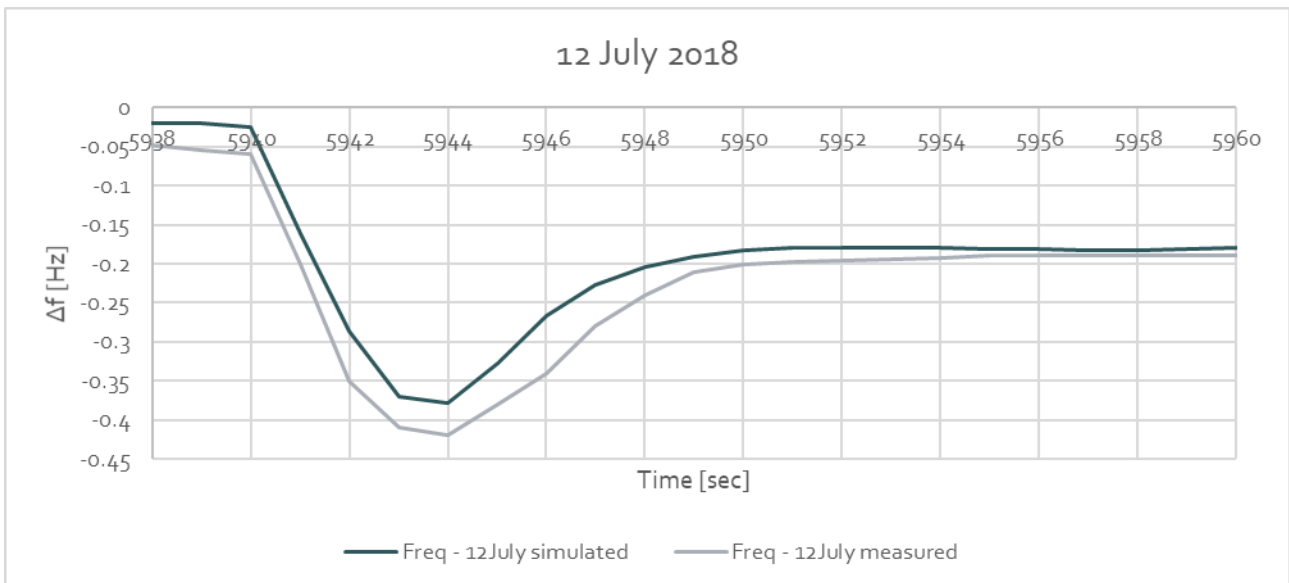
Figure 3-28: *Calibration model - 12 July*
Source: data downloaded from web portal [10] and from spreadsheet [11] and DNV GL simulation

3.2.9.1.3 CALIBRATION OF KERMIT DURING "NORMAL" SITUATION

The different FFR controller strategies of wind turbines will be verified during frequency events in the Irish grid as indicated in the previous section. In the case of the FFR control modes of droop and boost, the dead bands are chosen in such way to prevent these FFR modes being activated in normal situation (i.e. with a |Δfrequency| of 0.2 Hz). These control modes are typically used to support the frequency recovery after an event rather than in normal operation.

However, the control mode synthetic inertia can also be used within the |Δfrequency| of 0.2 Hz, i.e. during normal operation. In this mode the power control of the wind turbine is triggered based on the derivative of the frequency, df/dt. No dead bands are present on frequency. A synthetic inertia with unit rad/s is the tuning parameter. This control mode is verified during normal operation, thus not only during frequency events. Therefore it is important for this verification to have representative frequency variations.

The grid simulation should be able to mimic the real frequency behaviour as closely as possible. In order to do his, an artificial imbalance signal was generated which mimics the actual measured frequency behaviour closely.

The measured frequency throughout the day of a frequency event, is publicly available as indicated in the previous section (3.2.9.1.2). However, unlike the frequency measurements, the total power balance is not available on 5-second granularity but only on 15-minute granularity. When using linear interpolation between the 15-minute power balance values, the simulated frequency does not contain similar dynamics compared to the measured frequency. In Figure 3-29 below the measured frequency and the simulated frequency are illustrated for the day December 22 2018, which is one of the days of the frequency events.
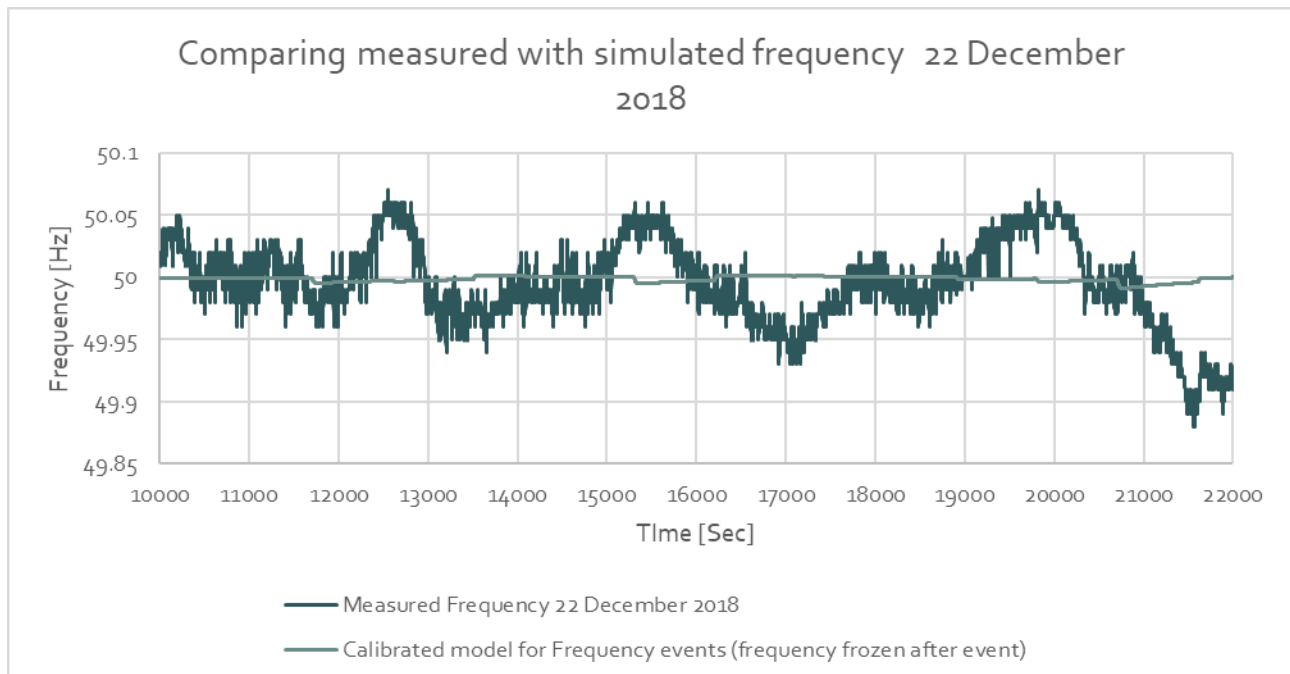
Figure 3-29: *Measured frequency versus simulated frequency during normal operation*
Source: data downloaded from web portal [10] and DNV GL simulation

In order to mimic the measured frequency more accurately, the power imbalance (generation – load – exchange) causing the frequency to deviate from its nominal value was obtained using a separate approach, illustrated below in Figure 3-30.
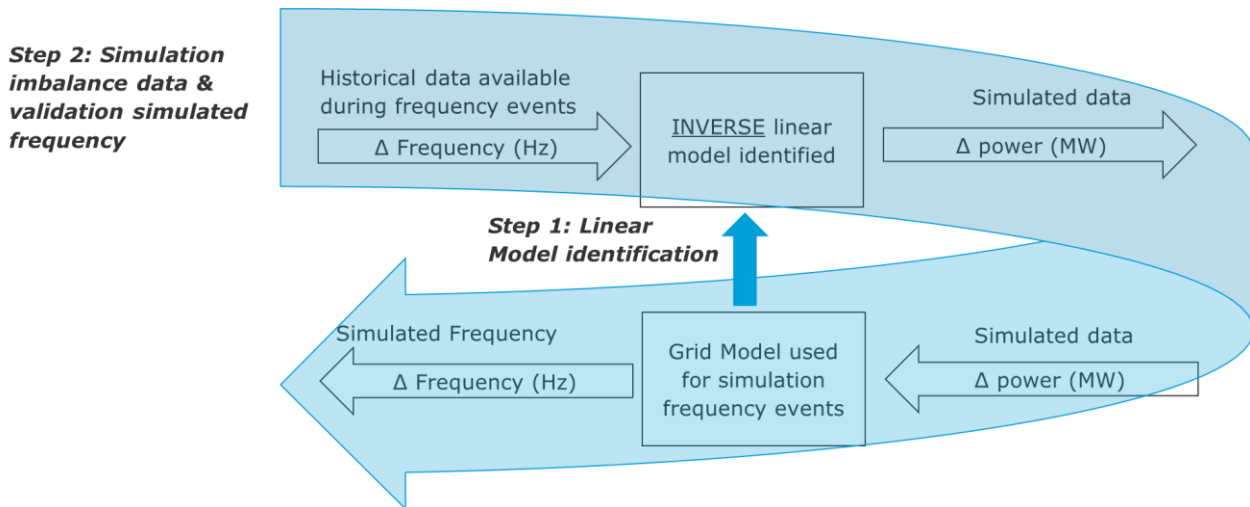
Figure 3-30: *Methodology to obtain imbalance power*
Source: DNV GL

In the first step by using model identification, an inverse linear model is created from the linear model obtained from the calibration of the grid (section 3.2.9.1.2). The system inertia and primary, secondary control settings are assumed constant within this linear model and therefore throughout the day.

In the second step using the inverse model and the measured frequency (Δfrequency), the (imbalance) Δpower can be obtained from the inverse linear model. A verification step can be performed, where the Δpower is then used to generate the simulated frequency (Δfrequency).

The use of the obtained imbalance power in the grid model (KERMIT), is illustrated in the figure below for a large part of 22 December 2018. The measured and simulated frequency have more or less dynamically the same behaviour, however some differences can be observed. As our focus is to verify the FFR controller strategy synthetic inertia with a more detailed frequency behaviour, the calculated imbalance can be used to simulate to frequency closer to reality.
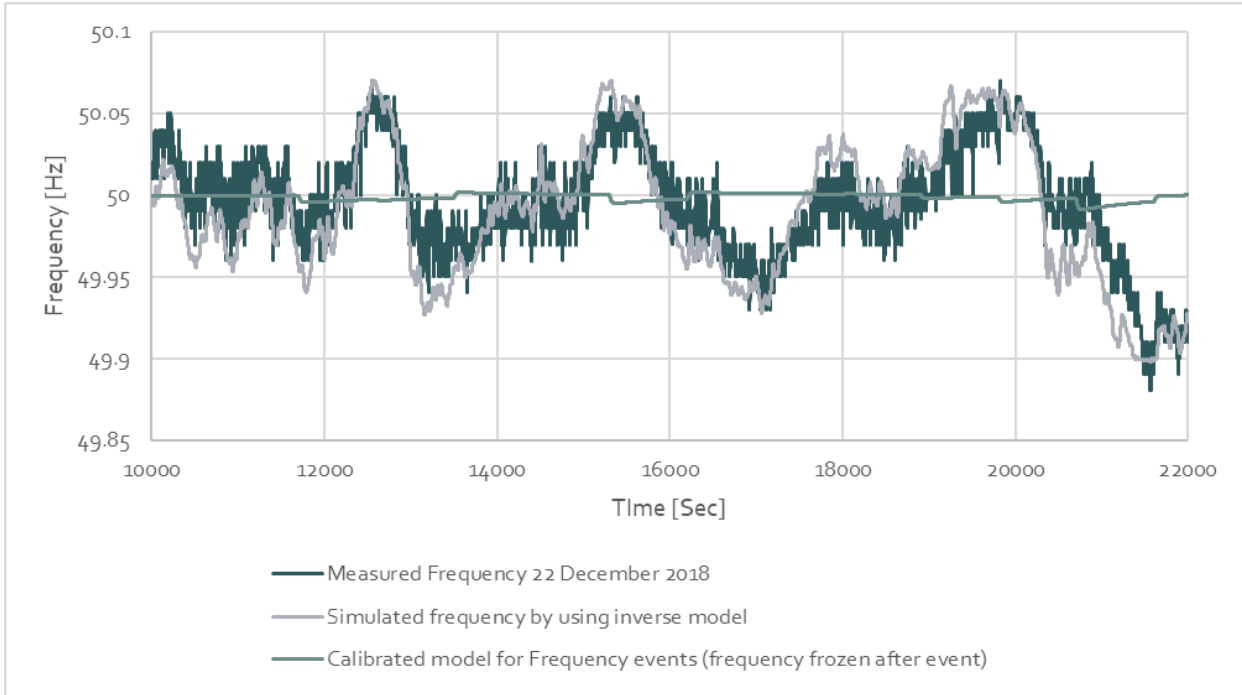
Figure 3-31: *Methodology to obtain imbalance power*
Source: DNV GL simulation

3.2.10   COMBINED LONGSIM AND KERMIT MODEL

The LongSim application is developed in the MATLAB application, while the KERMIT model is running in MATLAB Simulink. For the integration an S-Function was used in Simulink. In order to ensure the right data is fed from the LongSim model to KERMIT and visa-versa, an external time step in LongSim was applied. In FIGURE 3-32 the high-level interface between KERMIT and LongSim is illustrated.
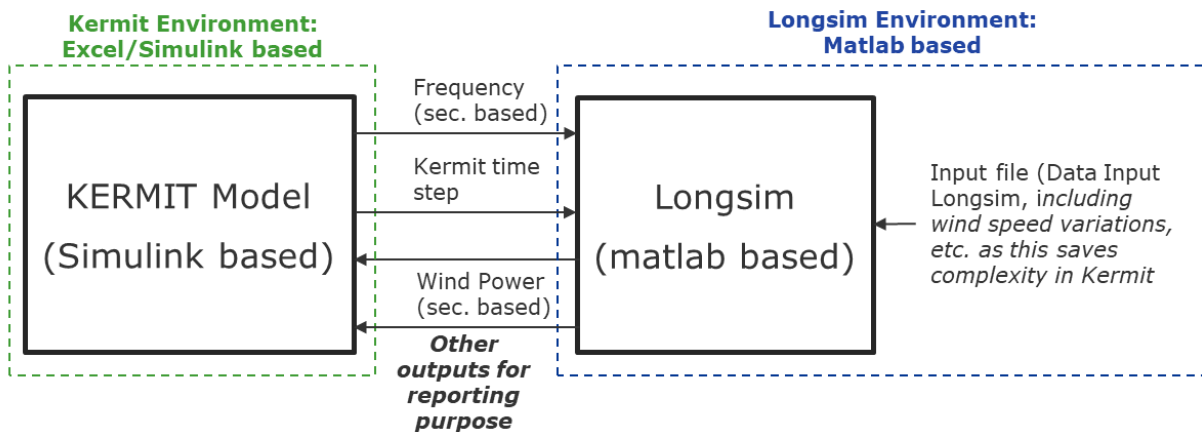
Figure 3-32: *Interface LongSim, KERMIT*
Source: DNV GL

As was described in section 3.1.2, based on the historical data obtained from the Eirgrid website [10], [11] the windspeed was calculated. In the simulation test cases a windfarm of 2000 turbines of 2MW rating each is used. The calculated wind speed during the frequency events is provided in *Figure 3-25*.

3.3 SIMULATION TEST CASES

As explained in Section 3.1.3, two different wind farm scenarios were used. Most of the simulations presented in this section used the simplest scenario, with a single 2MW turbine scaled up to represent 2000 turbines, but with the high-frequency variations due to turbulence smoothed out. In this section, this is called the 'simple' wind farm model. A second scenario, here called the 'complex' wind farm model, makes up the total wind power using multiple instances of a 9-turbine wind farm, in which different turbines see different wind conditions due to turbine wake effects and spatial wind field variations. This affects the results because the frequency response capability of a turbine at any instant depends on the wind conditions at the turbine. A more detailed explanation is provided in section 3.1.3.

As indicated in section 3.1 one of the strategies for wind farm control is Fast Frequency Regulation (FFR) which will be analysed for the current study. All three types of FFR as implemented in the turbine controller used for the simulations, as explained in section 3.1.4, were used:

- **Droop control**

  Droop control is a proportional action, linear to frequency deviation. LongSim implements droop in a more generic way as a look-up table, but here just a simple lookup table was used, defining a dead-band and a slope. This is similar to primary control (FCR) described in section 3.2.5.

- **Synthetic inertia**

  For synthetic inertial response, where the change in power is proportional to the RoCoF as described in Section 3.1.4.

- **Boost**

  Three parameters can be configured to tune the boost, namely the frequency threshold below which the power boost is triggered, and the (pre-determined) size and duration of the power boost.

In the different simulations a difference is made between open loop simulations and closed loop simulations. The definition of open loop and closed loop in the simulations:
- Open loop in this case means that the wind farm model in LongSim does not affect the frequency.
- Closed loop in this case means that the wind farm model in LongSim does affect the frequency.

In both cases, the wind power generated by LongSim responds to the grid frequency, but only in the closed loop case do the resulting power variations feed back into KERMIT to have an effect on the grid frequency.

In the following subsections the following simulations are described for the different configurations:

- Section 3.3.1 where the simple wind farm model in LongSim is used to simulate different controller strategies during frequency events in open loop. The calibrated Kermit model for "frequency events" is used (section 0).
- Section 3.3.2, where the simple wind farm model in LongSim is used to simulate different controller strategies during frequency events in closed loop. The calibrated Kermit model for "frequency events" is used (section 0).
- Section 3.3.3, where the complex wind farm model in LongSim is used to simulate synthetic inertia during "normal operation" closed loop and the droop controller strategy during a frequency event.

3.3.1 SIMPLE WIND FARM MODEL WITH OPEN LOOP LONGSIM SIMULATIONS DURING FREQUENCY EVENTS

In order to initially asses the performance of the LongSim controller settings, open loop tests are performed using the historical conditions measured on the days of the frequency events. As illustrated in *Figure 3-33* a fixed response of representative frequency is fed into LongSim and the additional FFR power from LongSim is assessed. The additional FFR power does not affect the frequency in the open loop simulations, making it possible to compare the different controller settings more easily. The effect on frequency will however be assessed in the closed loop simulations described in section 3.3.2.

To illustrate the difference in power generation response using the three FFR types, open loop simulations are defined in *Table 3-4*.

Table 3-4: *settings used in LongSim simulation (simple wind farm) of the three types of FFR*

Setting	Value
Case D1 - Droop Control	
Dead band	200 mHz
Desired power at 400 mHz based on droop setting	160 MW
Case I1 - Synthetic inertia	
Inertial synchronous speed	257 rad/sec
Case I2 - Synthetic inertia	
Inertial synchronous speed	357 rad/sec
Case B1 - Boost	
Thresh hold frequency which activated Boost	49.8 Hz
Amount of power to boost	160 MW
Boost time	4 sec
Case B2 - Boost	
Thresh hold frequency which activated Boost	49.8 Hz
Amount of power to boost	240 MW
Boost time	4 sec
Case D1 and case B1	
Dead band	200 mHz
Desired power at 400 mHz based on droop setting	160 MW
Thresh hold frequency which activated Boost	49.8 Hz
Amount of power to boost	160 MW
Boost time	4 sec
Case D1 and case I1	
Dead band	200 mHz
Desired power at 400 mHz based on droop setting	160 MW
Inertial synchronous speed	257 rad/sec

The results of the different cases are illustrated in *Figure 3-34*. The open loop frequency signal used is illustrated in *Figure 3-35*.

Figure 3-33: *Open loop LongSim simulation*
Source: DNV GL
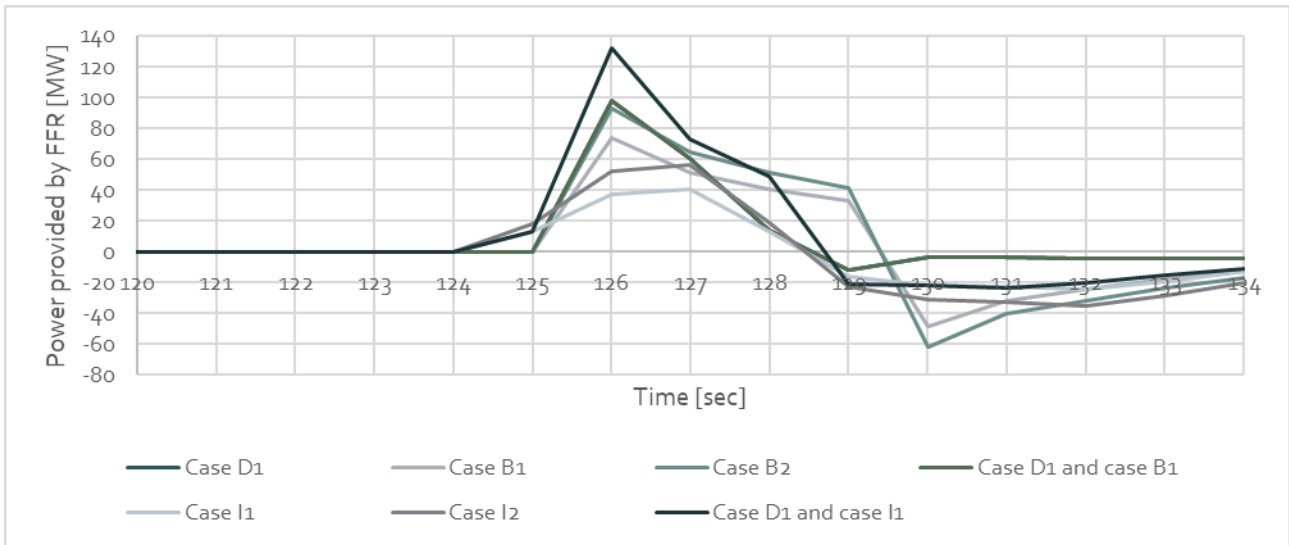
Figure 3-34: *Results open loop LongSim simulations*
Source: Simulation DNV GL
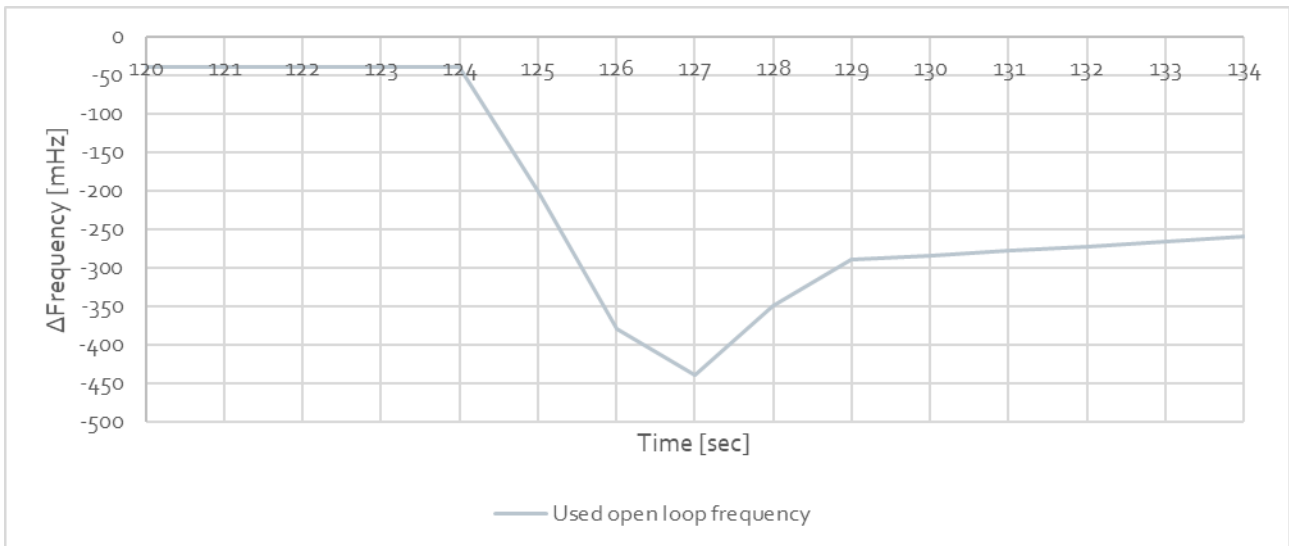
Figure 3-35: *Open loop frequency used in LongSim simulations*
Source: Simulation DNV GL

Since the power increase is derived from the rotor kinetic energy, which needs to be recovered later, it is important to select a strategy such that the subsequent power dip is as benign as possible. This power dip after a frequency event, can be postponed and/or sped up with parameters in LongSim. The Recovery Delay parameter postpones the dip a s long as possible, and the Decay Time adjusts how gradually it happens. At high wind speeds it was observed that the recovery dip is very small or not present at all. This is because above rated, the extra power requirement comes from surplus wind energy which is otherwise being discarded by the pitch control, and not from rotor kinetic energy, so the rotor speed does not need to recover.

The ultimate choice will of course be made using the closed-loop simulations in the next section, where the effect of any such power dip on the grid frequency will be seen.

3.3.2 SIMPLE WIND FARM MODEL WITH CLOSED LOOP SIMULATIONS DURING FREQUENCY EVENTS

For the closed loop simulations the additional power from LongSim is fed into KERMIT, causing the frequency in KERMIT to change, and the changed frequency is fed back to LongSim. The different cases evaluated in open loop have also been evaluated in closed loop, therefore the settings for the simulations are identical to the settings defined in *Table 3-4*. The effect during the three frequency events is assessed.

3.3.2.1 SIMULATION EFFECT OF P-ACTION DURING THE THREE FREQUENCY EVENTS

The closed loop effect for case D1 is assessed for all three frequency events. The settings of case D1 are defined in *Table 3-4*, and the effect on grid frequency is shown for each event in *Figure 3-36* to *Figure 3-38*. At the time of the frequency event, the amount of wind is largest on 22 December. Therefore the effect of FFR is largest in this simulation.
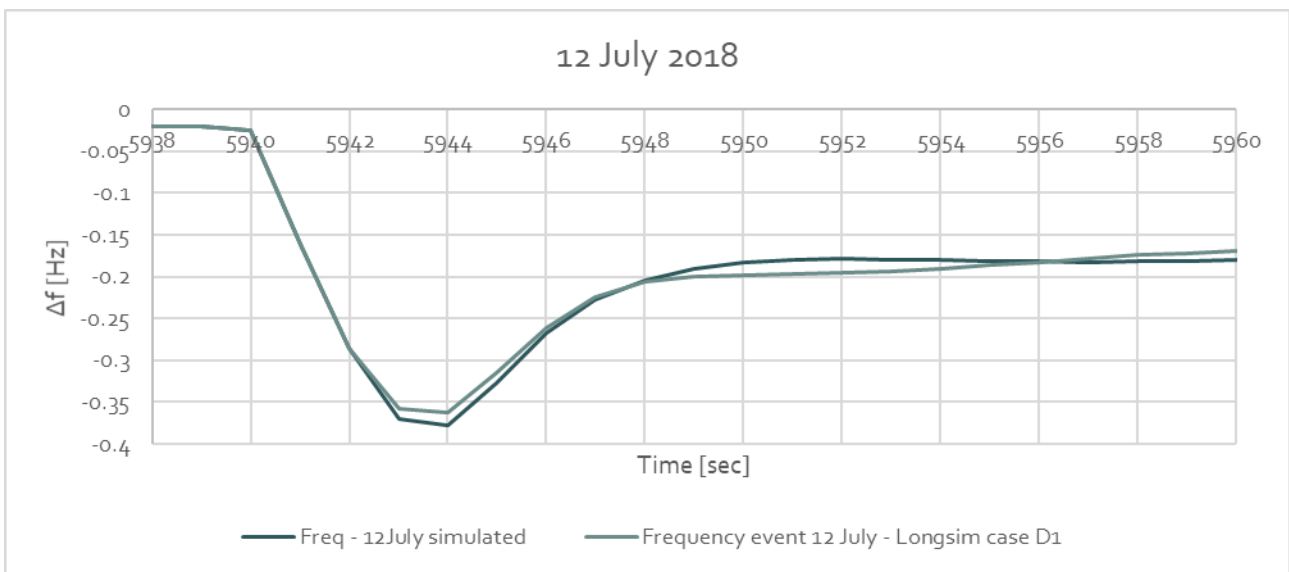
Figure 3-36: *Simulated closed loop simulation case D1 – 12 July 2018*
Source: Simulation DNV GL
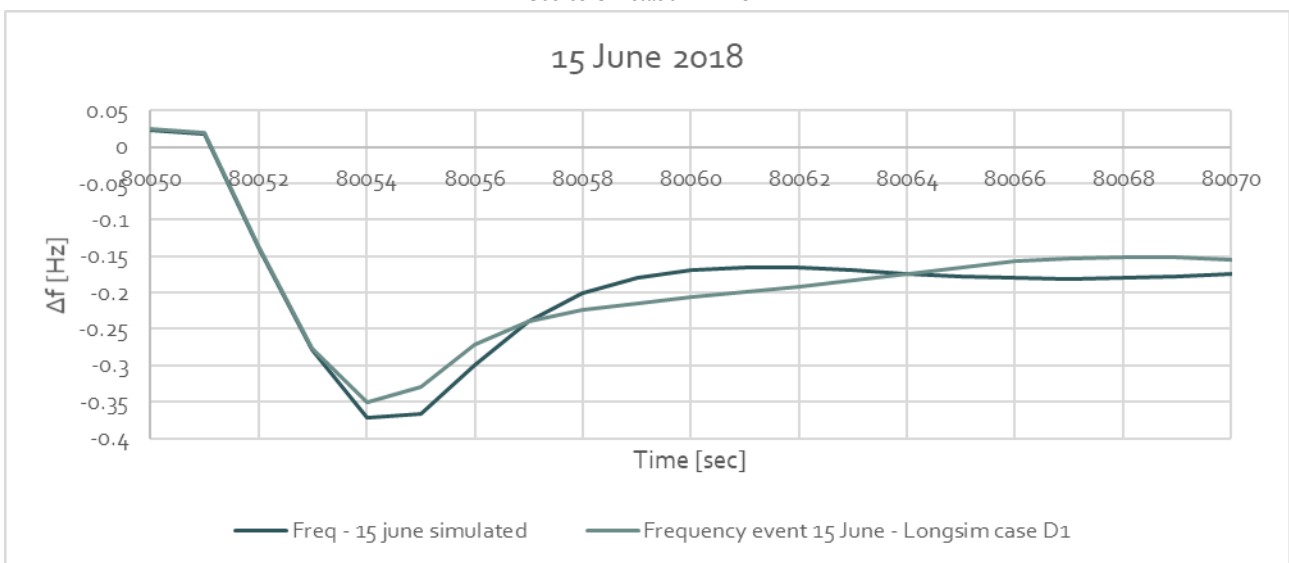
Figure 3-37: *Simulated closed loop simulation case D1 – 15 June 2018*
Source: Simulation DNV GL
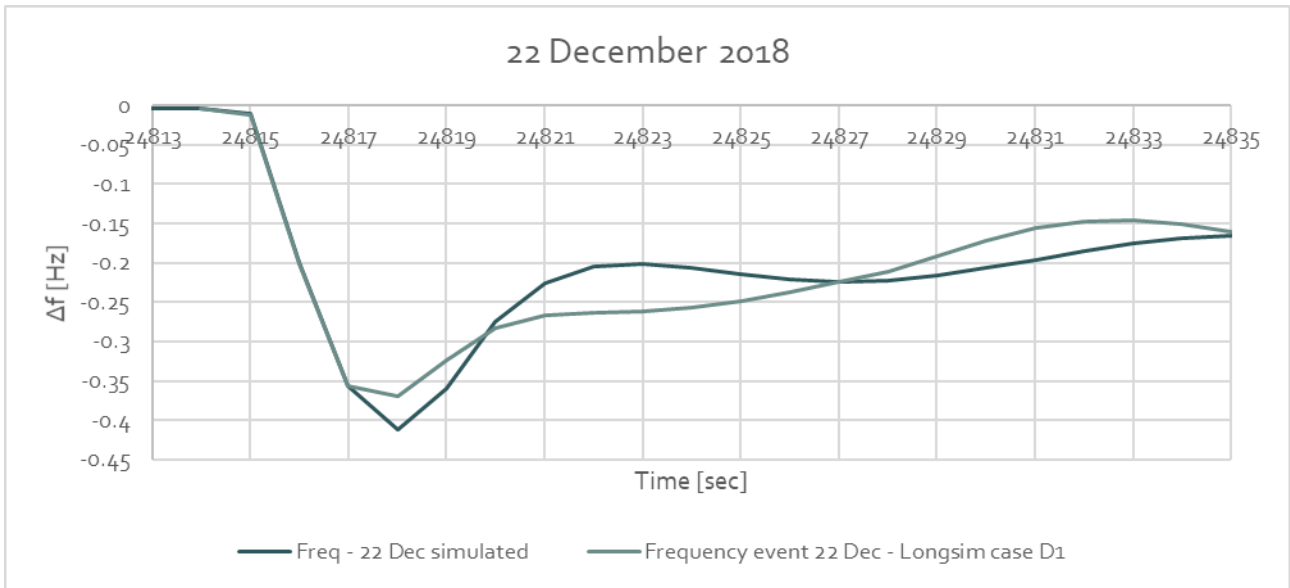
Figure 3-38: *Simulated closed loop simulation case D1 – 22 December 2018*
Source: Simulation DNV GL

3.3.2.2 SIMULATION EFFECT OF OTHER SETTINGS FOR FREQUENCY EVENT OF 22 DECEMBER

The closed loop effect for the following cases is assessed for the frequency event on 22 December, as this day has the largest wind at the time of the trip:

- Case B1 - Boost
- Case B2 - Boost
- Case D1 and case B1
- Case I1 - Synthetic inertia

The settings of the different cases are defined in *Table 3-4*. The results are shown in *Figure 3-39* - *Figure 3-41*.
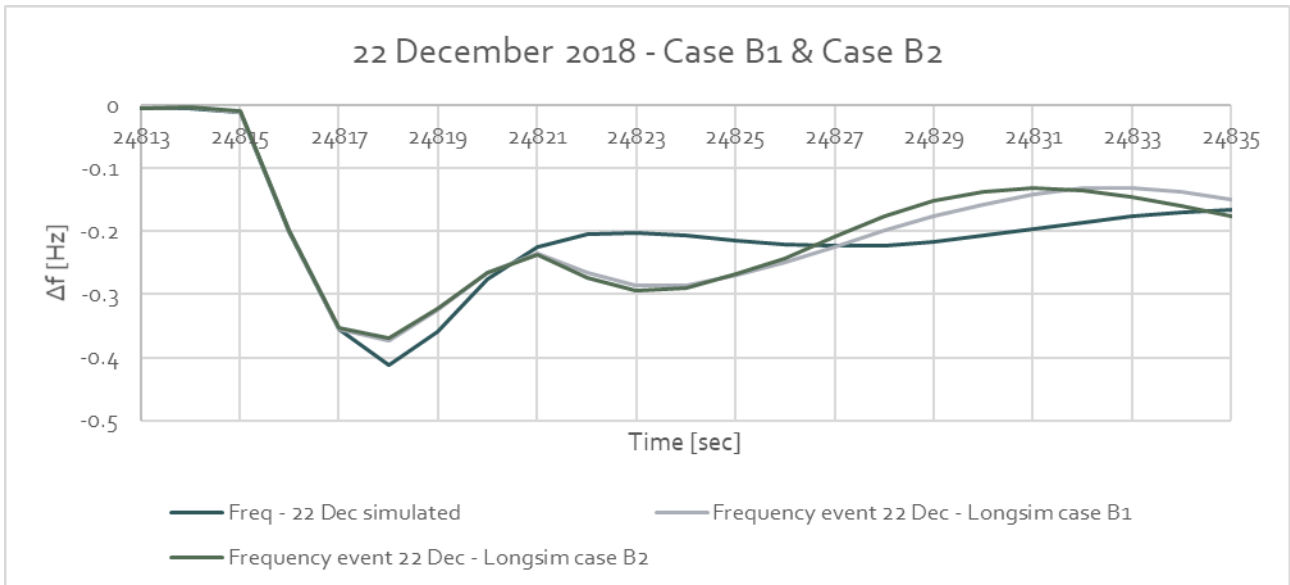
Figure 3-39: *Simulated closed loop simulation 22 December case B1 and case B2*
Source: Simulation DNV GL
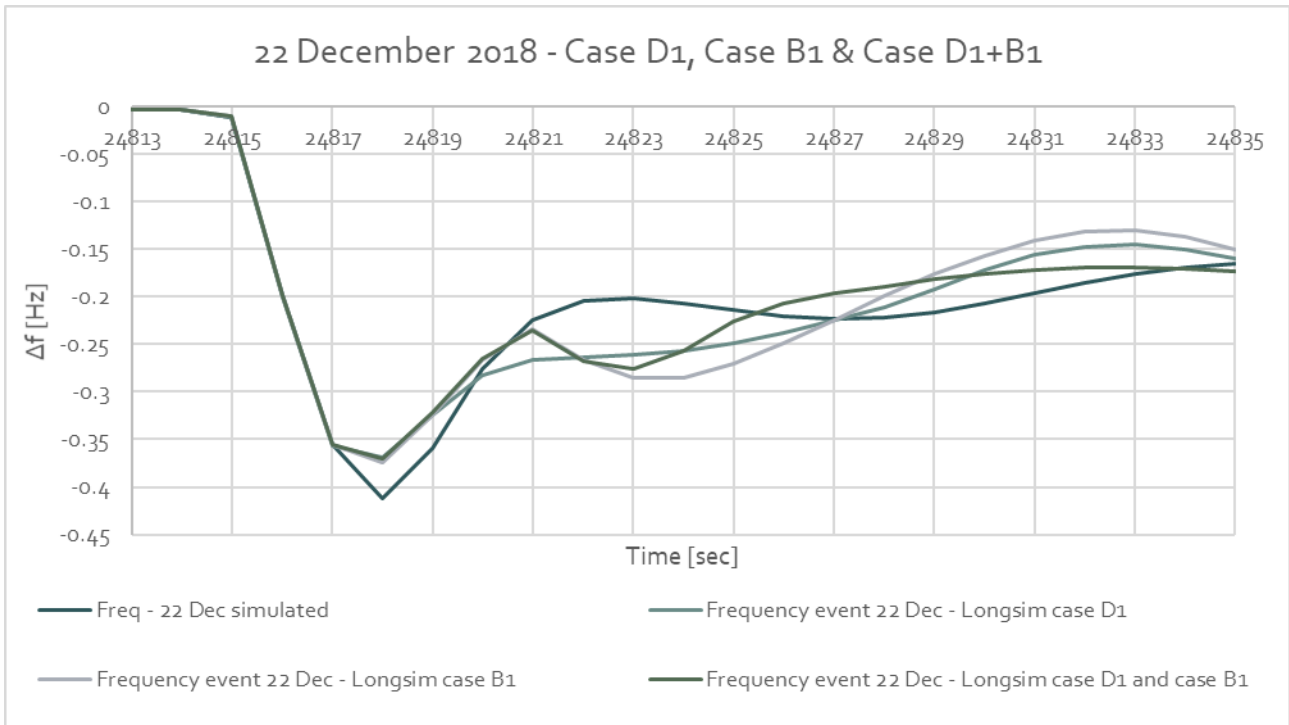
Figure 3-40: *Simulated closed loop simulation 22 December case B1 and case D1 and combination of D1, B1*
Source: Simulation DNV GL
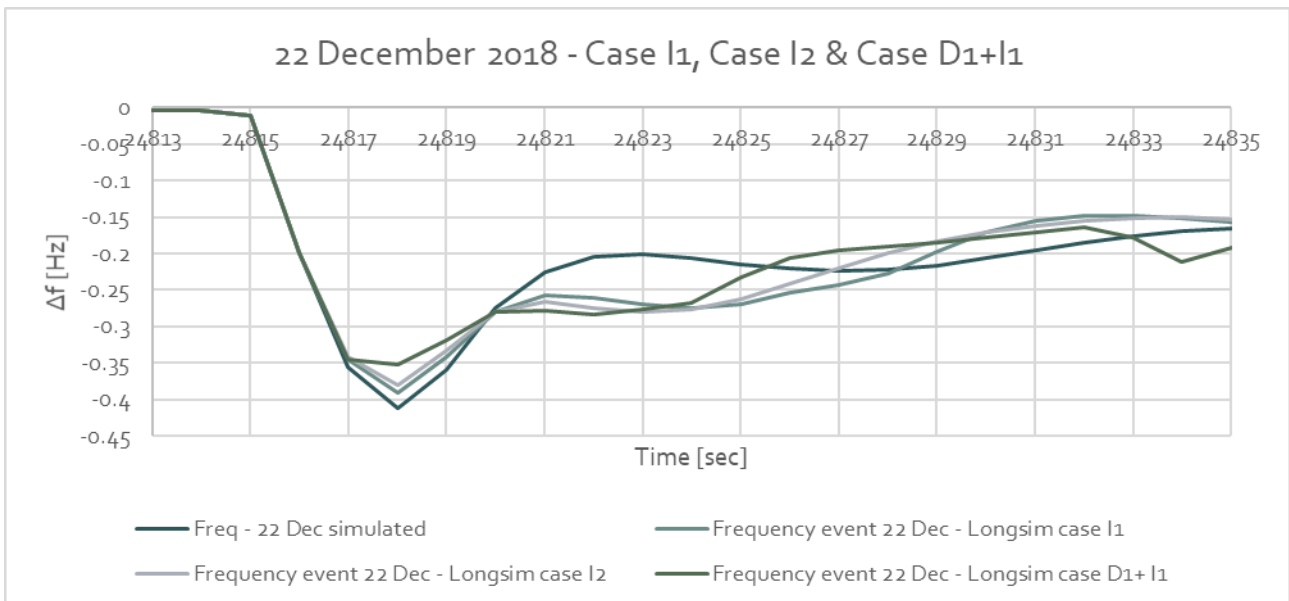
Figure 3-41: *Simulated closed loop simulation 22 December case I1, CASE I2 and combination of D1, I1*
Source: Simulation DNV GL

All these simulations show a beneficial effect on the frequency nadir, and any secondary dips are small enough not be an issue.

3.3.3 COMPLEX WIND FARM MODEL WITH CLOSED LOOP SIMULATIONS

Compared to the closed loop simulations with the simple LongSim windfarm model described in Section 3.3.2, simulations in this section contain two adjustments:

- Detailed wind farm model is used in LongSim, in detail described in section 3.1 evaluated for both frequency events and during "normal" operation.
- A simulated frequency closer to the measured frequency is used by using the calculated imbalance power in the calibration method described in section 3.2.9.1.3

Simulations are again performed in closed loop, where the additional power from LongSim is fed into KERMIT, causing the frequency in KERMIT to change, and the changed frequency is fed back to LongSim. The settings for the simulations are identical to the settings defined in TABLE 3-5.

Table 3-5: settings used in LongSim simulation for complex wind farm

Setting	Value
Case D1 and case I1 (droop control and inertia)	
Dead band	300 mHz
Desired power at 400 mHz based on droop setting	160 MW
Inertial synchronous speed	11 rad/sec

The simulation result of Case D1 and case I1 (droop control and inertia) is provided in FIGURE 3-42 for the frequency event using the detailed LongSim windfarm model. Note that the calibrated model is different compared to the calibrated model used for the closed loop simulations using the simple LongSim windfarm model (section 3.3.2), causing a difference in frequency behaviour (more detailed frequency behaviour using calculated imbalance vector is used).
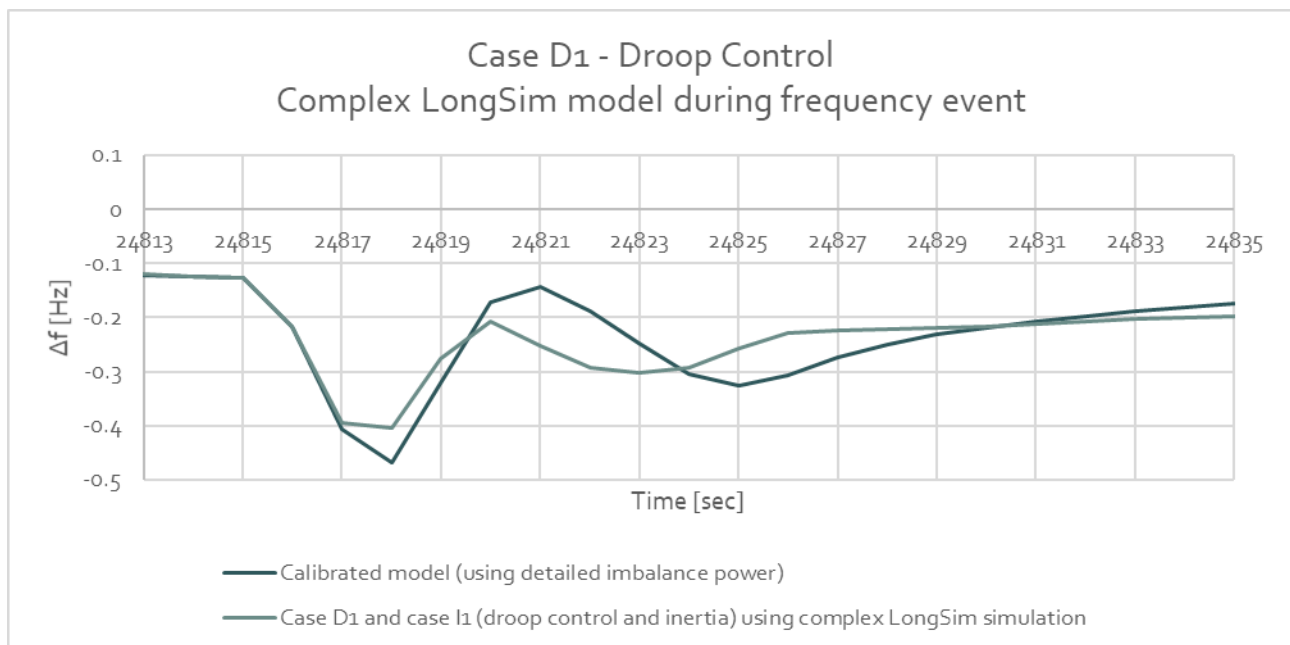
Figure 3-42: Simulated closed loop 22 December D1 and case I1 (droop control and inertia) with complex LongSim model during frequency event
Source: Simulation DNV GL

During normal operation, droop control is not activated as the deadband for droop control is set to 300 mHz. During normal operation the effect of synthetic inertia can be observed in FIGURE 3-43. The effect is limited, also due to the lower amount of inertial synchronous speed as indicated in TABLE 3-5.
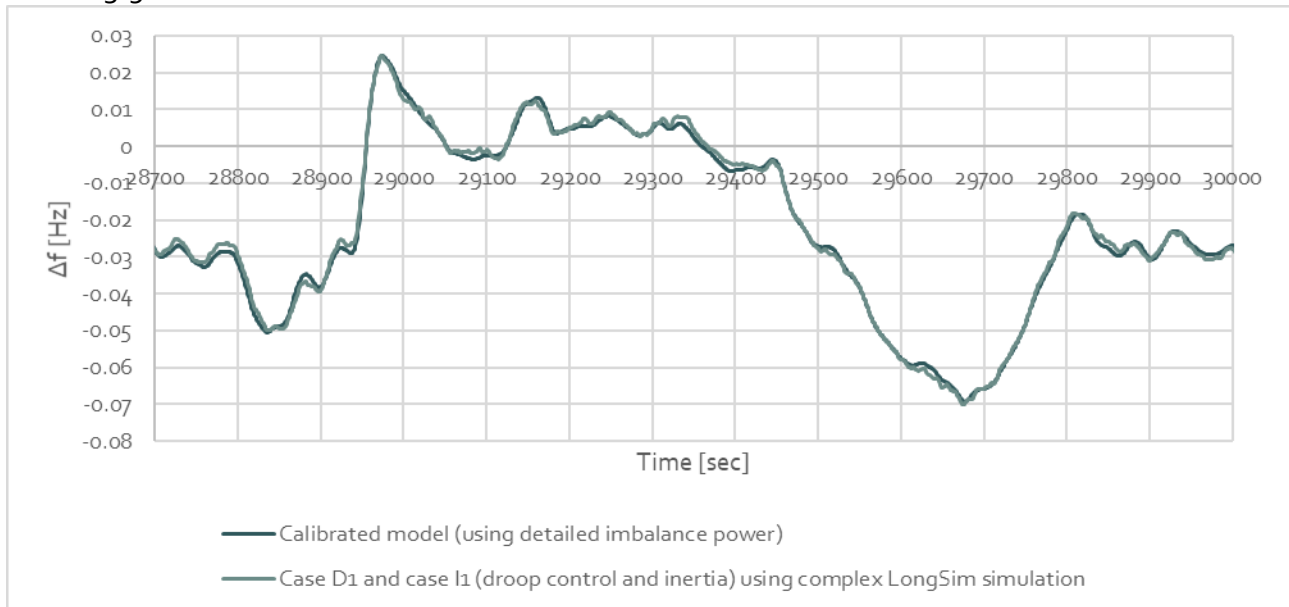
Figure 3-43: *Simulated closed loop 22 December D1 and case I1 (droop control and inertia) with complex LongSim model during normal operation*
Source: Simulation DNV GL

3.4 CONCLUSIONS

The task described in Section 3 was to couple together a wind farm simulator (LongSim) and a grid simulator (KERMIT), so that fast frequency response (FFR) strategies implemented in the wind turbine controllers can be defined and tuned to achieve the best performance in terms of helping to stabilise the grid frequency, while remaining within the operational constraints of the wind turbines in the wind conditions available at the time. The models are linked by feeding the active power output from LongSim into Kermit, and the grid frequency from KERMIT into LongSim, resulting in a closed-loop simulation of the whole system. In order for the simulations to run as fast as possible, the LongSim wind farm setup has been simplified as far as possible while retaining the important features, although some simulations have also been run with a more complex setup to demonstrate that wind farm wake effects can be taken into account. This may have an effect because the frequency response capability of each turbine depends on wind speed and may be different at each turbine.

This study is based on historical data for the Irish grid system, which is appropriate as it already has a high wind power penetration, and suitable data is publicly available. The work has demonstrated that the combined model is a useful tool for tuning and testing FFR strategies integrated into the wind turbine controller, and example closed-loop simulations have shown that with appropriate tuning of these control strategies, the wind farms can have a significant beneficial effect on the frequency stability of the grid. The strategies have been tested against three real frequency dip events recorded on the Irish system.

4 VIRTUAL SYNCHRONOUS MACHINE (SINTEF)

4.1 INTRODUCTION

The share of power generation interfaced with power electronics converter is expected to rise in the future to accommodate the necessity of increasing level of renewable generation. This will reduce the power from conventional synchronous generators and could create operational issues for the power systems. This drawback could be mitigated by modifying the classical control schemes for power converters in order to replicate part of the functions that the synchronous machines normally cover. This is referred in literature as controlling the converters as grid forming units rather than grid following units. Within the grid forming schemes, the concept of Virtual Synchronous Machines (VSM) has been widely analysed for applications in distribution and transmission systems. The application of VSM can be potentially extended also to wind farms in order to provide grid forming capabilities and inertia support. Moreover, this approach would also offer the possibility to black start and island operation.

This report presents the laboratory validation of the frequency support methodology initially described in a previous deliverable [6]. The aim is to apply in a controlled environment the concept of synthetic inertia and fast frequency support of a wind power system with a converter using the virtual synchronous machine (VSM) controller. Ideally, the strategy presented in this report shows how to use some of the kinetic energy stored in the wind turbine mechanical inertia and supplies this energy into an affected grid where the frequency requires support. Besides, the VSM injects power into the grid in order to correct the frequency deviation of the AC grid.

Preliminary experimental results indicated several limitations of the classical VSM schemes presented in literature when applied in the context of wind generation. Thus, modifications have been introduced to offer more flexibility in the inertia support and to increase responsiveness to changes in the power produced by the wind turbines. These modifications are presented and justified in this section. Finally, experimental tests highlights that the concept of VSM can be successfully applied also to wind farms and satisfactory performance can be achieved.

4.2 EXPERIMENTAL SETUP

Experimental tests have been conducted in the Norwegian National Smartgrid Laboratory (NSGL) to illustrate the possible implementation of a VSM scheme in a wind farm. The NSGL is a state-of-the-art facility jointly operated by NTNU and SINTEF offering a flexible environment to test smartgrid solutions and control strategies for power electronics converters and power systems. The wind farm is represented with an aggregate model consisting of a single WT conversion system as shown in *Figure 4-1*. The rating of the WT conversion system is scaled down both in terms of power rating and voltage rating to fit with the laboratory capabilities.

The aggregate model is composed by two power electronics converter units in a classical back-to-back configuration. The grid side converter is implementing the VSM control and the inertia support features and is connected to a receiving ac grid. The other converter acts as a rectifier and is connected to a WT. In conventional WT conversion system, the WT side converter controls the speed of the generator while the grid side converter is responsible to control the voltage on the dc bus. However, as presented already in a previous deliverable [6], this configuration cannot be adopted for a VSM based scheme. Indeed, in this case the grid side converter implements the VSM

controls and is responsible for controlling the generator speed while the WT side converter needs to control the dc voltage.
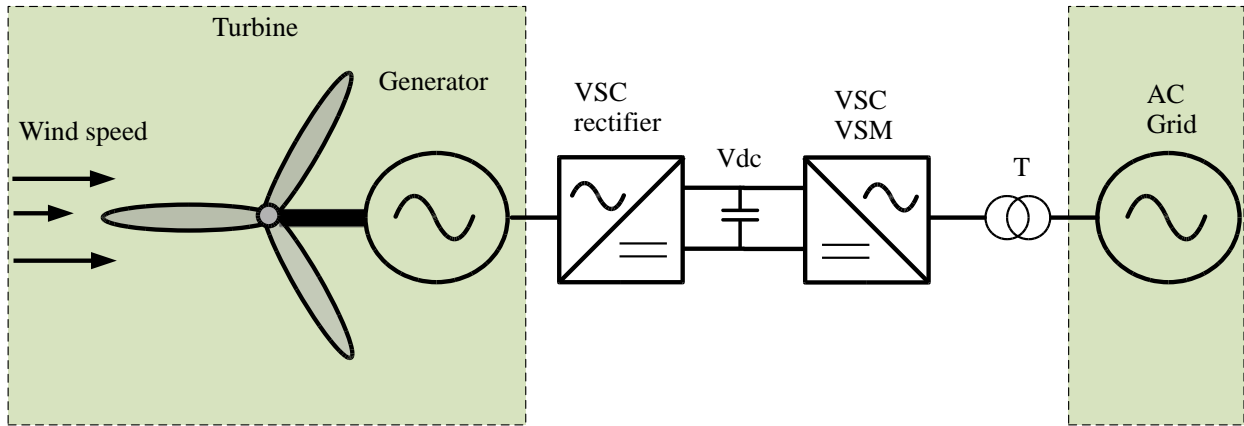
Figure 4-1: *Overview of the configuration of the WT conversion system.*

The scheme illustrated in *Figure 4-1* is translated into a laboratory setup according to the overview schematic diagram displayed in Figure 4-2. An overview of the setup is described in this section while the characteristics of the individual components are described separately in dedicated subsections. The two power electronics converters in the aggregated WT are represented with two 60 kW physical converters directly interconnected on the dc side in a back to back configuration (see blue line in Figure 4-2.). The ac side of the converters are connected via two delta-star transformers to a grid emulator unit. The transformers do not alter the voltage ratings (1:1 voltage ratio) but ensure galvanic insulation. The two converters are connected to a real time simulator platform via a fibre optic link (see dotted green line marked as communication bus 2 in Figure 4-2.). The control of the rectifier is implemented in an internal FPGA and receives only an external dc voltage reference. The control of the VSM is partly implemented in the internal FPGA (inner loops) and partly on the real time simulator.
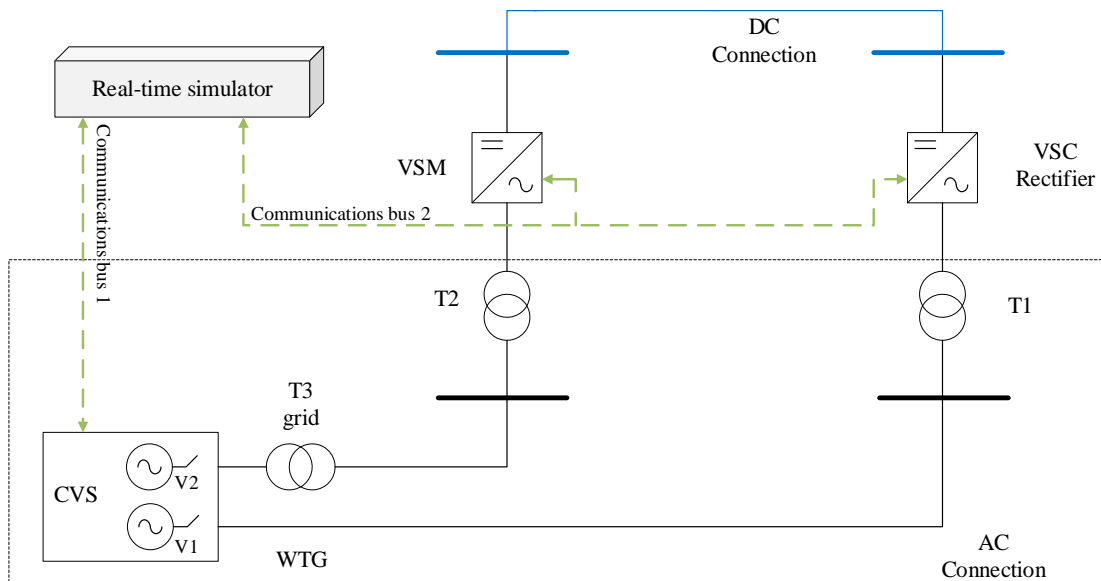
Figure 4-2: *Laboratory one-line diagram for experimental connections.*

The ac grid and the WT generator are both represented according to an approach referred to as Power Hardware in the Loop (PHIL) with a real time model executed in the real time simulator platform and a grid emulator acting as a high bandwidth power interface. An image of the laboratory is presented in Figure 4-4.

Figure 4-3: Norwegian National Smart Grid Laboratory. Marked in the figure: Grid emulator (1), Power electronics converters (3), Transformers (2), Control interface (4)

POWER ELECTRONICS CONVERTERS

This experimental setup includes two 2 level VSCs displayed in Figure 4-4 based on IGBT devices. The converter units are rated for a power of 60 kW with a rated voltage of 400 V ac and 600 V dc. The converters are connected to the external ac grid by an LCL filter with inductance L_f=0.5 mH, a capacitance C_f=50 µF and L_{fgrid}= 0.2 mH grid side.

The converter units embed a FPGA control board implementing the functions for measurements and protections. This board can be connected to the real time simulator via a fibre optic cable in order to distribute control functions between these two. In general, the inner loops are executed in the FPGA board while the slower outer loops are executed in the real time simulator.
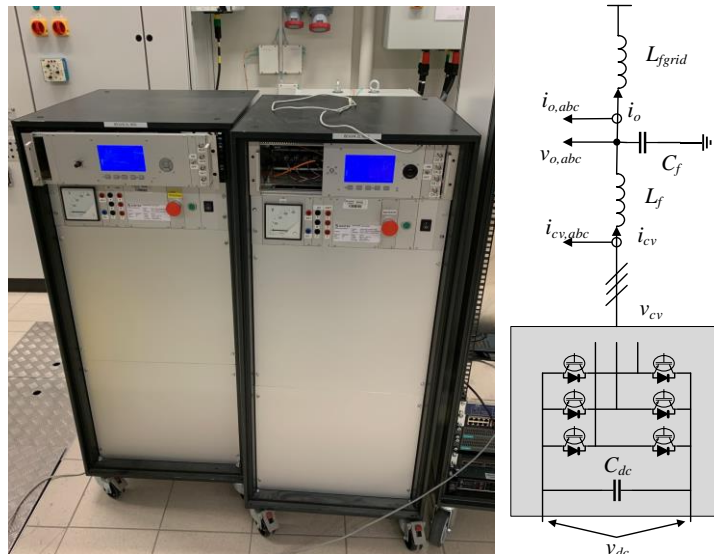
Figure 4-4: Two-level voltage source converter (60 kVA): photo of laboratory converters and circuit schematic.

Besides, the connection of the equipment requires some isolation to avoid short circuit problems or circulating currents provided by the VSCs. This isolation is obtained using 60 kVA transformers as the one shown in Figure 4-5.

Figure 4-5: Transformers (60 kVA).

4.3 GRID EMULATOR

The controlled voltage source shown in Figure 4-6 is used in order to emulate the grid equivalent and the WTG. The grid emulator allows up to 6 individual outputs that can be grouped to generate ac or dc voltages (e.g. 2 independent sets of three phase ac voltage). The total power rate for this

source is 200 kVA with sufficient bandwidth to be capable of reproducing voltages with frequency up to 10 kHz.

Figure 4-6: *Controlled voltage source (200 kVA).*

4.4 REAL TIME SIMULATOR

The controllers for the rectifier converter and the VSM converter, the dynamic models for the grid equivalent and the WTG are executed within a RT-simulator (see Figure 4-7). The RT-simulator has a fast processor and FPGA based boards that allow the models to run at a very high execution frequency. Besides, the RT-simulator uses IOs with fiber-optic cable to communicate with external devices sending and receiving the control and measures signals.
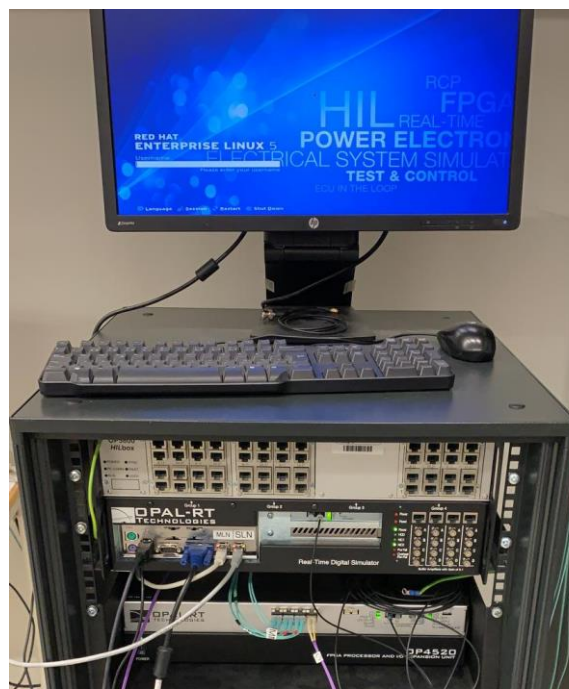
Figure 4-7: *Real time simulator.*

4.5 Control of power electronics converters

The general concept of VSM and conventional control structures for its adaptation to wind farm applications have been described in a previous deliverable [6]. The control schemes are partly repeated again in this deliverable to facilitate the reading and the description of the tests. Moreover, additional modifications that have been necessary to better control the power support are indicated and justified. These represent an improvement compared to the basic schemes documented in the previous deliverable and have been developed as an iterative process in parallel to the execution of the experiments. Besides, only a current control VSM strategy has been applied (i.e. scheme referred to as CCVSM QSEM).

4.6 Turbine side converter

The turbine side converter is responsible for controlling the voltage on the dc bus with power generated by the wind turbine. It should be noted that the speed regulation that normally is assigned to this unit is shifted in this configuration to the grid side converter. A block diagram of the control structure implemented in the rectifier is shown in Figure 4-8. There are three measurements from the grid and the output of the converter, one is for the voltage at the connection point, a second for the grid current and the third is the converter current in the filter. The converter controls are based on an inner current control based on a PI in the Synchronous rotating frame cascaded to a dc voltage control generating the reference for the d-axis component of the current. Both the controllers are executed in the internal FPGA. The reference for the dc voltage is received as an external input from the real time simulator.
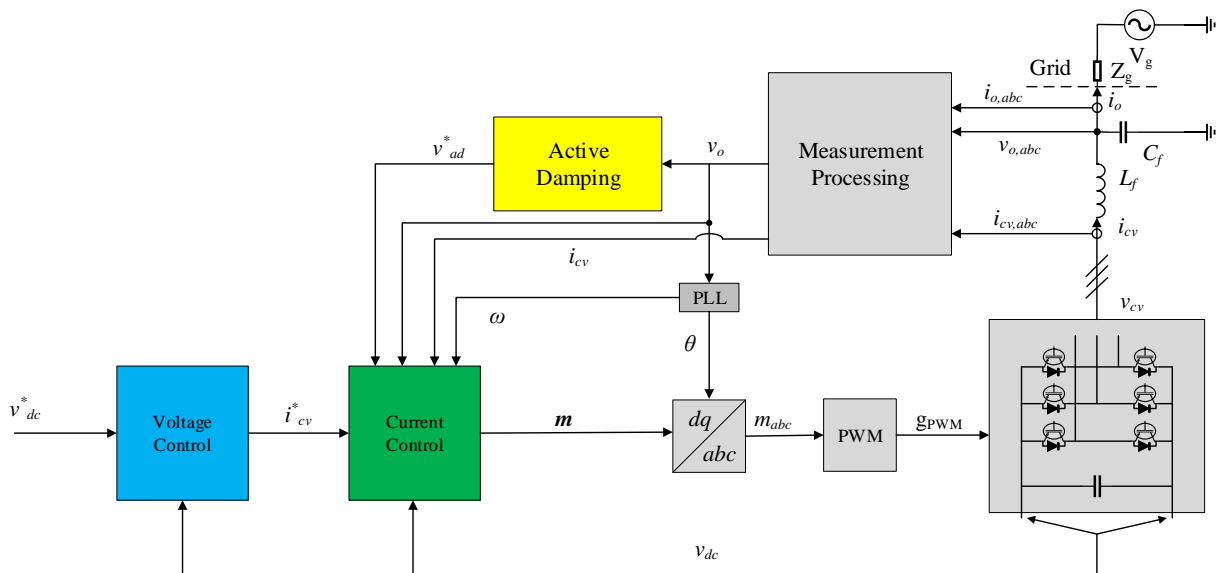
Figure 4-8: Block diagram of the controller loops of the rectifier.

4.7 Grid side converter

The grid side converter is the unit implementing the VSM and offering the inertia support to the external grid. Moreover, the converter implements also an external loop aiming at regulating the

turbine speed. An overview of the control structure for the VSM (i.e. a current controlled VSM) is presented in Figure 4-9.

The control consists of an inner current loop based on a PI in a rotating reference frame. However, the source of the angle for the Park transformation is the inertia model rather than a PLL like in the turbine side converter or the conventional grid connected control schemes. The regulator is complemented by an active damping block that attenuates the resonances introduced by the output filter. The active damping, the current control and the integrator for the angle generation are implemented in the internal FPGA board. The remaining control blocks are considered as external loops and implemented in the real time simulator.

The reference for the current controller is provided by the block marked as electrical model. This block reproduces the behaviour of the electrical impedance at the armature windings of the synchronous machine and has been formulated according to a quasi stationary model (i.e. CC VSM QSEM). The voltage control ensures that the amplitude of the voltage from the virtual machine is coordinated with the amplitude of the voltage at the external grid. Additional features as reactive power control are also included according to a droop term on the voltage amplitude but will not be targeted by the experiments in this report because rather conventional.

The core of the control scheme is in the blocks marked as Inertia model, Frequency control and WT speed control. These blocks generate the angle for the Park transformation and are the main responsible for the regulation of the active power. The frequency control block implements a droop between active power and frequency. This is a classical component in the governors for synchronous machines and it is normally included also in the VSM configurations. However, in the experiments carried out for the project and documented in this report, the droop coefficient has been set to zero thus actively disabling the droop features. The reason for disabling the droop is because a droop term would cause a steady state power contribution if the frequency is not equal to the rated value. However, in steady state the power transferred to the grid needs to be equal to the power generated by the wind turbine in order to maintain the speed of the wind turbine bounded and well controlled. Thus, the presence of a droop term should be offset by an opposite term of equal amplitude from the speed regulator. In the previous deliverable [6] the droop term was included to offer more flexibility in the power support during frequency transients. However, these approaches proved to be not convenient for the laboratory implementation because affecting the stability of the scheme and because not easy to tune. Flexibility for adjusting the power support is instead offered by an additional control term referred as additional power support and included in the speed regulator block.

Further details about modifications included in the laboratory implementation and the conventional VSM schemes are provided in the following subsections
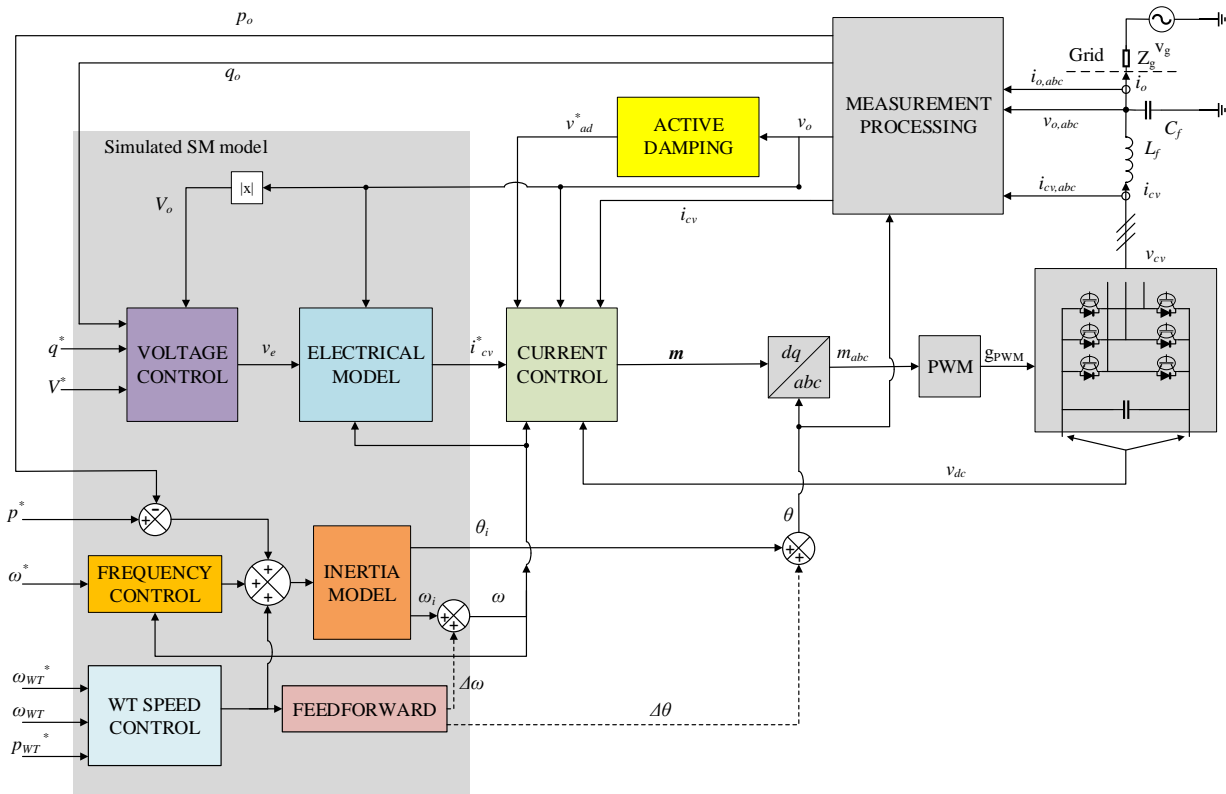
Figure 4-9: *Overview of the control structure for the grid side converter implementing a current controlled VSM.*

4.8 INERTIA MODEL WITH FEEDFORWARD TERM

The inertia model determines the rotational speed of the virtual inertia based on the power balance between a reference power for the VSM and the electrical power measured. This speed is integrated to generate the angle for the Park transformation. The power balance is responsible for the grid forming capabilities and for the power synchronization mechanism that ensure the synchronization to the external grid without a PLL or similar external function. In normal VSM schemes the inertia model is a translation of the swing equation and power unbalances affect only the speed and then reflect to the angle. This mechanism is also affected by the value of the virtual inertia that effectively acts as a filter. In practice higher values of virtual inertia correspond to more inertia support but also to a slower reaction of the VSM to changes of power reference. However, in the case of a wind turbine the grid side converter should promptly react to variations in the power generated by the WT in order to avoid speed deviations. Thus, a feedforward term has been introduced linking the reference power to an additional contribution summed to the angle of the VSM. The sum of these two angles is then forwarded to the Park transformation (see Figure 4-10 and Table 6).
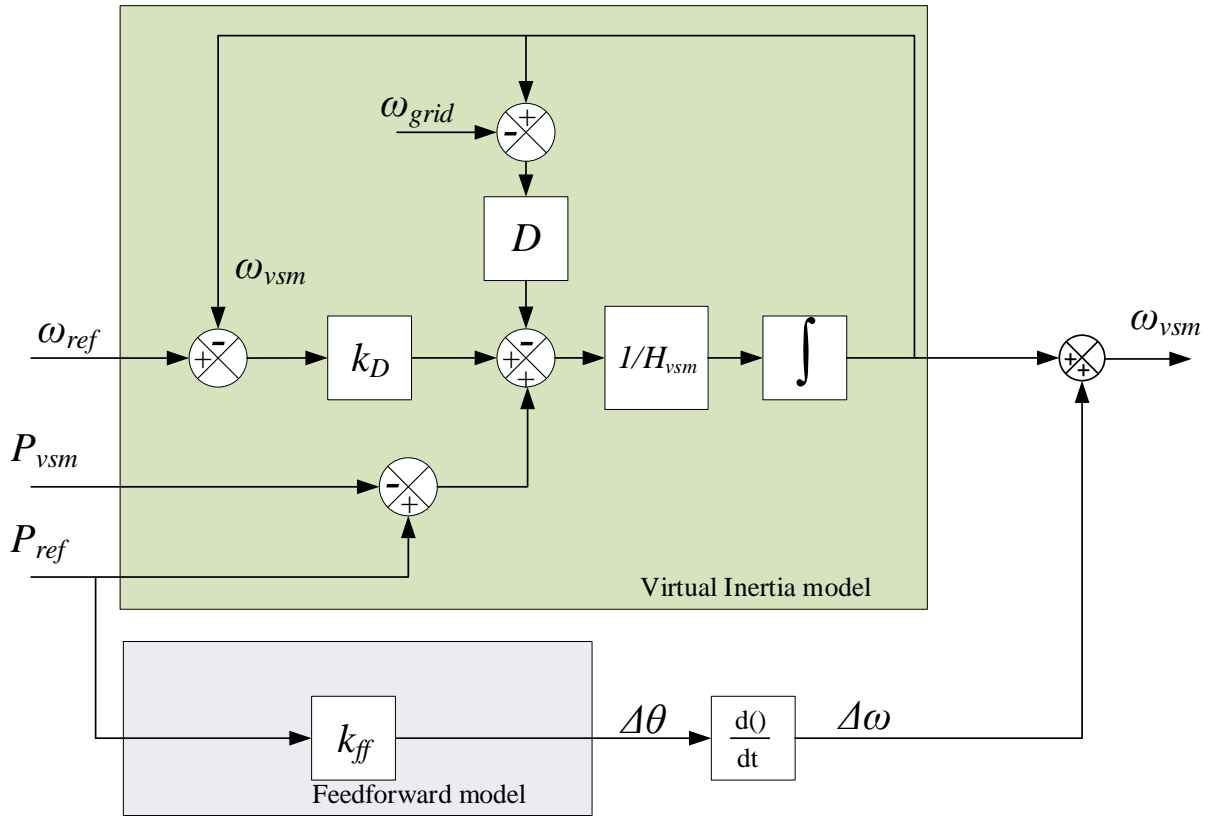
Figure 4-10: Virtual inertia and feedforward models.

Table 6: Parameters VSM virtual inertia and feedforward.

Parameter description	Symbol	Parameter description	Symbol
Damping gain	D	Grid electrical frequency speed	ω_{grid}
Virtual inertia VSM	H_{vsm}	Speed reference	ω_{ref}
Droop gain	k_D	VSM frequency speed	ω_{vsm}
Feedforward gain	k_{ff}	Reference power	P_{ref}
		VSM power	P_{vsm}

4.9 WT SPEED REGULATION

The grid side converter is responsible for the regulation of the speed in the WT. The speed regulation is obtained by regulating the power reference to the VSM according to the speed error. If the turbine is rotating too fast, the speed regulator will increase the power reference for the VSM resulting in higher power transferred to the grid (see Figure 4-11). When the power transferred to the grid plus the internal converter losses exceeds the power generated by the WT, the rotational speed decreases and reduces the overspeed. The same mechanism is operating in inverted terms in case of speed slower than the reference. The speed regulation is obtained with a PI that generates a power reference for the VSM from a speed error input. The regulator gains have been tuned for the PI controller to be sufficiently slow not to interact negatively with the inner loops and the dynamics of the virtual inertia. The parameters are shown in Table 7.
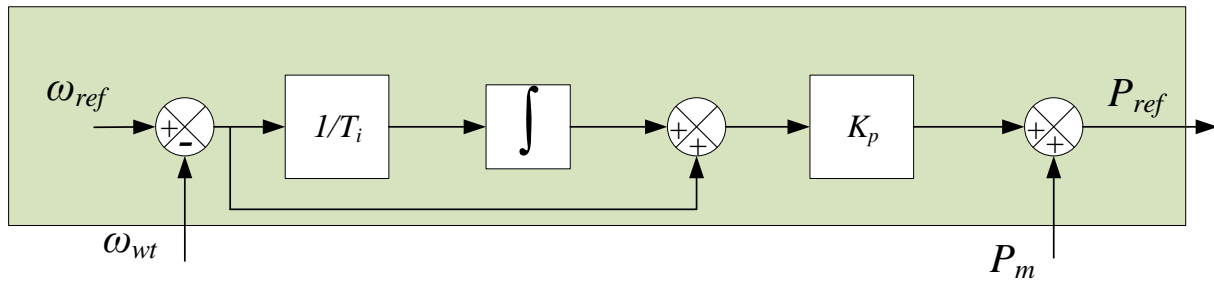
Figure 4-11: *WT speed regulator.*

Table 7: Parameters WT speed regulator.

Parameter description	Symbol	Parameter description	Symbol
Proportional gain	K_p	Speed reference WT	ω_{ref}
Integral time	T_i	WT speed	ω_{wt}
Mechanical power	P_m	Reference power	P_{ref}

4.10 ADDITIONAL POWER SUPPORT AND BACKTRACKING ANTI-WIND UP

During a frequency transient, the grid side converter should support the external grid providing a power surplus for a time duration in the order of a few seconds. This power should help in reducing the frequency deviations while waiting for the response of the conventional synchronous generators and their governors. In the implementation phase, the power support provided by the VSM revealed to be difficult to adjust by acting only on the virtual inertia value and on the droop coefficient in the VSM. This implied that a rather negligible energy was provided from the rotating masses in the wind turbines. In order to alleviate this issue and to offer more flexibility, an additional power support has been added to the output of the speed regulator. Thus, the input reference power of the VSM is a combination of several terms as indicated in the Figure 4-12. This additional term is activated when a frequency transient is detected and maintained for a fixed time interval duration (i.e. 6 s in the majority of the tests). This term could be set according to multiple criteria based on the present operating conditions but for sake of simplicity has been assumed constant in the experimental tests. Thus, during the frequency transient the VSM will support the external grid with this constant power term in addition to the power due to the virtual inertia.

It should be considered that during a frequency disturbance the speed regulation should be deactivated in order to avoid it conflicting with the main VSM inertia support objective. Indeed, if the external frequency is decreasing, the VSM will react by injecting more power. This will reflect in a reduction of the rotating speed of the WT and in an action from the speed regulator aiming at cancelling the additional power transferred. The deactivation of the controller is applied for a fixed time duration. Once the controller is activated again the WT will need to recover back the kinetic energy in order to repristinate the original speed. Thus, the speed controller reduces to zero the power output from the VSM leading to an increase in the speed. The experimental tests revealed a wind-up effect when the speed returned to the reference value with speed overshot and oscillatory power transients. The wind up of the integrator in the speed regulator has been compensated with an anti-wind up scheme based on back tracking.
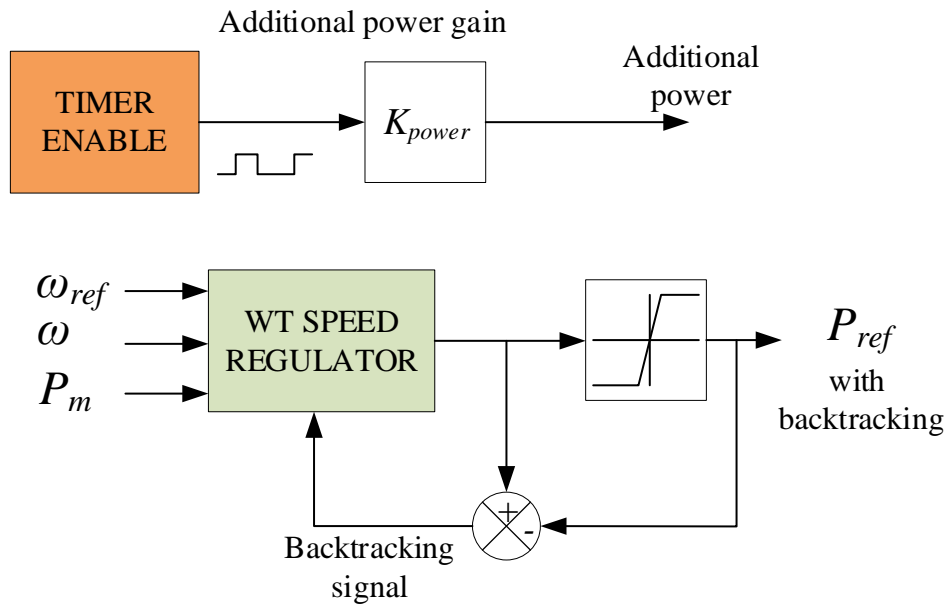
Figure 4-12: Additional power and WT speed regulator.

Table 8: Parameters additional power WT speed regulator.

Parameter description	Symbol	Parameter description	Symbol
Additional power gain	K_{power}	Speed reference WT	ω_{ref}
WT speed	ω	Mechanical power	P_m
		Reference power	P_{ref}

4.11 MODELS FOR REAL TIME SIMULATION

The experimental configuration combines physical hardware represented by the two converter units with a simulated wind turbine and an external grid according to the PHIL approach. In the experimental tests the real time simulator was executing real time models for grid and wind turbine and control algorithms for the VSM converter with a fixed time step of 100 μs. An insight in the implementation of these real time model is provided in this section.

4.12 WIND TURBINE MODEL

It has been shown in the previous report [6] that is necessary to carry a strict stability analysis that identifies the modes presented in the interaction between WTG and VSM. These modes represent the states-transient behaviour of the set WTG plus VSM. Therefore, as the main goal in this report is to find the limitations and performance of the WTG-VSM methodology for frequency support and synthetic inertia in the integration of the WTG; the dynamic model used to emulate the WTG system can be reduced to a first order equation (the swing equation) in order to ease the implementation and validation of the topology. This simplification approach has been also presented in [7] and [8]. Besides, in [8] the model is used to analyse the frequency stability improvement using synthetic inertia of WTs. The authors in [8] presented the validation of the simplified model against the full model of a WT with double feed induction generators (DFIG), this validation is shown in Figure 4-13.
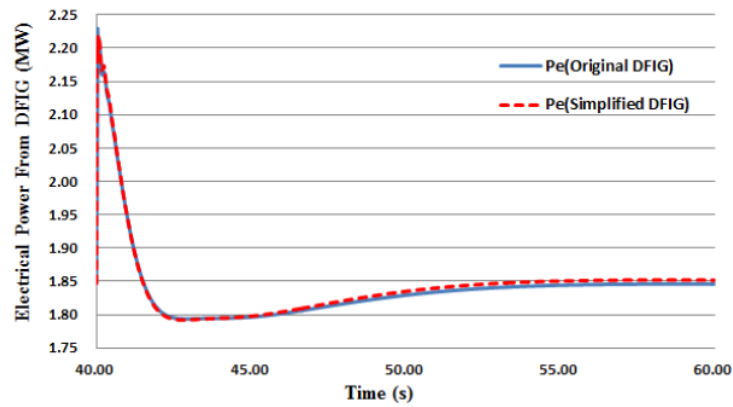
Figure 4-13: *Validation of the simplified wind farm model and the full electrical model (From [8]).*

The model can be represented with the following differential equation:

$$H_{wt} \frac{d\omega_{wt}}{dt} = P_m - Pe - K_d(\omega_{wt}) \tag{1}$$

where, the rotational speed is ω_{wt}, the mechanical input power is P_m, the electrical power is P_e, the parameters for the inertia and the damping constant are H_{wt}, K_d, respectively. P_m is the available wind power. This model uses the electric power measured in the rectifier DC link. The mechanical power is used as input to produce enough torque in the axis of the turbine and generator. A friction gain has been applied to dissipate kinetic energy of the turbine emulating a the first order model and keeping control on the rising time of the time response for ω_{wt}. Additionally, this gain K_d can be set to zero to avoid the losses in the model.

A 3 s time response of the rotational speed as shown in Figure 4-14 is used as the base response of the WTG model and it is close to the response shown in [8]. Therefore, based on the time response the parameters of the WTG can be calculated. This response shows the behaviour of ω_{wt} for a small 0.01 pu power step in the electric power. With initial condition $\omega_{wt} =1$ pu, this power step produces a deceleration of the turbine ω_{wt}.
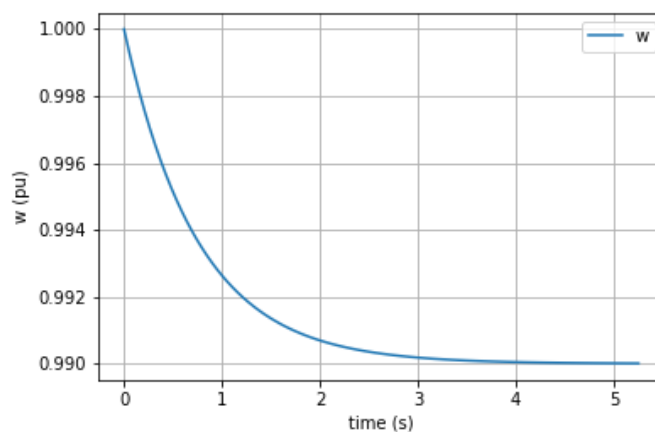
Figure 4-14: *Base response for the emulated WTG model.*

The approach described above assumes the WTG is operating around the optimal rotational speed. In this model the optimal value for $\omega_{wt} = 1$ pu. Besides, this optimal operation assumes that the tip

speed ratio of a WT is at the optimal point for all feasible wind power inputs. Hence, the extracted power from the WTG is around the optimal rotational speed.

4.13 EXTERNAL GRID MODEL

The grid equivalent is RT-simulated with a per unit equivalent turbine, governor and a synchronous generator inertia dynamic (see Figure 4-15). Moreover, a generic first order power response is used with the governor-turbine for the prime mover (P_{Gen}), this model has a integral gain k_i, a droop gain k_p and a droop gain R. The reference angular speed deviation in per unit is $\Delta \omega_{ref} = 0$. Besides, the AC voltage magnitude is represented with an ideal voltage source, and the generator dynamic uses the swing equation with rotational speed deviation $\Delta\omega$, H inertia constant, and the damping gain D in the generator. In order to disturb the frequency in the system a load is connected to the model (P_{Load}). The power generated by the VSM is P_{vsm} and the penetration degree of the VSM is scaled with a proportional gain g_r. Therefore, the electric power measure P_{el-m} is calculated with the difference between the load power P_{Load} and the power injected by the VSM P_{vsm}.
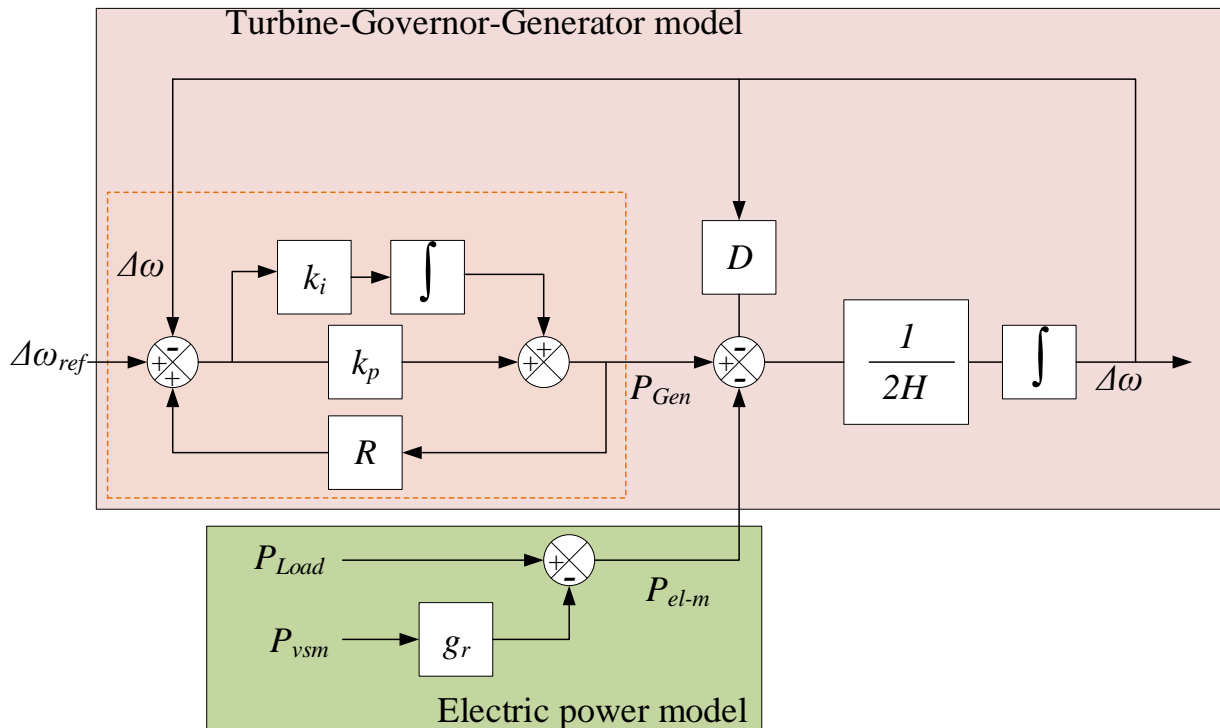
Figure 4-15: *Dynamic model for the Turbine-Governor-Generator.*

4.14 EXPERIMENTAL RESULTS

The operation of the inertia support implementation from WT based on VSM has been validated experimentally in a sequence of tests and the main experimental results are presented in this section. The results have been grouped in separate cases aiming at highlighting the response of the combined system to external disturbances or references. Further tests have been added to demonstrate the role of the modification of the implementation compared to conventional VSM schemes published in the technical literature.

Parameter	Value	Parameter	Value
Rated grid voltage (LL rms)	400 V	Time extra power support	8 s
Rated grid frequency	50 Hz	Time PI speed disabled	6 s
VSM virtual inertia	1 s	WT inertia constant	3 s
VSM damping factor	40 pu	WT power	20 kW
VSM backtracking coefficient	0.5		
Extra power support	0.1 pu		

4.15 RESPONSE TO VARIATIONS OF POWER GENERATED BY THE WIND TURBINE

A first test case aims at characterising the response of the system to changes in the power production from the wind turbine. In general, the power produced by the wind turbine should be constantly balanced with the power injected in the grid to avoid accumulating energy in the form of kinetic energy in the rotating masses or in the form of electrical energy in the dc bus capacitance. In the configuration implemented, the dc voltage controller has a relatively higher bandwidth compared to the other control loops regulating power and power mismatches will translate into variations of the turbine rotational speed. It should also be noted that a conventional VSM scheme presents a rather sluggish response for changes of power reference and this could be conflicting with requirements of prompt speed regulation of the WT. This deficiency of the VSM scheme has been correcting by adding a feedforward term that increases the responsiveness to changes of power reference without affecting the power synchronization mechanism and the grid forming capabilities of the VSM unit. In case of a variation of power produced from the turbine, the power reference for the VSM is changed and due to the feedforward term the power injected in the grid rapidly follows the variation. Any difference will result in a variation of speed that will be more slowly corrected by a speed controller (i.e. PI regulator) having the speed error as an input and the VSM power reference as an output.

An experimental test has been conducted where the configuration operates at steady state injecting 3 kW in the grid until the power produced by the WT is ramped linearly up to 30 kW (i.e. .5 pu) and then again linearly decreased with same slope till the initial value. The response in terms of measured power and WT speed are reported in Figure 4-16. Results clearly indicate that the power from the VSM and from the rectifier converter promptly follow the change of power and that this results in a negligible speed variation. The differences between the power from the VSM and the power from the rectifier are due to the power losses in the two converter units.
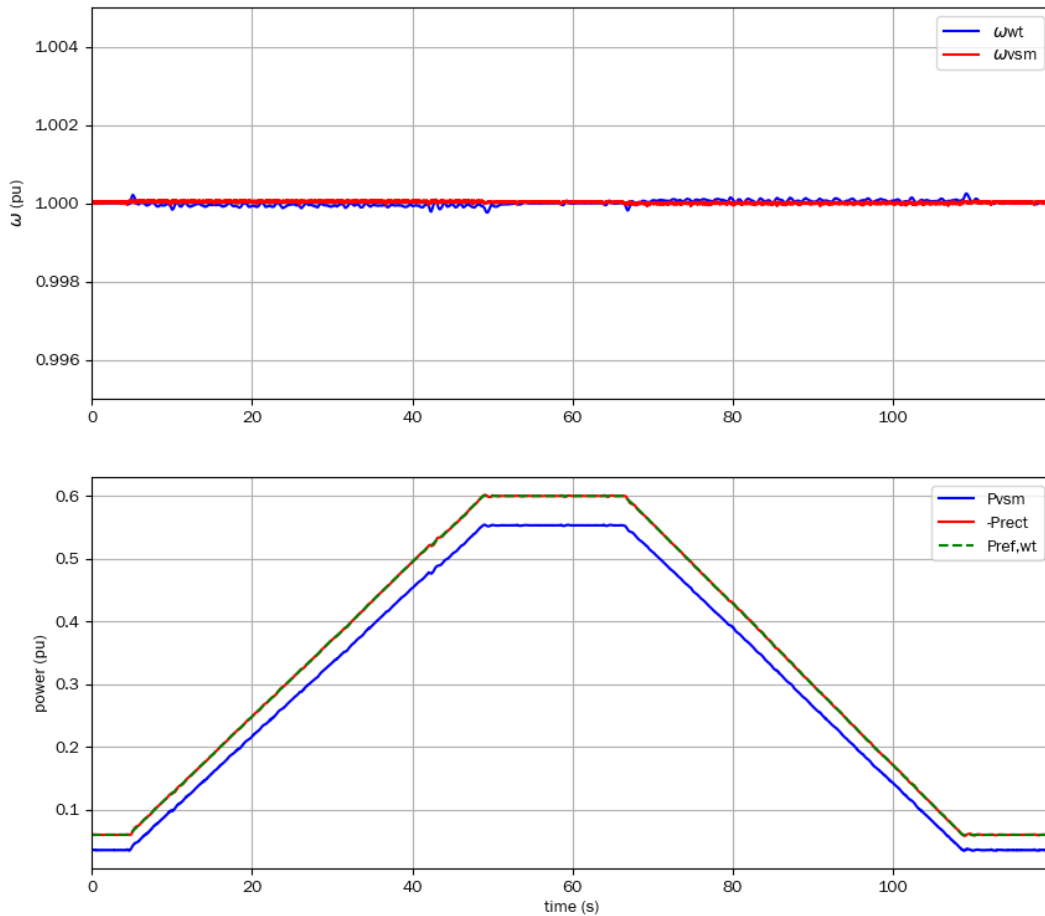
Figure 4-16: *Response to a ramp variation in power generated by the WT from 3 kW to 30 kW.*

4.16 RESPONSE TO VARIATIONS IN GRID FREQUENCY

The second test case illustrates the main feature of the inertia support scheme as response to grid frequency variations. In order to better isolate the behaviour and the dynamics of the converter control system, the grid is assumed as an ideal voltage source experiencing a step change in the frequency. The VSM control scheme inherently detects the frequency variation in the grid and provides inertia support. Indeed, the power response depends on the overall amplitude and derivative o the frequency change according to the power synchronization mechanism that the VSM implements. However, it should be considered that the pure inertia contribution may be associated to a relatively limited contribution both in terms of time duration and overall energy. A conventional VSM scheme does not offer in this perspective sufficient flexibility since the response can be adapted mostly by modifying the values of the virtual inertia and of the damping coefficient. Both these parameters have an impact on the time and on the energy, but variations are relatively limited and they imply also critical effects on the stability and damping of the response. Thus, an extra power term is added to increase flexibility.

In a first test the system is exposed to a frequency step from 1 pu to 0.998 pu corresponding to a step from 50 Hz to 49.9 Hz (Figure 4-17). It should be noted that this variation is rather large in the perspective of a large transmission system. The system reacts to the frequency variation by increasing the power in the first seconds mostly due to the contribution from the virtual inertia (power peak) and then from the extra power term (constant power). The constant extra power is

maintained for 6 s that is considered a time sufficient for the main grid to start recovering from the frequency transient where inertia support is beneficial. After this the power injected is equal to the power produced by the WT for 2s. The dynamics of the power are reflected in the wind turbine speed that is progressively reduced in the first 6 s and then remain approximately constant for these last 2 s. These setting bring the WT speed to a value equal to approximately 0.8 pu. After 8 s the speed controller is activated and the power injected to the grid is controlled to be equal to zero. This imply that the power generated in the wind turbine is transferred to the rotating masses to re-establish the reference speed. When the WT speed is approaching the reference speed the system reduce the power to reach steady state conditions without overshoots. These dynamics are heavily affected by the settings of the backtracking term.
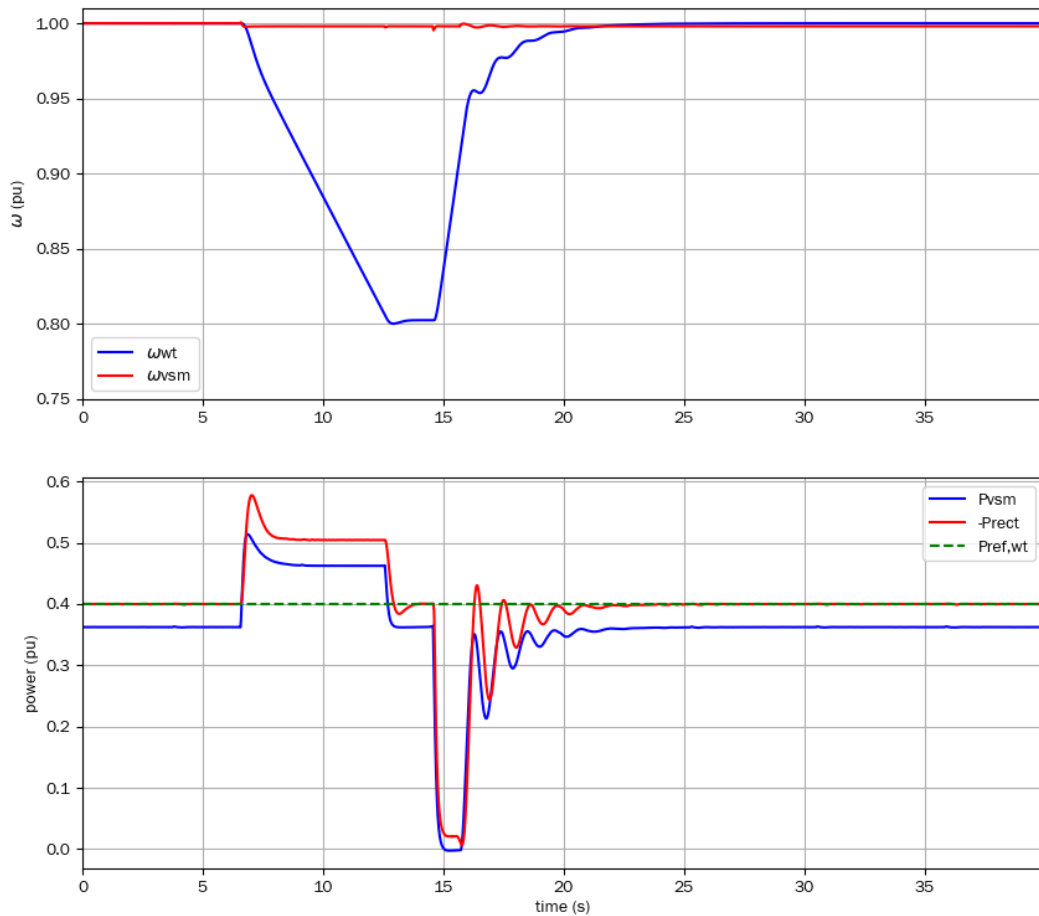
Figure 4-17: Response to a frequency step in grid frequency from 1 to .998 pu.

In a second test the system is exposed to a larger frequency step from 1 pu to 0.995 pu corresponding to a variation from 50 Hz to 49.75 Hz (Figure 4-18). This corresponds to a very extreme variation for a transmission system while could be more realistic for operation in islanded conditions and is added for further reference. The behaviour is largely similar to the previous case with main differences in the power peak due to the support associated to the virtual inertia. Indeed, this behaviour fits with the expected support from a virtual inertia.
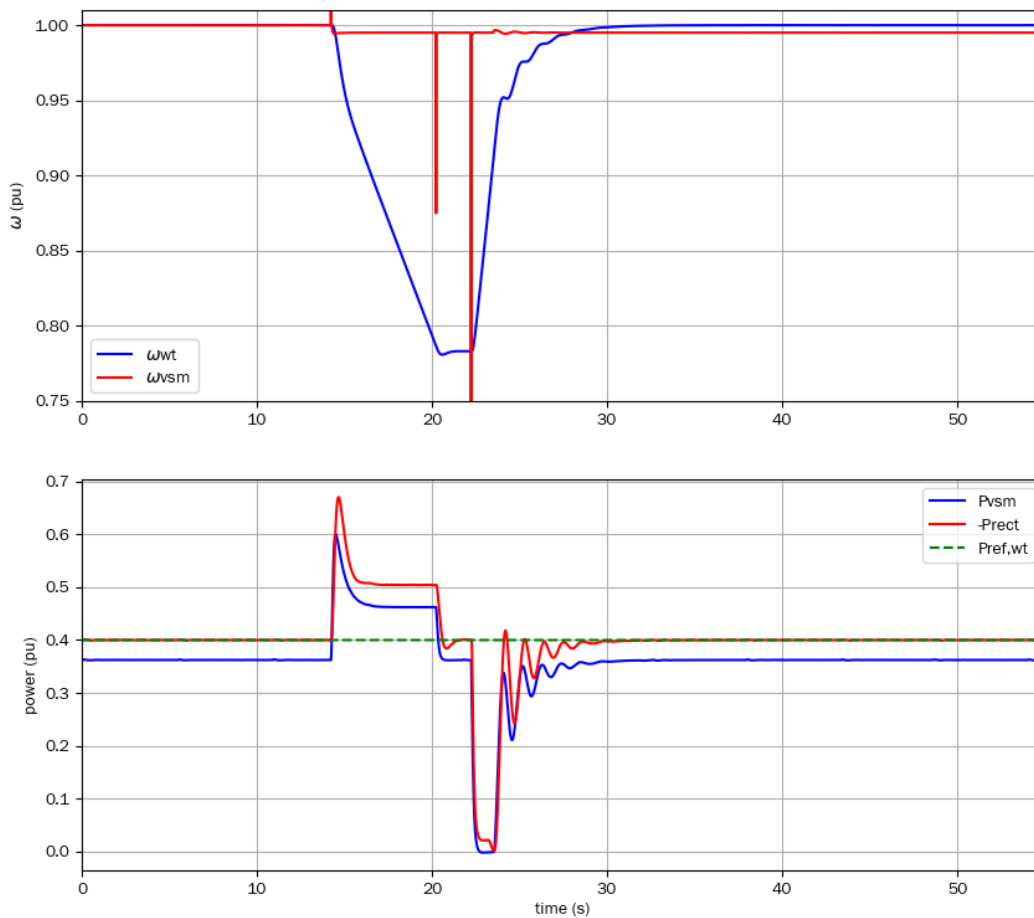
Figure 4-18: *Response to a frequency step in grid frequency from 1 to 0.995 pu.*

4.17 DISABLING ADDITIONAL POWER SUPPORT

The conventional VSM schemes provide inertia support during frequency variation due to the dynamics of the virtual inertia and the presence of possibly a droop term. In this implementation for WT the droop term is omitted because at steady state the power injected into the grid should be equal to the power produced independently by the frequency of the grid. However, power support due to only the virtual inertia could be rather small in terms of energy and duration except for very extreme tuning of the VSM parameters that could have serious implications on the general stability. Thus, in the previous experiments an extra power has been added to offer more flexibility in defining the amount of support. This contribution is defined by two main parameters: the amount of extra power (i.e. 0.1 pu in the previous cases) and the duration of the extra power support (i.e. 6s in the previous cases). In order to demonstrate the role of this extra power term to the general behaviour the two cases presented in the previous subsections are repeated disabling the extra power term.

In a first test the frequency is again reduced as a step from 1 pu to 0.998 pu. The speed regulator is disabled for 2 s only. The experimental results are presented in Figure 4-19. Results clearly demonstrate that the amount of inertia support is quite limited and that only a few percent of the kinetic energy in the rotating masses is transferred to the grid. The test has been repeated with a step of the grid frequency from 1pu to 0.995 pu and extending the time where the speed regulator is disabled to 4 s. However, the results reported in Figure 4-20 indicate still that the energy provided during the inertia support is rather limited.
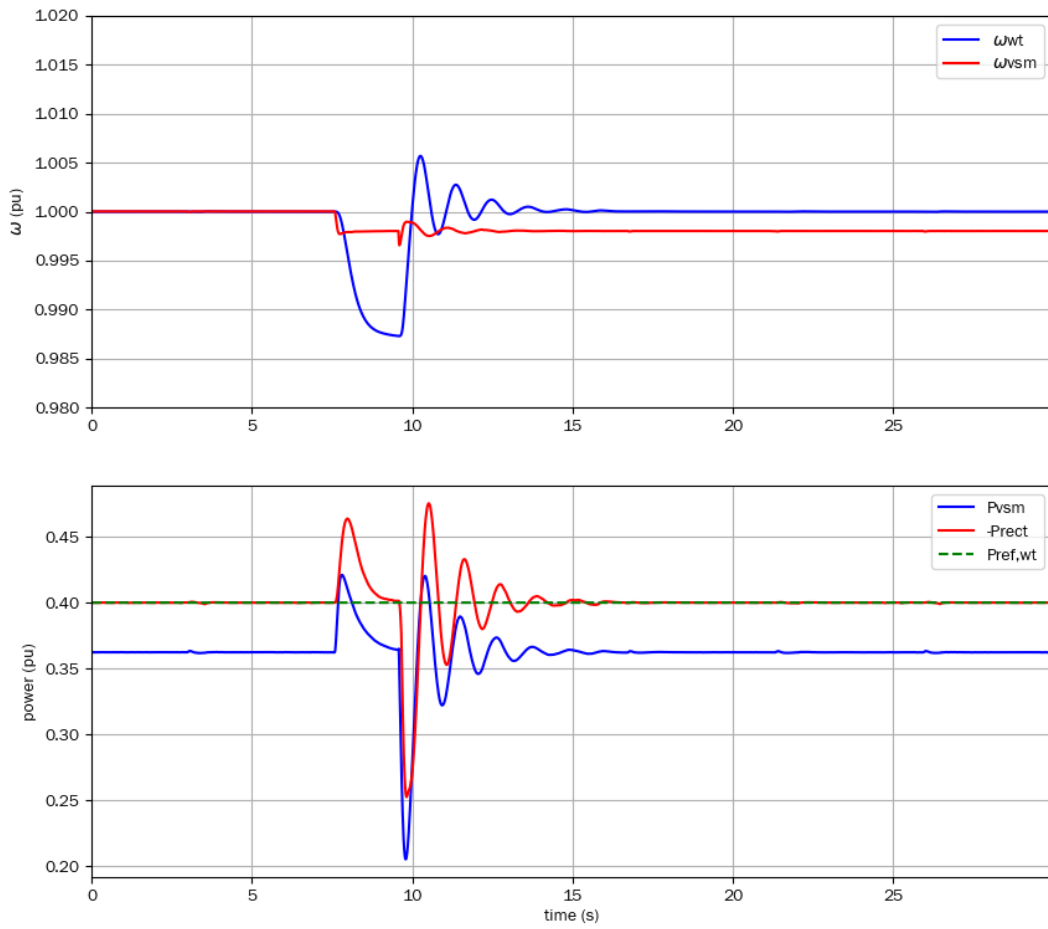
Figure 4-19: *Response to a frequency step in grid frequency from 1 to 0.998 pu without extra power support.*
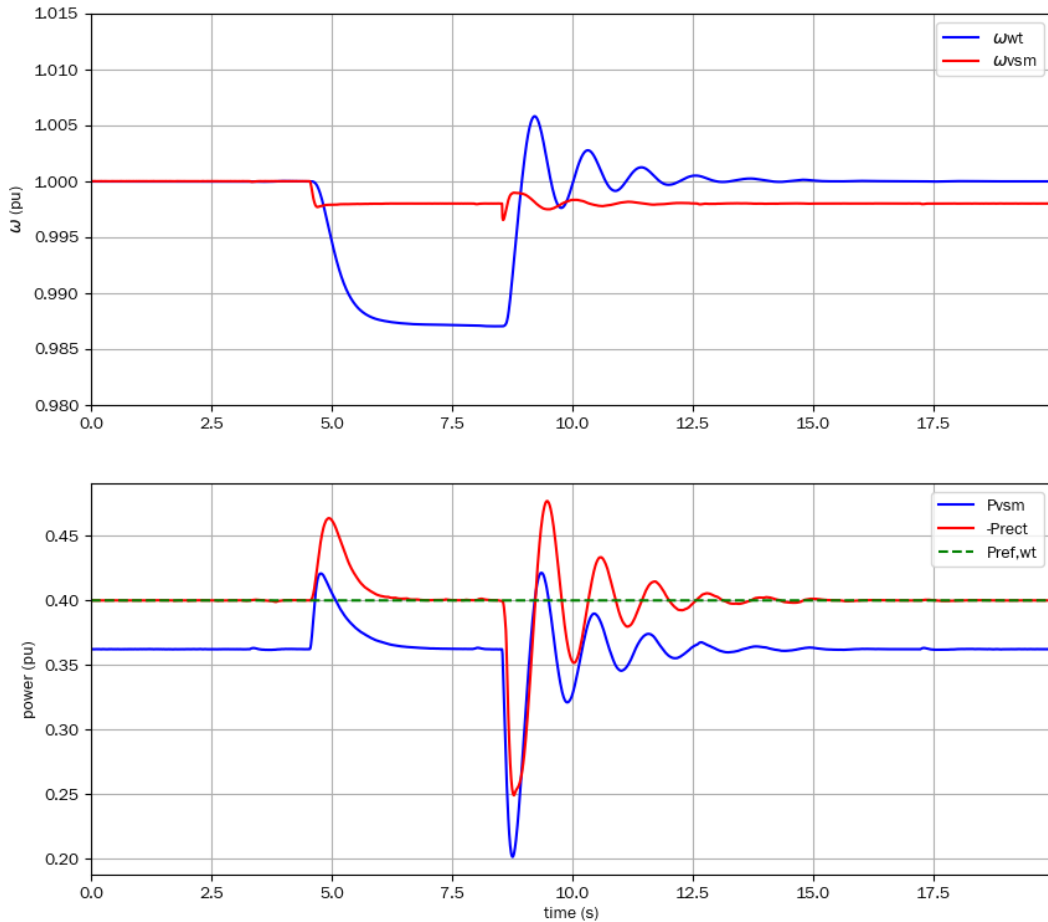
Figure 4-20*: Response to a frequency step in grid frequency from 1 to .995 pu without extra power support.*

4.18 DISABLING FEEDFORWARD TERM

In the conventional VSM schemes a change in the power reference determines an unbalance on the virtual inertia and a variation of its speed. This speed variation leads to a variation of the power angle and finally in the power transferred to the grid. Thus, the link between the change of power reference and the actual change in the power transferred to the grid is not direct but filtered by the inertia dynamic. This link implies also that a higher inertia support would require a higher value of inertia and this would result also in a slower dynamic performance. In order to avoid this issue, a feedforward term has been added to the scheme in order to create a more direct link between the change in the power reference and the power injected in the grid. The differences produced by the presence of the feedforward term has been highlighted by dedicated tests where the term has been disabled. Moreover, since the differences are more evident for steep variations of the reference power the slew rate limiter present on the power reference has been modified allowing a change of 100 pu/s and 500 pu/s.

The responses to a power step from 20 kW to 10 kW at a slew rate of 100 pu/s without and with feedforward are presented in Figure 4-21 and Figure 4-22 respectively. The results demonstrate that the feedforward term contributes in a faster and better damped response.
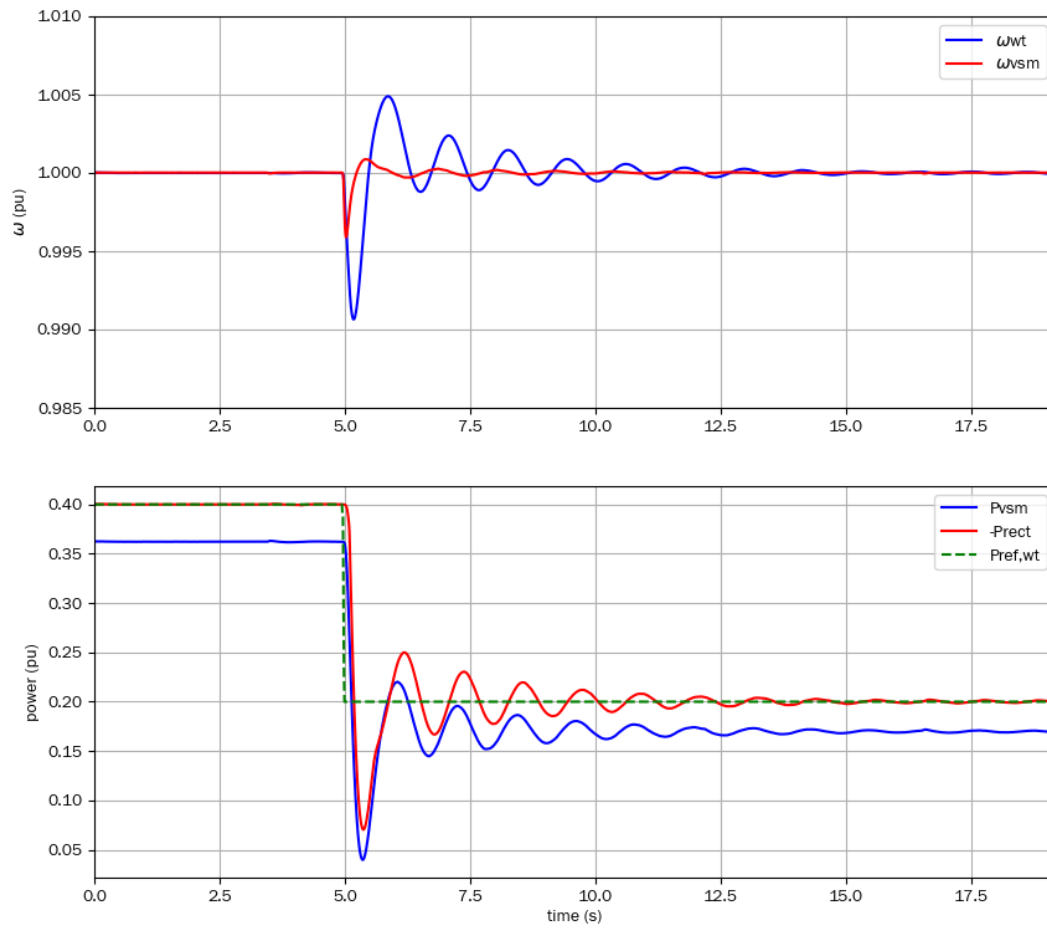
Figure 4-21: *Response to a variation of the WT power from 20 kW to 10 kW with a slew rate of 100 pu/s and no feedforward.*
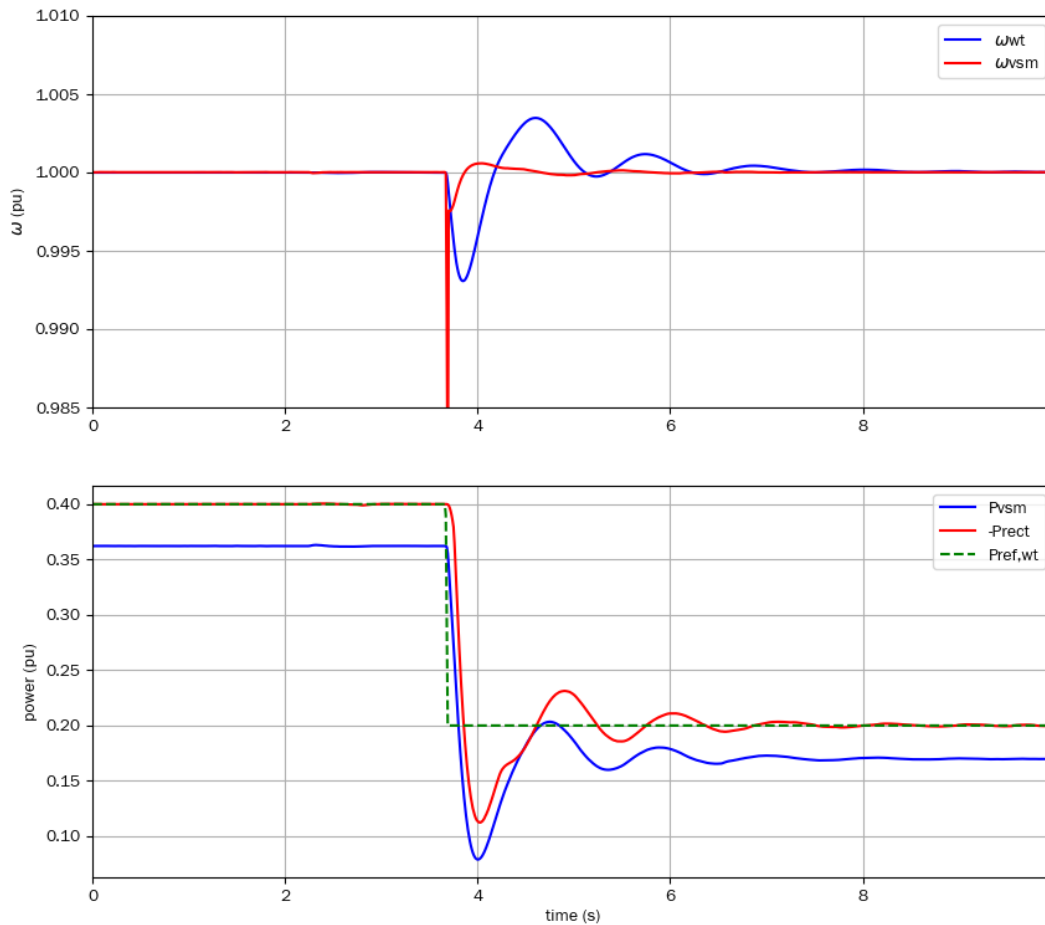
Figure 4-22: Response to a variation of the WT power from 20 kW to 10 kW with a slew rate of 100 pu/s and feedforward.

The test is repeated further increasing the slew rate limiter to 500 pu/s. Experimental results are again consistent with the previous test (see Figure 4-23 feedforward and Figure 4-24 no feedforward). The feedforward term significantly reduces transient oscillations and produce a faster and better damped response. It should be noticed that in the real laboratory implementation the feedforward term is implemented only partially due to control constraints in the control implemented in the converter FPGA boards. This indeed partly reduces the effect of the term and introduces oscillations. It is expected that a non-limited version of the feedforward term would result in a much better transient response with even less overshooting and oscillations. However, this could not be tested within the time frame of the project task.
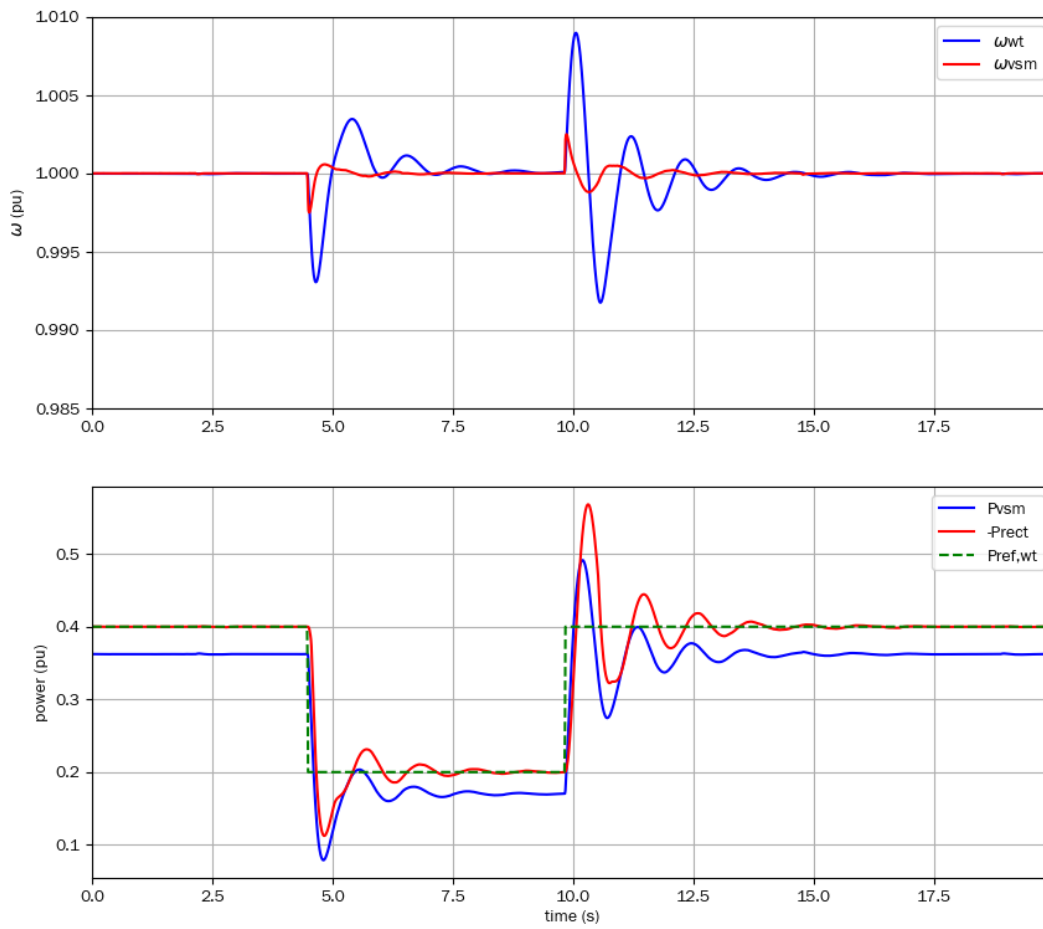
Figure 4-23: *Response to a variation of the WT power from 20 kW to 10 kW with a slew rate of 500 pu/s and feedforward.*
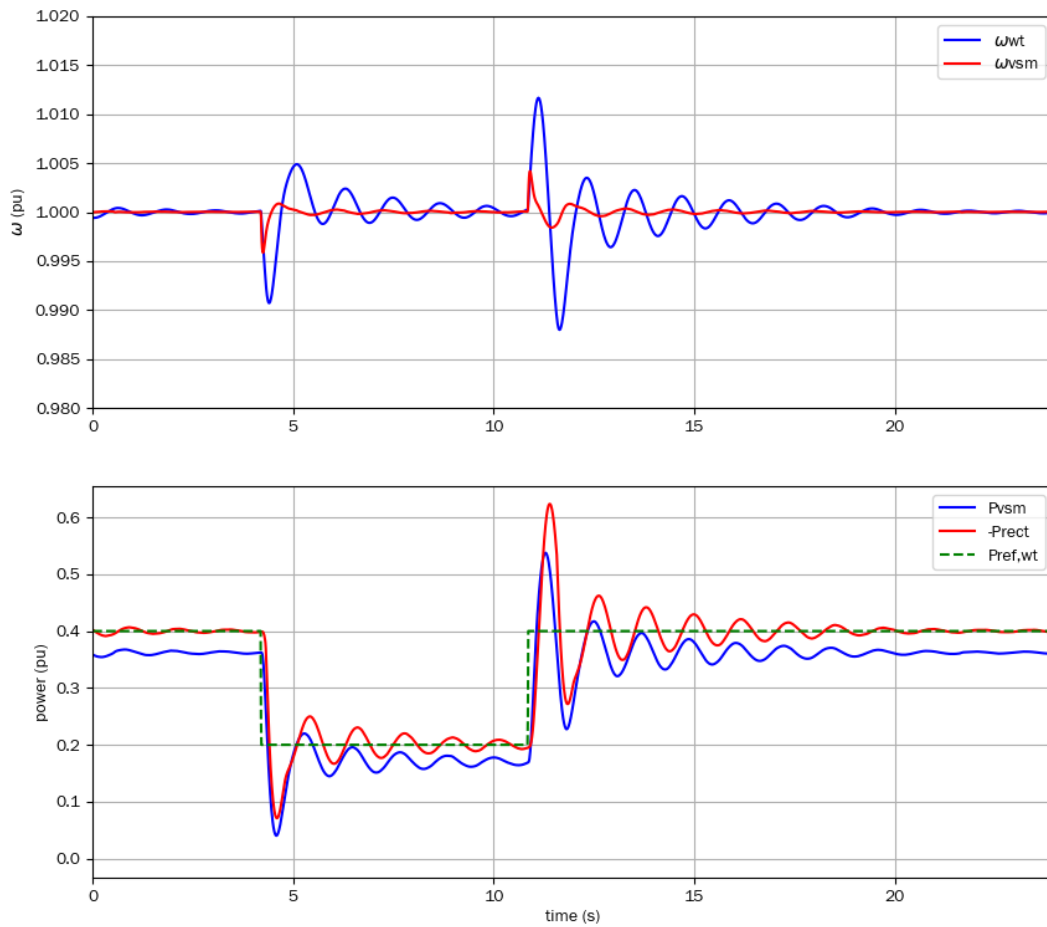
Figure 4-24: *Response to a variation of the WT power from 20 kW to 10 kW with a slew rate of 500 pu/s and no feedforward*

4.19 INFLUENCE OF BACKTRACKING COEFFICIENT

A set of tests has been conducted to highlight the effect of the backtracking coefficient on the response of the system. This coefficient affects the behaviour of the speed controller when the speed is in the proximity of the reference after a period where the output of the regulator was saturated. The term aims at reducing the wind up of the integrator in the PI controller for the speed and avoids a possible overshoot of the speed and associated power oscillations. The behaviour is largely dependent on the power of the wind turbine and the relevance of the grid disturbance. The coefficient has been set to a default value of 0.5 since it proved to be a reasonable compromise within all the power range.

An example of response for the coefficient set to 0.3 is presented in the Figure 4-25 and Figure 4-26 for grid frequency steps from 1 pu to 0.998 and 0.995, respectively. The differences are relatively minor with a more smooth transition to the steady state conditions.
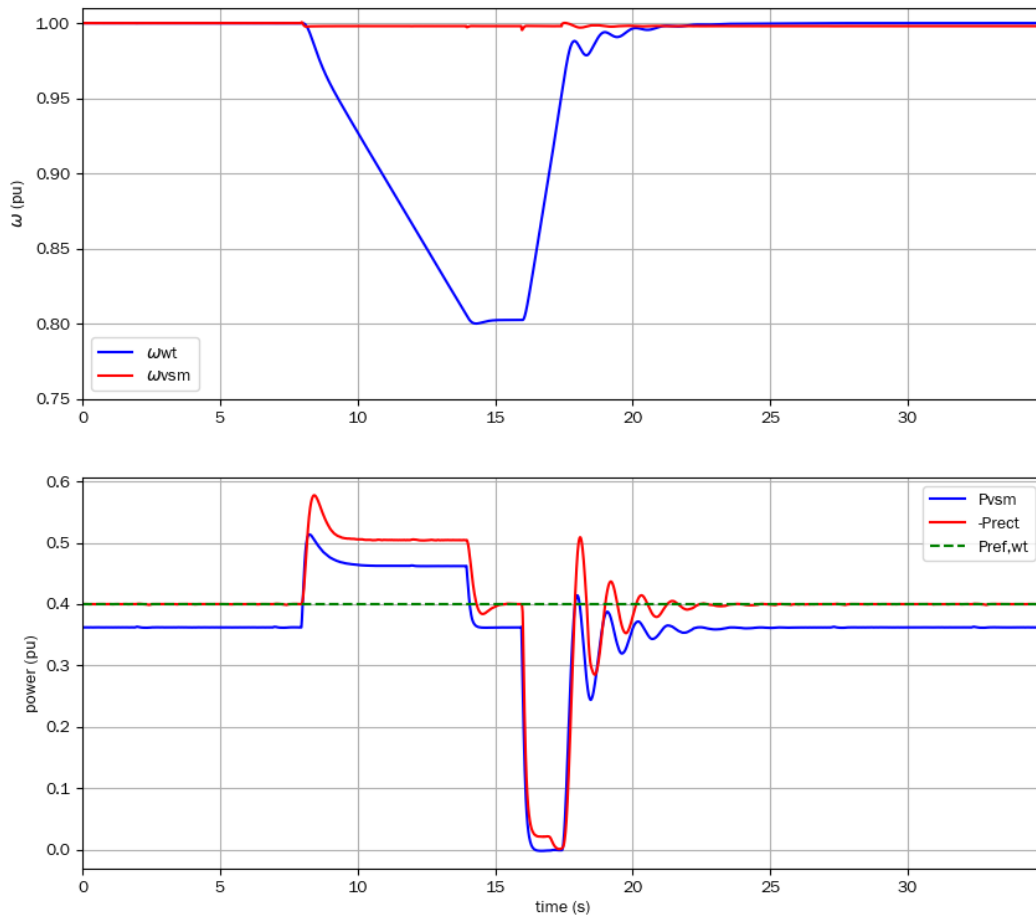
Figure 4-25: *Response to a frequency step in grid frequency from 1 to .998 with backtracking set to 0.3.*
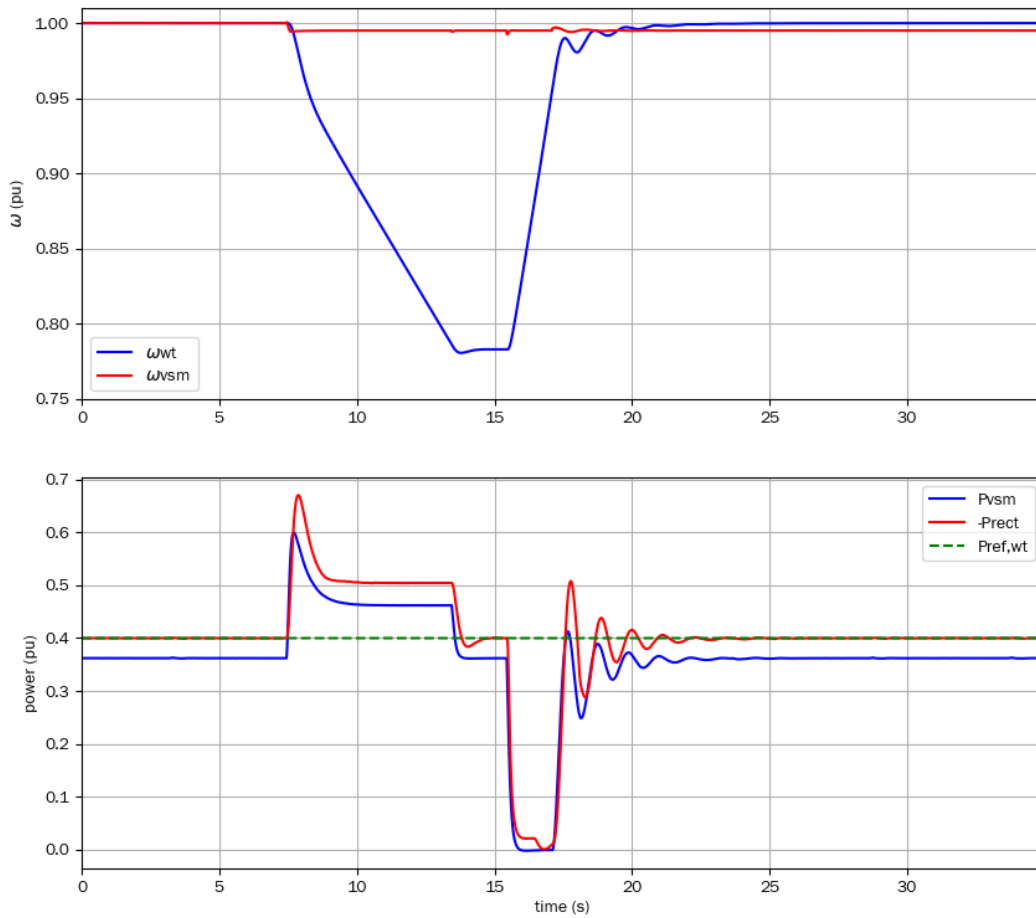
Figure 4-26: *Response to a frequency step in grid frequency from 1 to .995 with backtracking set to 0.3.*

The Figure 4-27 indicates the behaviour if the backtracking term is completely disabled for a similar transient triggered by a frequency step in the grid. The first part of the transient presents negligible differences compared to the previous case with backtracking activated. However, when the speed of the turbine approaches the reference speed at the end of the transient support the speed controller suffers from wind up and leads to a frequency overshoot. This is reflected also in power oscillations that are not present in the other cases.
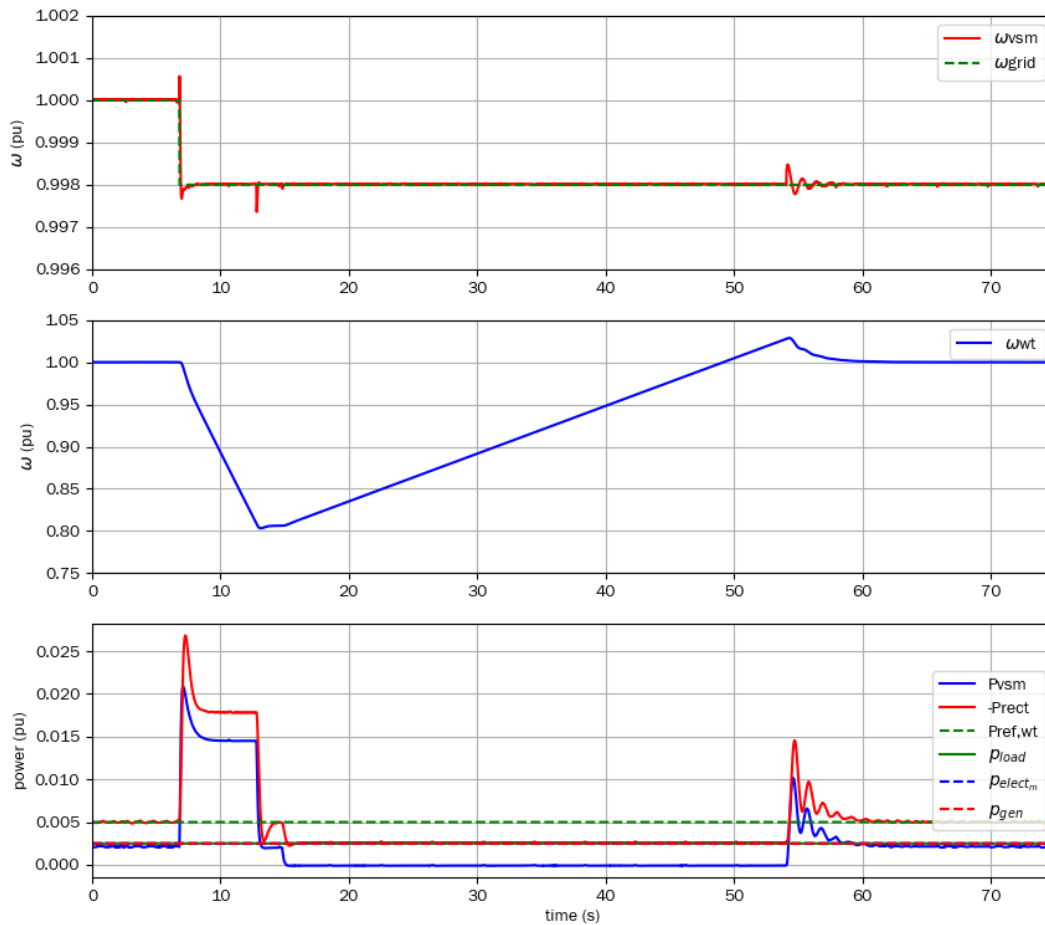
Figure 4-27: *Response to a frequency step in grid frequency from 1 to .998 without backtracking.*

4.20 RESPONSE TO VARIATIONS OF POWER LOAD IN THE GRID

As a last set of tests, the VSM implementation has been tested according to a PHIL approach with a simulated grid as described in the previous dedicated subsection. The following cases show the behaviour when a load disturbance creates a frequency variation in the grid. The reaction of the grid to a load disturbance is a reduction of the frequency as seen in Figure 4-28. The test is performed with and without inertia support and demonstrate how the inertia support can reduce the rocof in the initial transient and improve the frequency nadir. Finally, the power in each subsystem are reported in Figure 4-29.
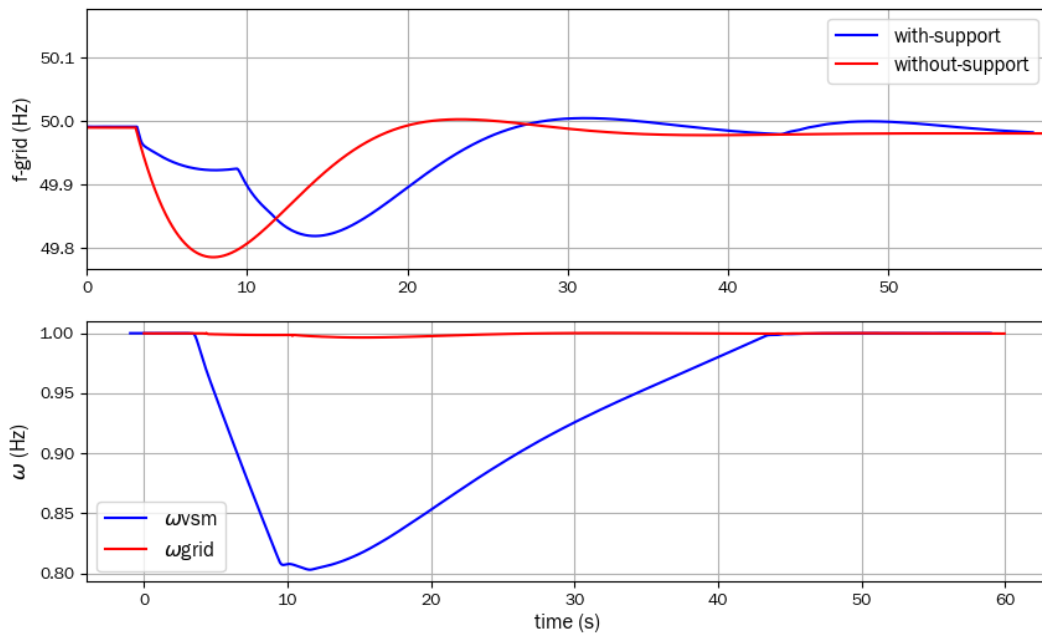
Figure 4-28*: Grid frequency response for power load step (top) and rotational speed for VSM and WT (bottom).*
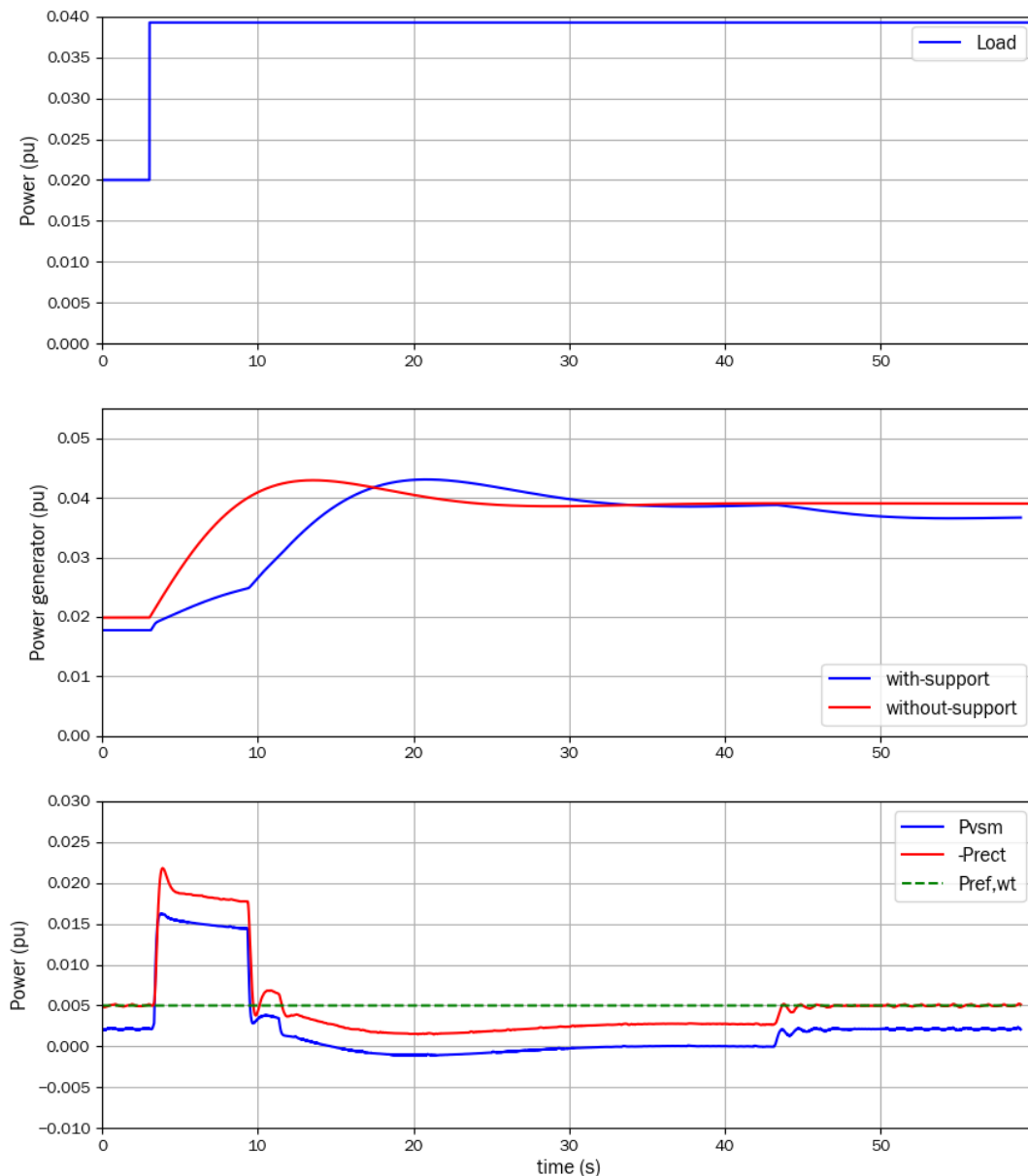
Figure 4-29*: Power responses for the load step. Load behaviour (top), power of the generator with and without support (middle) and support power of the VSM, support Rectifier and support WT (bottom).*

4.21 CONCLUSIONS

The concept of VSM offers the possibility to provide inertial support from power converter together with grid forming capabilities. These features are considered very relevant for future power systems where the penetration of power from renewables interfaced via converters will be even higher than presently.

Many implementations of VSM has been presented in literature and a selection of a few best candidates has been considered in the project. However, classical schemes while offering inertia support seemed to be very difficult to parametrize in order to obtain a sufficient transfer of energy to support frequency disturbances. Moreover, conventional VSM schemes suffer for an inherent limitation due to the link between inertia and speed response. Thus, high inertia support implies

possibly unacceptable dynamic performances. These two aspects are relatively minor for classical microgrid applications but do not seem suitable for a wind turbine application.

Modification to classical schemes have been proposed in the document and documented with experimental tests in the laboratory setup. The experimental tests demonstrated that a modified VSM scheme can be implemented within a WT conversion system and offer inertia support during grid disturbances. Moreover, the tests indicated that the proposed changes offer enough flexibility in modulating the amount of support to provide and a satisfactory speed response.

4.22 TABLE OF PARAMETERS FOR THE SIMULATED SYSTEMS

This section presents the parameters used in the simulation and the PHiL test for the dynamic models described in the previous sections.

Table 9: Parameters for the WT.

Symbol	Value	Description
H_{wt}	3 (s)	Inertia constant
k_d	4 (pu)	Damping constant

Table 10: Parameters for Turbine-Governor-Generator.

Symbol	Value	Description
H	5.0 (s)	Inertia constant
D	0.5 (pu)	Damping gain
k_p	2.3 (pu)	Turbine-governor proportional gain
k_i	0.625 (pu)	Turbine-governor integral gain
R	0.01 (pu)	Droop gain
g_r	0.125	Scale proportional gain

Table 11: Parameters for the VSM and WT speed regulator.

Symbol	value	Description
H_{vsm}	1 (s)	Inertia constant
D	40 (pu)	Damping factor
K_D	0 (pu)	Droop gain
K_p	15 (pu)	Proportional gain PI WT speed regulator
K_i	8 (pu)	Integral gain PI WT speed regulator

4.23 REFERENCES FOR SECTION 4

[1] The Grid Code, "nationalgrid ESO," 4 September 2019. [Online]. Available: https://www.nationalgrideso.com/codes/grid-code?code-documents .

[2] Connection and Use of System Code, "nationalgridESO," 1 April 2019. [Online]. Available: https://www.nationalgrideso.com/codes/connection-and-use-system-code-cusc?code-documents.

[3] Requirements for Generators, "Entso-e," 16 April 2016. [Online]. Available: https://www.entsoe.eu/network_codes/rfg/.

[4] DNV GL - ST - 0125, "Grid code compliance standard," 2016.

[5] nationalgridESO, "Power Park Module Signal Best Practice Guide for Intermitent Generation v1.0," July 2019. [Online].

[6] A. M. Urban, M. de Batista, H. G. Svendsen, S. D'Arco and S. Sahcez, "Turbine controller adaptation for varying conditions and ancillary services: Deliverable TotalControl Project," DNV GL, 2019.

[7] N. Ding, Z. Lu, Y. Qiao and Y. Min, "Simplified equivalent models of large-scale wind power and their application on small-signal stability," *J. Mod. Power Systems, Clean Energy,* vol. 1, no. 1, pp. 58-64, 2013.

[8] Q. Gao and R. Preece, "Improving frequency stability in low inertia power systems using synthetic inertia from wind turbines," in *IEEE PowerTech2017,* Manchester , 2017.

[9] nationalgridESO, "Future of Frequency Response - Industry Update," February 2019. [Online].

[10] Power Networks Demonstration Centre (PNDC), "PNOR Phase 1 report," The University of Strathclyde, Glasgow, 2018.

[11] R. Eriksson, N. Modig and K. Elkington, "Synthetic inertia versus fast frequency response: a definition," *IET Renewable Power Generation,* vol. 12, no. 5, pp. 507-514, 2016.

[12] ENTSO-E, "ENTSO-E Network Code for Requirements for Grid Connection Applicable to all Generators," ENTSO-E, Brussels, 2013.

5 CONCLUSIONS

This report is concerned with the addition of special features to wind plant controllers so that they can actively contribute to the stable operation of the electricity grid system and make it possible for larger penetrations of wind power to be integrated. After an brief overview of relevant grid codes in Section 2.1, section 2.2 describes how wind farms may contribute to both frequency and voltage stability. The remainder of the report is concerned mainly with grid frequency support.

The task described in Section 3 was to couple together a wind farm simulator (LongSim) and a grid simulator (KERMIT), so that fast frequency response (FFR) strategies implemented in the wind turbine controllers can be defined and tuned to achieve the best performance in terms of helping to stabilise the grid frequency, while remaining within the operational constraints of the wind

turbines in the wind conditions available at the time. The models are linked by feeding the active power output from LongSim into Kermit, and the grid frequency from KERMIT into LongSim, resulting in a closed-loop simulation of the whole system. This tool was used for a study based on historical data for the Irish grid system, which is appropriate as it already has a high wind power penetration, and suitable data is publicly available. The results demonstrate that the combined model is a useful tool for tuning and testing FFR strategies integrated into the wind turbine controller, and example closed-loop simulations have shown that with appropriate tuning of these control strategies, the wind farms can have a significant beneficial effect on the frequency stability of the grid. The strategies have been tested against three real frequency dip events recorded on the Irish system, and a day-long simulation during normal conditions was also run successfully.

The virtual synchronous machine (VSM) concept offers the possibility to provide inertial support from power converters. Section 4 describes a laboratory setup to test the VSM concept experimentally, using a hardware-in-the-loop setup with a VSM power converter and a grid emulator. Classical VSM schemes were found not to work well for the wind turbine case, so alternative configurations are proposed. The experimental tests demonstrated that a modified VSM scheme can be implemented within a wind turbine system, and is able to provide inertia support during grid disturbances. There is enough flexibility in modulating the amount of support to provide and a satisfactory speed response.

Taken together, the results of the different tasks covered in this report demonstrate that wind power plant can be of significant help to the grid system by providing fast frequency response to help stabilise grid frequency, so increasing the allowable penetration of wind power plant on the system.

REFERENCES FOR SECTIONS 2.2 AND 3

[1]   Q Li, Y Zhang, T Ji, X Lin and Z Cai, "Volt/Var control for power grids with connections of large-scale wind farms: a review", IEEE Access, 2018, 6, 26675-26692

[2]   "Technical report on the events of 9 August 2019", 2019

[3]   W Qiao, R G Harley and G K Venayagamoorthy, "Coordinated reactive power control of a large wind farm and a STATCOM using heuristic dynamic programming", IEEE Transactions on Energy Conversion, 2009, 24(2), 493-503

[4]   L Wang and D-H Truong, "Dynamic stability improvement of four parallel-operated PMSG-based offshore wind turbine generators fed to a power system using a STATCOM", IEEE Transactions on Power Delivery, 2012, 28(1), 111-119

[5]   Q Wu, J I B Solanas, H Zhao and L H Kocewiak, "Wind power plant voltage control optimization with embedded application of wind turbines and STATCOM", Asian Conference on Energy, Power and Transportation Electrification (ACEPT), 2016

[6]   E Bossanyi & R Ruisi, "Simple dynamic wind farm model", TotalControl deliverable D1.9, March 2019, http://www.totalcontrolproject.eu/-/media/Sites/TotalControl/Publications/Public-deliverables/Deliverable_D1-9_Final.ashx?la=da&hash=EF18A43B4B71438DB0453683EE10BFFF3BEE3728

[7]   Eirgrid, Soni, All-Island Transmission System Performance Report 2018,
        http://www.eirgridgroup.com/site-files/library/EirGrid/All-Island-Transmission-System-
        Performance-Report-2018.pdf

[8]   Eirgrid, Soni - Operational Constraints Update 29/03/2019, link:
        http://www.eirgridgroup.com/site-files/library/EirGrid/Operational-Constraints-Update-
        Mar_2019.pdf

[9]   ENTSOE, Future system inertia, Nordic system,
        https://docstore.entsoe.eu/Documents/Publications/SOC/Nordic/Nordic_report_Future_Sys
        tem_Inertia.pdf

[10]   SMART grid dashboard, historical data (day of the frequency events can be downloaded) of
        load, generation, frequency, wind forecast and wind actuals. See:
        http://smartgriddashboard.eirgrid.com/

[11]   System Data Quarter Hourly 2018-2019 – EirGrid, http://www.eirgridgroup.com/site-
        files/library/EirGrid/System-Data-Qtr-Hourly-2018-2019.xlsx

[12]   2018 – Eirgrid - All-Island Transmission System Performance Report

[13]   2019 – Eirgrid – Operation Constraints Update

[14]   2017 - Eirgrid - DS3 System Services Protocol

[15]   2018 - Future System Inertia 2, ENTSOE, https://www.statnett.no/globalassets/for-aktorer-
        i-kraftsystemet/utvikling-av-kraftsystemet/nordisk-frekvensstabilitet/future-system-
        inertia-phase-2.pdf

[16]   E. A. Bossanyi, Generic grid frequency response capability for wind power plant. Proc.
        European Wind Energy Association Conference, Paris, November 2015.